Models of HPV as an Infectious Disease and as an Etiological Agent of Cancer

by

Andrew Frederick Brouwer

A dissertation submitted in partial fulfillment
of the requirements for the degree of
Doctor of Philosophy
(Applied and Interdisciplinary Mathematics)
in the University of Michigan
2015

Doctoral Committee:

Assistant Professor Marisa C. Eisenberg, Co-Chair
Assistant Professor Rafael Meza, Co-Chair
Professor Charles R. Doering
Professor Trachette L. Jackson
Professor Kerby A. Shedden

ACKNOWLEDGEMENTS

This thesis would not exist if not for Drs. Rafael Meza and Marisa Eisenberg, who introduced me to the problem, supported me throughout, guided my growth as a mathematical modeler, and advised the writing of this document. You both have my deep gratitude.

I would like to thank my committee members, Drs. Charlie Doering, Tracy Jackson, and Kerby Shedden for their advice and direction in this project. I would like to thank the Department of Mathematics for their support, in particular Dr. Peter Miller for helping me prepare for my preliminary exams and Dr. Charlie Doering for advising me in my first years. I would also like to thank Drs. Bill Hazelton, Jihyoun Jeon, and Suresh Moolgavkar at the Fred Hutchinson Cancer Research Center for their help and guidance in the area of multistage clonal expansion models. In addition, I would like to thank Dr. Tom Carey for his input in my NHANES analysis.

Fianlly, I would not have been able to complete this thesis without financial support, for which I want to thank the Department of Mathematics, the University of Michigan MCubed program, and NIH grant 1U01CA182915-01A1 in particular.

PREFACE

A version of Chapter 3 will be submitted for publication with the following authors: Brouwer AF, Eisenberg MC, Carey TE, Meza R. A version of Chapter 4 will be submitted for publication with the following authors: Brouwer AF, Meza R, Eisenberg MC. A version of Chapter 5 will be submitted for publication with the following authors: Brouwer AF, Eisenberg MC, Meza R.

TABLE OF CONTENTS

LIST OF FIGURES

Figure

LIST OF TABLES

Table

CHAPTER I

Introduction

In 2013, the National Cancer Institute published its Annual Report to the Nation on the Status of Cancer, 1975–2009, highlighting the trends in the burden of human papillomavirus (HPV) associated cancers. Although total cancer incidence has recently declined, incidence of HPV-related oropharyngeal and anal cancers have increased (Chaturvedi et al., 2011; Jemal et al., 2013).

The human papillomavirus (HPV) infects multiple sites in the human epithelial layer, in particular the genitals, oral cavity, and anal canal, and is the etiological agent for over 90% of anogenital cancers and an increasing percentage of oropharyngeal cancers (Jemal et al., 2013). While the progression from cervical HPV infection to cervical cancer is well understood because of data from annual gynecological exams, very little is known about the progression to cancer in the head and neck. Further, the association between infection at different sites and their relation to seroconversion is not well characterized.

The National Health and Nutrition Examination Survey (NHANES), a United States-wide survey conducted by the Centers for Disease Control and Prevention (CDC), samples approximately 10,000 people in each biennial study. Begun in the 1960s and becoming continuously run in 1999, NHANES combines both interviews and physical examinations and is a major program within the National Center for Health Statistics. It is used to determine prevalence of and risk factors for major diseases as well as information about nutrition and basic biometrics (Centers for Disease

Control and Prevention, 2014b). The NHANES program, which first began including cervical HPV infection and serum antibodies in 2003 and oral HPV infection in 2009, offers an opportunity to assess not only associations between oral and genital HPV infection and seropositivity for certain genotypes, but HPV infection and seroprevalence trends as well. Most knowledge of the natural history of HPV comes from cohort and case-control studies, which, although relevant, cannot give information about patterns and trends at the population level. Additionally, although testing for HPV at cervical sites has been standard for some time, characterization of oral prevalence has only recently begun.

NHANES also provides key time-course data on disease prevalence at multiple sites that can serve as inputs for modeling HPV-related cancers whose dynamics depend on HPV transmission in the population. Thus, although direct analysis of NHANES is left primarily to Chapter III, the analysis of genital–oral concurrence informs the multisite infectious disease model developed in Chapter IV, and population-level HPV prevalence informs the cancer models of Chapters V and VI.

There are many strains of the human papillomavirus, and these are typically classified according to their oncogenic risk. Genotypes 16, 18, 26, 31, 33, 35, 39, 45, 51, 52, 53, 56, 58, 59, 66, 68, 73, 82 are considered to be high risk, that is have the potential to be oncogenic, and genotypes 6, 11, 40, 42, 54, 55, 61, 62, 64, 67, 69, 70, 71, 72, 81, 82 subtype IS39, 83, 84, 89 [CP6108] are low risk for oncogenesis but may cause other complications such as condylomas (genital warts) (Muñoz et al., 2003). (Classification into low- and high-risk types can very slightly between studies. This classification is consistent with Gillison et al. (2012a)). HPV infection is associated with nearly every cervical cancer, 90% of anal cancers, 60% of some subsites of head and neck cancers, and 40% of other genital cancers (Jemal et al., 2013). HPV 16, in particular, causes about 70% of genital cancers and together 16 and 18 are responsible for 90% (Jemal et al., 2013). HPV 6 and 11 cause 90% of anogenital warts (Jemal et al., 2013). HPV 16 is also found in 90% of HPV-positive squamous cell carcinomas (SCCs) in the head and neck (Gillison et al., 2012a).

Most HPV infections clear within a year or two (Ho and Bierman, 1998; Franco et al., 1999; Molano et al., 2003; Moscicki et al., 2012), but some infections may persist for decades and result in intraepithelial lesions and squamous cell carcinomas (IARC, 2007). HPV-positive cancers are associated with overexpression of the cyclin-dependent kinase inhibitor p16 relative to HPV-negative cancers and inhibition of two tumor-suppressors: gene product p53 and retinoblastoma protein pRb (IARC, 2007; Gillison et al., 2012a).

Vaccines have been developed to target certain strains of HPV. Two vaccines are currently approved by the FDA: GlaxoSmithKline Biologicals devolped the bivalent (16, 18) vaccine Cervarix®, and Merck makes the quadravalent (6, 11, 16, 18) vaccine Gardisil® (Kreimer, 2014). Merck's nonavalent (6, 11, 16, 18, 31, 33, 45, 52, 58) vaccine has been shown to be effective in trials (Joura et al., 2015). Vaccination against HPV is targeted at females ages 11–12 but is recommended in the United States for both men and women with minimal sexual activity under the age of 26. Australia, which has an aggressive vaccination campaign and a national health monitoring system, achieved a vaccination rate of 83% for one dose and 70% for all three doses among 12–17 year old females during 2007–2009 (Tabrizi et al., 2012). Vaccination of school-aged females and males has been routine there since 2009, and incidence of genital warts has decreased dramatically (Ali et al., 2013; Harrison et al., 2014). In contrast, vaccine coverage in the United States has been low, though increasing, especially among boys. Coverage for at least one dose (all three doses) in 2013 was 57.3% (37.6%) for girls and 34.6% (13.9%) for boys in the targeted age group (Centers for Disease Control and Prevention, 2014a). Markowitz et al. (2013) found that cervical HPV prevalence among women ages 14–19 decreased from 11.5% in 2003–2006 to 5.1% in 2007–10, a difference largely attributable to vaccination. Concerns that administering a vaccine for a sexually transmitted infection to young girls would give them license to be sexually active were recently refuted (Mayhew et al., 2014), and the President's Panel on Cancer called for urgent acceleration of vaccine uptake (Rimer et al., 2014). It remains to see what effect these developments will have on future vaccination coverage. Modeling may

provide a useful approach to predicting the effects of vaccination, and existing vaccination models are discussed in Chapter II.

Few studies have thus far considered multisite concurrence or type-concordance. Steinau et al. (2014) reported that, in the 2009–2010 NHANES survey, oral HPV infection was five-fold higher in women with a current genital infection, and that type-specific concordance was low. The Hawaii cohort study reported a relative risk of 20.5 for acquiring a type-concordant anal infection after a cervical infection and a relative risk of 8.8 for acquiring a type-concordant cervical infection after an anal infection (Goodman et al., 2010). Data from the HPV in Men (HIM) study have suggested that seroconversion in men differs by anatomical site for some genotypes, with anal infections more likely to result in seroconversion than genital infections (Lu et al., 2012). Modelers have similarly neglected consideration of multisite concurrence. Although multistrain models have been considered (e.g. van den Driessche and Watmough (2002)), including for HPV (e.g. Kim and Goldie (2008)), there has been no analysis of a dynamical systems multisite infection model. Thus, Chapters III and IV address these gaps in the literature through both epidemiological and mathematical approaches.

Like many sexually transmitted diseases, prevalence of HPV varies widely by demographic group in the United States, possibly due, in part, to sexual assortativity (Morris et al., 2009). Prevalence among non-Hispanic blacks, for instance, is significantly higher at both oral and genital sites of infection than for non-Hispanic whites and Hispanics. Further, prevalence varies significantly with age. However, no attempt has yet been made to disentangle the effects of age, birth cohort, and time period for trends in HPV prevalence. One way to differentiate these effects is by the use of age–period–cohort (APC) models developed by Holford (1983, 1991) and Clayton and Schifflers (1987a,b). APC models have been used for myriad public health issues, from infant and adult mortaility (Meza et al., 2010c), to smoking histories (Holford et al., 2014), to the incidence of colorectal (Luebeck and Moolgavkar, 2002), breast (Holford et al., 2006), esophageal and gastric (Jeon et al.,

2006), thyroid (Kilfoy et al., 2009), bone (Anfinsen et al., 2011), and oropharyngeal (Chaturvedi et al., 2013) cancer.

Analysis of HPV-related oral (oralpharyngeal and oral cavity) squamous cell carcinomas (OSCC) incidence in the Surveillance, Epidemiology, and End Results (SEER) cancer registries, have identified gender disparities but diminishing racial differences in the United States (Brown et al., 2011, 2012). Overall OSCC incidence rates for men are two to four times that of women across all races, though this varies slightly for the different cancer subsite groups (Brown et al., 2012). Racial differences between rates of OSCC in white and black women have largely disappeared. Although rates for black men have historically been higher than for white men, declining rates among black men have been met by a recent increase in incidence for white men (Brown et al., 2011). These results, however, only address overall temporal trends and neither distinguish between age, period, and birth cohort trends nor make implications about the underlying biological and epidemiological causes. Multistage clonal expansion (MSCE) models, a class of inhomogeneous, continuous time Markov models, capture the initiation–promotion–progression hypothesis of tumorigenesis, in which normal cells undergo a genetic transformation that leads to clonal expansion, followed by transformations that lead to malignancy (Moolgavkar and Venzon, 1979; Moolgavkar and Knudson, 1981; Luebeck and Moolgavkar, 2002; Meza et al., 2008). Using models that account for the natural history of cancers is important because the effects of carcinogens acting as initiators or promoters results in different temporal effects on the the age-specific incidence of cancer, which can be inferred from population level data (Heidenreich et al., 1997; Meza et al., 2008). MSCE models have been shown to capture temporal patterns of cancer risk and provide insight into the underlying mechanisms leading to population level cancer incidence patterns (Meza et al., 2008, 2010b; Luebeck and Moolgavkar, 2002; Luebeck et al., 2013). Chapter V uses an MSCE model coupled with an APC model to address incidence of oral squamous cell carcinomas.

One challenge of combining mathematical models of infectious diseases and cancer

is the inherently multiscale nature of the problem. Infectious disease dynamics play out at the population level, infection and disease progression occur at the individual level, and cancer incidence is of interest once more on the population scale. Working on multiple time scales is also challenging: disease transmission and clearance occurs on scales of a year or less, but a decade or more may pass between the infection and the detection of the cancer. These challenge must be addressed if we are to quantify the risk for oropharyngeal cancer associated with HPV infection and to model the impact of interventions (e.g. vaccination) targeting HPV on incidence of HPV-related oropharyngeal cancer. Chapter VI takes steps in this direction by introducing MSCE models with infection-related initiation pathways.

This dissertation is organized in seven chapters. Chapter II explores the mathematical background of infectious disease, age–period–cohort, and multistage clonal expansion models, including the relevant literature, and presents new exposition and several minor results that will be expanded on in later chapters. Chapter III presents a statistical analysis of data in NHANES. We consider HPV prevalence at oral and genital sites and prevalence of HPV antibodies in serum, with special attention to concurrent infection and genotype-concordant infection. Age–period–cohort models are leveraged to describe cohort trends in genital HPV-prevalence and in seroprevalence. Chapter IV introduces a multisite model of HPV or other multisite infectious disease and presents derivations of the form and properties of the basic reproductive number under a variety of assumptions and limiting cases. Autoinoculation and the effects of heterogeneity in the same-site and cross-site transmission pathways are considered. Chapter V presents an analysis of the incidence of oral squamous cell carcinomas reported in the SEER cancer registries, considering HPV-related, HPV-unrelated except oral tongue, and HPV-unrelated oral tongue anatomical subsite groups. Multistage clonal expansion models are combined with age–period–cohort models to assess not only temporal trends in the data but also aspects of the underlying tumor biology. Chapter VI explores two extensions of the two-stage clonal expansion model that incorporate HPV prevalence as an age-dependent driver of initiation. I derive the equations under the assumption that i)

HPV-related and HPV-unrelated cancers have the same promotion and malignant conversion rates and ii) that they differ. Structural identifiability of each model is considered. Chapter VII contains the final remarks and conclusions.

CHAPTER II

Background and Minor Results

2.1 Infectious disease models

Infectious diseases have been effectively modeled with a dynamical systems approach, the heart of which is the SIR—susceptible, infectious, recovered—model. The SIR model assumes susceptible people come into contact with infectious people at rate β and recover at a rate γ. Typically, the birth and death rates μ are assumed to be the same, which keeps the population size is constant. The equations of the basic SIR model (Kermack and McKendrick, 1927) are

$$\begin{aligned} \dot{S} &= \mu - \beta SI - \mu S, \\ \dot{I} &= \beta SI - \gamma I - \mu I, \\ \dot{R} &= \gamma I - \mu R, \end{aligned} \tag{2.1}$$

where S is the fraction of the population that is susceptible to infection, I the fraction that is infectious, and R the fraction that have recovered. Many variations of the basic SIR model exist: models without immunity or with waning immunity, with vaccination, with a presymptomatic lag period, with seasonal forcing, with stratification by risk group or demographics, etc. (Anderson and May, 1991; Hethcote, 2000; Diekmann and Heesterbeek, 2000; Keeling and Rohani, 2008).

Infectious disease dynamical systems models can easily be translated into a stochas-

tic simulation framework by means of the Gillespie algorithm (Doob, 1942, 1945; Gillespie, 1976, 1977) or extended to incorporate heterogeneity and stochasticity of social structure and mixing by embedding the process withing a sexual network model or an agent-based simulation framework (e.g. Bartlett (1953), Newman (2002), Eubank et al. (2004), Meyers et al. (2006),Morris et al. (2009), Perez and Dragicevic (2009), Conway et al. (2011),Valente (2012)).

2.1.1 Basic reproduction number

The *basic reproduction number* R_0, also called the *basic reproductive ratio*, is an important quantity in infectious disease systems epidemiology, defined as the average number of secondary cases arising from an typical primary case in an entirely susceptible population (Diekmann et al., 1990; Anderson and May, 1991; Diekmann and Heesterbeek, 2000). The basic reproduction number acts as a threshold value that controls the local stability of the disease-free equilibrium: if $R_0 < 1$, the disease will die off quickly, while if $R_0 > 1$, the disease will become epidemic (Diekmann and Heesterbeek, 2000; van den Driessche and Watmough, 2002). The values of R_0 vary greatly by disease (Anderson and May, 1991), ranging from close to 1 for seasonal influenza to 5–7 for smallpox and polio to 12–18 for measles and pertussis, but are also dependent on some attributes of the population. Mathematical modeling is often used to estimate the basic reproductive ratio and other relevant quantities. In practice, R_0 is calculated as a threshold parameter that may not precisely correspond to the number of secondary cases per infection, especially in the case of an environmentally transmitted infections (van den Driessche and Watmough, 2002). The basic reproduction number is widely considered the most useful contribution of mathematics to epidemiology (Heesterbeek and Dietz, 1996).

In the basic SIR system, the basic reproduction number is given by the ratio of the transmission rate to the recovery rate β/γ (Keeling and Rohani, 2008). Several methods exist for calculating R_0 in more complex systems. One of the most commonly used approaches, the Next Generation Method, is described in detail

elsewhere (Diekmann et al., 1990; van den Driessche and Watmough, 2002; Diekmann et al., 2010), though we give a brief formulation here. Denote the vector of states by x and the disease free equilibrium by x_0. For each infected compartment i, let $\mathcal{F}_i(x)$ be the rate at which previously uninfected people enter compartment i. Let $\mathcal{V}_i(x)$ be the rate of transfer of individuals out of compartment i minus the rate of transfer into compartment i. Then

$$\frac{dx_i}{dt} = \mathcal{F}_i(x) - \mathcal{V}_i(x). \tag{2.2}$$

Denote by F and V the matrices whose entries are

$$F_{ij} = \frac{\partial \mathcal{F}_i(x)}{\partial_{x_j}}\Big|_{x=x_0}, \tag{2.3}$$

$$V_{ij} = \frac{\partial \mathcal{V}_i(x)}{\partial_{x_j}}\Big|_{x=x_0}. \tag{2.4}$$

The matrix FV^{-1} is called the next generation matrix.

> To interpret the entries of FV^{-1} and develop a meaningful definition of R_0, consider the fate of an infected individual introduced into compartment k of a disease free population. The (j,k) entry of V^{-1} is the average length of time this individual spends in compartment j during its lifetime, assuming that the population remains near the DFE and barring reinfection. The (i,j) entry of F is the rate at which infected individuals in compartment j produce new infections in compartment i. Hence, the (i,k) entry of the product FV^{-1} is the expected number of new infections in compartment i produced by the infected individual originally introduced into compartment k. (van den Driessche and Watmough, 2002)

Then, R_0 is defined to be the spectral radius of the matrix FV^{-1} (Diekmann et al., 1990), and, under certain assumptions trivially satisfied for realistic infectious disease models, the disease free equilibrium is locally asymptotically stable if $R_0 < 1$

and unstable if $R_0 > 1$ (van den Driessche and Watmough, 2002). An equivalent method to finding R_0 is solving to the polynomial equation $\det(Fx - V) = 0$ (De-Camino-Beck et al., 2009).

The basic reproduction number also has implications for infection control. If a fraction of the population greater than $1 - \frac{1}{R_0}$ is permanently protected from infection (e.g. through immunization), the infection cannot become epidemic (Roberts and Heesterbeek, 2003). The concept of the basic reproductive number, at least in these infection control terms, can be extended to examine infection control in populations with multiple subgroups using the type and target reproductive numbers, which provide R_0-like threshold quantities under the assumption that only a specific population group or transmission pathway is being controlled. Suppose that there are n host types. Let $K = FV^{-1}$ be the next generation matrix, and P_i the projection matrix with $P_{ii} = 1$ and all other entries 0. Then, if $\rho((I - P_i)K) < 0$, that is, if the other host groups are not self-sustaining disease reservoirs, the infection can be controlled by protecting a greater fraction than $1 - \frac{1}{T_i}$ of host type i, where

$$T_i = e_i' K(I - (I - P_i)K)^{-1} e_i \tag{2.5}$$

is called the type reproduction number for host type i. It is known that $T_i > 1$ if and only if $R_0 > 1$ (Roberts and Heesterbeek, 2003). If $\rho((I - P_i)K) \geq 1$, then another host type acts as a reservoir for infection, the infection cannot be controlled only through intervention on host type i, and T_i is not defined. If several host types are to be controlled simultaneously, the target reproduction number is defined as

$$M_\ell = E_\ell' K(I - (I - P_\ell)K)^{-1} E_\ell, \tag{2.6}$$

where $(E_\ell)_{ii} = (P_\ell)_{ii} = 1$ for $i \in \ell$ and 0 otherwise (Roberts and Heesterbeek, 2003). The type reproduction number is especially of interest for vector-borne and other multiple-species infections. The target reproduction number may be further generalized to consider individual entries of the next generation matrix, not just

whole rows. For any matrix A such that $A_{ij} = K_{ij}$ or 0, then the target reproduction number for the nonzero entries of A is

$$T_A = \rho(A((I - (K - A))^{-1}). \tag{2.7}$$

The target reproduction number has the same properties as the type reproduction number (Shuai et al., 2013).

2.2 Identifiability

When estimating model parameters from data, a key consideration is model identifiability. A model is said to be *identifiable* if the model parameters may be uniquely determined from the observed data (Bellman and Åström, 1970; Rotherberg, 1971; Cobelli and DiStefano, 1980). Identifiability is a key step in ensuring successful parameter estimation and is often considered in two forms: structural identifiability, which considers a best-case scenario in which the data is noise-free and continuously measured in order to uncover identifiability issues inherent in the model structure, and practical identifiability, which addresses issues such as noise, bias, and frequency of sampling (Raue et al., 2009). While the best-case scenario is unrealistic, structural identifiability is necessary for practical identifiability and can often lead to useful insights for model reparameterization and data collection strategies for ODE models. Structural identifiability for dynamical systems is defined as follows. Consider a vector of states $x(t)$ (unobserved), vector of parameters μ, and observable input and output $u(t)$ and $v(t)$ in the ODE model

$$\begin{aligned} x'(t) &= f(x(t), u(t), \mu), \\ v(t) &= g(x(t), \mu). \end{aligned} \tag{2.8}$$

The above model is identifiable if μ may be uniquely recovered by $u(t)$ and $v(t)$ (Bellman and Åström, 1970). Equivalently, one often frames the identifiability problem

as testing the injectivity of the map from the parameters to the output trajectories (implicitly defined by the ODE system and output equation above) (Saccomani et al., 2001). There are a wide range of approaches to answering questions of identifiability, including Laplace transformation, Taylor series, similarity transformation, and differential algebra (Cobelli and DiStefano, 1980; Vajda et al., 1989; Chappell et al., 1990; Evans and Chappell, 2000; Saccomani et al., 2001; Audoly et al., 2001; Meshkat et al., 2009; Raue et al., 2014). Identifiability of models in mathematical biology are commonly considered, but the issue appears in a wide range of statistical and mathematical contexts, including in infectious disease (Eisenberg et al., 2013), age–period-cohort (Holford, 1991), cancer (Heidenreich et al., 1997; Little et al., 2009), and other models.

If a model is not structurally identifiable, there exist identifiable combinations of parameters that represent the parametric information possible to extract from the data. These combinations can provide structure for other aspects of the model, determine what additional data or constraints would render the model identifiable, and generate identifiable reparameterizations of the model (Cobelli and DiStefano, 1980). It is important to remember that identifiability is a data dependent concept. Identifiability analysis seeks to find combinations of parameters that can be estimated from some given data (input and output). If additional data becomes available later on, an unidentifiable model can become identifiable.

To assess identifiability of certain models in this dissertation, I will use a differential algebra approach, which is a method for evaluating the structural identifiability of rational-function differential equation models. This method is built on the idea of treating the differential equations as elements of a differential polynomial ring, that is, a polynomial ring in the variables and their derivatives, with an additional derivative operation. Once framed in this algebraic perspective, reduction techniques such as characteristic sets or Gröebner bases can be used to reduce the model to a form in which the identifiability properties can be determined, called the input–output equations. Like many structural methods, the differential algebra ap-

proach yields identifiability results globally for the whole parameter space; however because there may be specific or degenerate parameter sets and initial conditions at which the results break down (e.g. if all parameters or initial conditions are zero), structural identifiability is defined for almost all parameter values and initial conditions. Technical details of the differential algebra approach to identifiability may be found in Saccomani et al. (2001) and Eisenberg (2013), and additional information on the subject of differential algebra may be found in Ritt (1950).

To illustrate the differentiable algebra approach using input–output equations, we borrow an example from Eisenberg (2013). Consider the following linear model with two compartments of drug uptake in an organ:

$$\begin{aligned} \dot{x}_1 &= u(t) + k_{12}x_2 - (k_{01} + k_{21})x_1, \\ \dot{x}_2 &= k_{21}x_1 - (k_{02} + k_{12})x_2, \\ y &= x_1/V. \end{aligned} \tag{2.9}$$

Here, $x_1(t)$ is the mass of drug in the blood, $x_2(t)$ is the mass of drug in an organ. The mass of drug administered $u(t)$ and concentration of the drug in the blood $y(t)$ are known. The drug decays in the blood and organ at rates k_{01} and k_{02} respectively. The rate of transfer from blood to organ and from organ to blood are k_{21} and k_{12} respectively. To determine whether this system is structurally identifiable, we find the input–output equation for this system, that is, a monic, polynomial representation of the system in terms of u and y (and their derivatives) only. We eliminate the unmeasured variables as follows:

$$\begin{aligned} \dot{y}V &= u(t) + k_{12}x_2 - (k_{01} + k_{21})yV, \\ \dot{x}_2 &= k_{21}x_1 - (k_{02} + k_{12})x_2, \end{aligned} \tag{2.10}$$

$$\begin{aligned} x_2 &= \frac{1}{k_{12}}\left(-u(t) + k_{01}Vy + k_{21}Vy + V\dot{y}\right), \\ \dot{x}_2 &= k_{21}x_1 - (k_{02} + k_{12})x_2, \end{aligned} \tag{2.11}$$

$$0 = k_{12}k_{21}Vy + (k_{02} + k_{12})(u(t) - V(k_{01} + k_{21})y + V\dot{y}) + \dot{u}(t) - V(k_{01} + k_{21})\dot{y} + V\ddot{y}, \tag{2.12}$$

$$0 = \ddot{y} + (k_{01} + k_{02} + k_{12} + k_{21})\dot{y} + (k_{01}k_{02} + k_{01}k_{12} + k_{02}k_{21})y - \frac{1}{V}\dot{u}(t) - \frac{k_{02} + k_{12}}{V}u(t). \tag{2.13}$$

We see that eq. 2.13 is a monic, polynomial equation of y, u, and the parameters and is thus an input–output equation for the model (eq. 2.9). The coefficients of the input–output equation are identifiable combinations and represent the complete set of structural identifiable information for the model and data. The underlying idea for input–output equations is that testing injectivity of the map from the parameters to the outputs can be reduced to testing injectivity of the map from the parameters to the input–output coefficients. (Eisenberg, 2013). From the coefficients, we see that V, $k_{01} + k_{21}$, $k_{02} + k_{12}$, and $k_{21}k_{12}$ are identifiable. This result suggests a reparameterization $x_3 = k_{12}x_2$, which gives the model in terms of the identifiable combinations only:

$$\begin{aligned} \dot{x}_1 &= u(t) + x_3 - (k_{01} + k_{21})x_1, \\ \dot{x}_3 &= (k_{12}k_{21})x_1 - (k_{02} + k_{12})x_3, \\ y &= x_1/V, \end{aligned} \tag{2.14}$$

with estimated parameters $p_1 = V$, $p_2 = k_{01} + k_{21}$, $p_3 = k_{12}k_{21}$, and $p_4 = k_{02} + k_{12}$.

2.3 Age–period–cohort models

Age–period–cohort (APC) models are a class of epidemiologic models used to disentangle effects of age, period (factors affecting all people at a given time), and birth cohort (factors affecting all people born in a given time period) given prevalence (e.g. HPV prevalence) or incidence (e.g. incidence of oral cancer). APC models are a form of generalized linear regression developed by Holford (1983, 1991) and Clay-

ton and Schifflers (1987a,b). The traditional model posits that incidence rates λ are described by a multiplicative model with age (A), period (P), and birth cohort (C). This is usually treated in the logarithmic form, in which we fit the following generalized linear model (using Poisson family and log link function).

$$\log \lambda = \beta_0 + \beta_A(A) + \beta_P(P) + \beta_C(C), \tag{2.15}$$

where β_0 is a constant and β_A, β_P, and β_C are some functions, often chosen to be splines or discrete functions.

Given an incidence I and at-risk population N, it is straightforward to model $\lambda = I/N$. If, alternatively, one wishes to model prevalence (P), one may convert as follows (Holford et al., 2014).

$$\log \lambda = \log \frac{I}{N} = \log \frac{\frac{I}{I+N}}{\frac{N}{I+N}} = \log \frac{P}{1-P} = \text{logit } P. \tag{2.16}$$

This allows us to use a generalized linear model with binomial family and logit link function. We then model

$$\text{logit } P = \beta_0 + \beta_a(a) + \beta_p(p) + \beta_c(c). \tag{2.17}$$

One drawback of full APC models is their inherent unidentifiability: $P = A + C$. To resolve the unidentifiability, one may consider only two effect models, typically age–period or age–cohort, or constrain the age effects to have a given shape, such as a hazard function (Holford, 1991; Luebeck and Moolgavkar, 2002; Meza et al., 2008; Luebeck et al., 2013). Alternatively, one can introduce an additional assumption, such as equating two effects (e.g. two adjacent period effects) or making the mean of successive differences zero (i.e. equating the first and last effect); unfortunately, there "generally is not a sound basis" for making such assumptions (Holford, 1991).

Given a set of observed cases $\{x_i\}$ with corresponding population-at-risk sizes $\{n_i\}$,

we may derive a likelihood for the APC model in the following way. We assume that observed incident cases x_i for a given population all of age A_i at time P_i from birth cohort $C_i = P_i - A_i$ are Poisson distributed with mean $\mu_i = n_i \cdot \lambda(A_i, P_i, C_i)$, where λ is the incident rate function dependent on parameter β_0 and functions β_A, β_P, and β_C. Observations are assumed to be independent, and thus the likelihood for the whole data set of observations $\{x_i\}$ is given by

$$L(\beta_0, \beta_A, \beta_P, \beta_C) = \prod_i \frac{e^{-\mu_i} \mu_i^{x_i}}{x_i!}. \tag{2.18}$$

2.4 Cancer models

Many models of carcinogenesis have been developed using a variety of techniques and with different goals. Here, we work toward multistage clonal expansion (MSCE) models, beginning with Armitage–Doll model of carcinogenesis. Before investigating model development, however, we present a few preliminary definitions.

2.4.1 Preliminaries: survival and hazard

Let X be the random variable giving the time of malignant transformation or, more generally, of a failure event. We define the *survival* function to be the probability that failure has not occured by time x, namely

$$S(x) = P[X > x]. \tag{2.19}$$

The standard measure of cancer risk is the *hazard* function, $h(x)$, also known in this context as the age-specific cancer incidence function. The hazard is defined as the instantaneous rate of change of failure probability:

$$h(x) = \lim_{\Delta x \to 0} \frac{P[x < X < x + \Delta x | X > x]}{\Delta x}. \tag{2.20}$$

We can also write the hazard in terms of the survival function.

$$\begin{aligned} h(x) &= \lim_{\Delta x \to 0} \frac{P[x < X < x + \Delta x | X > x]}{\Delta x} \\ &= \lim_{\Delta x \to 0} \frac{P[x < X < x + \Delta x]}{\Delta x \cdot P[X > x]} \\ &= \lim_{\Delta x \to 0} \frac{S(x) - S(x + \Delta x)}{\Delta x \cdot S(x)} \\ &= -\frac{S'(x)}{S(x)} \\ &= -\frac{d}{dx} \ln S(x) \end{aligned} \tag{2.21}$$

We will seek to find the hazard and survival functions for several models of carcinogenesis. Since the hazard is a representation of incidence (or mortality), the hazard can connect theory with data, allowing model verification and parameter estimation (Moolgavkar and Knudson, 1981; Luebeck and Moolgavkar, 1991; Heidenreich et al., 1997; Luebeck and Moolgavkar, 2002; Meza et al., 2008). Similarly to the ODE models discussed previously, considerations of parameter identifiability given the survival and hazard are also given.

2.4.2 The Armitage–Doll model

The first mechanistic models of cancer were developed by Armitage and Doll (1954) and Nordling (1953, 1954) to describe cancer as an accumulation of genetic transformations. The mathematical formulation is as follows. Suppose n sequential genetic transformations must accrue in a cell, or its progeny, before it becomes malignant. We say that a cell is in stage E_k after k transformations. Each transformation occurs in order and after a time exponentially distributed with rate λ_k. The process is illustrated in a schematic in Figure 2.1.

Let $Z(t)$ be the number of genetic transformations the cell has undergone by time t, and let

$$p_k(t) = P[Z(t) = k], \tag{2.22}$$

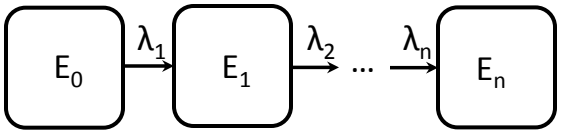

Figure 2.1: Schematic of the Armitage–Doll model of carcinogenesis

be the probability that the cell is in state E_k (i.e. has k genetic transformations) at time t. Because the rates are exponentially distributed, this system is Markov and may be analyzed in the context of stochastic processes. The Armitage–Doll process is in fact a birth process, a kind of continuous-time Markov chain. Define the following quantities for a homogeneous continuous-time Markov process:

$$P_{ij}(t) = P[Z(t+u) = j | Z(u) = i], \tag{2.23}$$

$$\nu_i = \lim_{t \to 0} \frac{1 - P_{ii}}{t}, \tag{2.24}$$

$$q_{ij} = \lim_{t \to 0} \frac{P_{ij}}{t}. \tag{2.25}$$

The transition probabilities $P_{ij}(t)$ are homogeneous, that is, they do not depend on u. In particular,

$$P_{ij}(t) = P[Z(t+u) = j | Z(u) = i] = P[Z(t) = j | Z(0) = i]. \tag{2.26}$$

We will develop the theory of inhomogeneous continuous-time Markov chains in a later section. Here, we also have

$$q_{ij} = \nu_i P_{ij}. \tag{2.27}$$

For our Armitage–Doll notation, $p_k(t) = P_{0k}(t)$, $\nu_k = \lambda_{k+1}$ for $k \in \{0, \ldots, n-1\}$ and 0 otherwise, and $q_{kj} = \lambda_k$ if $j = k+1$ and 0 otherwise. By the Markov property of

the process, we have the following infinitesimal transition probabilities:

$$P_{ij}(h) = hq_{ij} + o(h), \tag{2.28}$$

$$P_{ii}(h) = 1 - h\nu_i + o(h). \tag{2.29}$$

The Chapman–Kolmogorov equations give us that, for any t and h,

$$P_{ij}(t+h) = \sum_{k=0}^{n} P_{ik}(t)P_{kj}(h). \tag{2.30}$$

Subtracting $P_{ij}(t)$, dividing by h, and taking the limit as $h \to 0$, we arrive at the Kolmogorov forward equations:

$$\frac{d}{dt}P_{ij}(t) = \sum_{k\neq i} q_{kj}P_{ik}(t) - \nu_j P_{ij}(t). \tag{2.31}$$

[Note: the same operations on the equation $P_{ij}(t+h) = \sum_{k=0}^{n} P_{ik}(h)P_{kj}(t)$ would give the Kolmogorov backward equations $\frac{d}{dt}P_{ij}(t) = \sum_{k\neq i} q_{ik}P_{kj}(t) - \nu_i P_{ij}(t)$].

For the Armitage–Doll model, the Kolmogorov forward equations of interest are

$$\begin{aligned}
\frac{dp_0}{dt} &= -\lambda_1 p_0(t), \\
\frac{dp_1}{dt} &= \lambda_1 p_0(t) - \lambda_2 p_1(t), \\
&\vdots \\
\frac{dp_k}{dt} &= \lambda_k p_{k-1}(t) - \lambda_{k+1} p_k(t), \\
&\vdots \\
\frac{dp_{n-1}}{dt} &= \lambda_{n-1} p_{k-2}(t) - \lambda_n p_{n-1}(t), \\
\frac{dp_n}{dt} &= \lambda_n p_{n-1}(t).
\end{aligned} \tag{2.32}$$

This system may be written in matrix form, $\frac{d}{dt}P = P(t)Q$, and solved using matrix exponentials, $P(t) = e^{Qt}$. The survival function for one cell is $S(t) = 1 - p_n(t)$.

Suppose a person begins with N normal cells, and let $T_1, \ldots, T_N$ be the random times to malignant conversion for each cell. The time of first conversion is $T = \min\{T_1, \ldots, T_N\}$ and, assuming independence, we have the survival function

$$\begin{aligned} S(t) &= P[t < T], \\ &= P[t < \min\{T_1, \ldots, T_N\}], \\ &= (1 - p_n(t))^N. \end{aligned} \tag{2.33}$$

The hazard function can be shown under this formulation to be

$$h(t) = \frac{N p_n'(t)}{1 - p_n(t)}. \tag{2.34}$$

If we assume the probability of malignant conversion is small, $p_n(t) \approx 0$, we may make a Taylor series approximation of the hazard:

$$\begin{aligned} h(t) &\approx \frac{N \lambda_1 \ldots \lambda_n t^{n-1}}{(n-1)!}, \\ \log h(t) &\approx \log \frac{N \lambda_1 \ldots \lambda_n}{(n-1)!} + (n-1) \log t. \end{aligned} \tag{2.35}$$

This model predicts that cancer rates should be linear with age on a log–log scale. The slope of the relationship is one less than the number of genetic transformations necessary for malignant conversion. Armitage and Doll (1954) demonstrated that this framework explained death rates for certain cancers (e.g. colon and rectal cancers) quite well, though it did not fully match for others (e.g. lung, bladder, prostate).

The approximation $p_n(t) \approx 0$ does not hold asymptotically, and thus the Armitage–Doll linear hazard should not be used for very large ages.

2.4.3 Technical interlude: Markov branching processes

Before deriving the multistage clonal expansion model, we need to develop some theory for Markov branching processes, a kind of non-homogeneous continuous time Markov chain $Z(t)$, which we adapt from Harris (1963). The first part of this section concerns non-homogeneous continuous time Markov chains in general. The transition probabilities are defined as

$$P_{ij}(\tau, t) = P[Z(t) = j | Z(\tau) = i]. \tag{2.36}$$

Because the process is not homogeneous, $P[Z(t) = j|Z(\tau) = i]$ is not necessarily equal to $P[Z(t - \tau) = j|Z(0) = i]$. We do allow $Z(t)$ to be multistate. If $Z(t) = (Z_1(t), \ldots, Z_n(t))$, let $i = (i_1, \ldots, i_n)$ and $j = (j_1, \ldots, j_n)$ and define

$$P_{ij}(\tau, t) = P[Z_1(t) = j_1, \ldots, Z_n(t) = j_n | Z_1(\tau) = i_1, \ldots, Z_n(\tau) = i_n]. \tag{2.37}$$

Given $Z(t) = i$, the probability of a change in state in the interval $(t, t + h)$ is $\nu_i(t)h + o(h)$, and the probability that the change is to state j is denoted $p_{ij}(t)$. We do not allow $j = i$ (e.g. simultaneous birth and death) as this is treated as though no change in state has occurred. We have $\sum_j p_{ij}(t) = 1$. We use the notation $q_{ij}(t) = \nu_i(t)p_{ij}(t)$ to make the connection to the homogeneous theory clearer.

Since the process is Markov, we may use the Chapman-Kolmogorov equations, which, in this formulation are, for $0 \leq \tau \leq t$,

$$P_{ij}(\tau, t + h) = \sum_{k=0}^{\infty} P_{ik}(\tau, t) P_{kj}(t, t + h). \tag{2.38}$$

Then, the forward equation Kolmogorov differential equations (with initial condi-

tions $P_{ik}(\tau,\tau)=\delta_{ik}$) are

$$\frac{\partial P_{ij}}{\partial t}(\tau,t)=-\nu_j(t)P_{ij}(\tau,t)+\sum_{k\neq j}P_{ik}(\tau,t)q_{kj}(t). \tag{2.39}$$

and the backward equations (with initial conditions $P_{ik}(t-0,t)=\delta_{ik}$) are

$$\frac{\partial P_{ik}}{\partial \tau}(\tau,t)=\nu_i(\tau)P_{ik}(\tau,t)-\sum_{k\neq j}q_{ik}(\tau)P_{kj}(\tau,t). \tag{2.40}$$

Note the differences in the form of the backward equation between the homogeneous and inhomogeenous forms which arise because, in the homogeneous backward equation, increasing t increases the length of the time interval but, in the inhomogeneous equation, increasing τ decreases the length of the interval.

The rest of this theory, we develop for branching processes only and not inhomogeneous chains in general. We define a Markov branching process as follows. Let $Z(t)$ be the number of independent objects at time t. Suppose that an object existing at time t has a chance $\nu(t)h+o(h)$ of dying in an interval $(t,t+h)$. Consequently, the probability density of life length ℓ of an object born at time τ is $\nu(\tau+\ell)e^{-\int_\tau^{\tau+\ell}\nu(x)\,dx}$, which is exponential if $\nu(t)$ is constant. If the object dies at time t, suppose it is replaced with j objects with probability $p_j(t)$ for $j\neq 1$. Together $\nu(t)$ and $\{p_j(t)\}$ define a continuous time Markov process: because the objects are independent, $\nu_i(t)$ in the notation of the continuous time Markov chain is $i\nu(t)$ in the notation of the branching process, and $p_{ij}(t)=p_{j-i+1}(t)$. Then, the forward and backward Kolmogorov equations are

$$\frac{\partial P_{ij}}{\partial t}(\tau,t)=-j\nu(t)P_{ij}(\tau,t)+\nu(t)\sum_{k\neq j}P_{ik}(\tau,t)kp_{k-j+1}(t), \tag{2.41}$$

$$\frac{\partial P_{ik}}{\partial \tau}(\tau,t)=i\nu(\tau)P_{ik}(\tau,t)-\nu(t)\sum_{k\neq j}ip_{k-i+1}(\tau)P_{kj}(\tau,t). \tag{2.42}$$

A Markov branching process is defined to be a Markov chain that satisfies these

forward equations. The backward equations will then automatically be fulfilled.

We now introduce two generating functions. For $|s| \leq 1$,

$$\eta(s,t) = \sum_{k=0}^{\infty} p_k(t) s^k, \tag{2.43}$$

$$F_i(s,\tau,t) = \sum_{k=0}^{\infty} P_{ik}(\tau,t) s^k. \tag{2.44}$$

Then η is the generating function for the number of objects that replace one object after its death and F_i is the generating function of the probability that $Z(t) = k$ when $Z(\tau) = i$ for $\tau \leq t$. Multiplying the forward equation by s^k and summing over k, we get , for $i \geq 0$ and with initial condition $F_i(s,\tau,\tau+0) = s^i$,

$$\frac{\partial F_i}{\partial t}(s,\tau,t) = \nu(t)\left[\eta(s,t) - s\right] \frac{\partial F_i}{\partial s}(s,\tau,t). \tag{2.45}$$

The generating function satisfies $F_i = (F_1)^i$. From this relation, the backward equations give, for $t > 0$ and $F_1(s,t-0,t) = s$,

$$\frac{\partial F_1}{\partial \tau}(s,\tau,t) = -\nu(t)\left[\eta(F_1,\tau) - F_1\right]. \tag{2.46}$$

We will be interested in using the multistate form of the Markov branching process. Suppose there are k different types of objects, and that an object of type i that exists at time t has a chance $\nu_i(t)h + o(h)$ of being transformed in the interval $(t, t+h)$ for any $h > 0$. Let $\eta_i(s_1,\ldots,s_k,t)$ be the generating function for numbers of objects born in the different states after the transformation. Let $\Phi_i(s_1,\ldots,s_k,t)$ be the generating function for the numbers of different objects at time t if there is one object of type

i at time $\tau \leq t$. That is

$$\begin{aligned}\Phi_i(s_1, \ldots, s_k, \tau, t) &= \sum_{(j_1,\ldots,j_k)} P[N_\ell(t) = j_\ell \; \forall \ell | N_i(\tau) = 1, N_\ell(\tau) = 0 \; \forall \ell \neq i] s_1^{j_1} \cdots s_k^{j_k}, \\ &= E[s_1^{N_1(t)} \cdots s_k^{N_k(t)} | N_i(\tau) = 1, N_\ell(\tau) = 0 \; \forall \ell \neq i].\end{aligned} \tag{2.47}$$

Then, we have the following forward and backward equations for $\tau \leq t$ with $\Phi_i(s_1, \ldots, s_k, \tau, \tau + 0) = \Phi_i(s_1, \ldots, s_k, t - 0, t) = s_i$:

$$\frac{\partial \Phi_i}{\partial t} = \sum_{j=1}^{k} \nu_j(t) \left[\eta_j(s_1, \ldots, s_k, t) - s_j\right] \frac{\partial \Phi_i}{\partial s_j} \tag{2.48}$$

$$\frac{\partial \Phi_i}{\partial \tau} = -\nu_i(t) \left[\eta_i(\Phi_1, \ldots, \Phi_k, \tau) - \Phi_i\right] \tag{2.49}$$

Derivation of the backward equation requires the following fact, which can be derived from the forward equation:

$$\begin{aligned}&E\left[s_1^{N_1(t)} \cdots s_k^{N_k(t)} \middle| \forall_i \; N_i(\tau) = j_i\right] \\ &\qquad = \prod_{i=1}^{k} E\left[s_1^{N_1(t)} \cdots s_k^{N_k(t)} \middle| N_i(\tau) = 1, \; \forall \ell \neq i \; N_\ell(\tau) = 0\right]^{j_i}.\end{aligned} \tag{2.50}$$

It is these differential equations for the generating functions Φ_i that we will use for the multistage clonal expansion models.

2.4.4 Multistage clonal expansion models

From the Armitage–Doll model, cancer models evolved over the years, notably Armitage and Doll (1957), Fisher (1958), Kendall (1960), Neyman and Scott (1967), Whittemore and Keller (1978), before the two-stage clonal expansion model was proposed by Moolgavkar, Venzon, and Knudson (Moolgavkar and Venzon, 1979; Moolgavkar and Knudson, 1981). This Markov model captures the initiation–promo-

tion–progression hypothesis, in which normal cells undergo a genetic transformation that causes clonal expansion, followed by progression to malignancy. The initiation–promotion–progression paradigm is important because carcinogenic factors may be understood as initiators or promoters given their mechanism of action and result in different effects at different stages of life.

2.4.4.1 Two-stage clonal expansion model: Forward derivation

Moolgavkar, Venzon, and Knudson (Moolgavkar and Venzon, 1979; Moolgavkar and Knudson, 1981) described a non-homogeneous Poisson process followed by a Markov branching process. Although we could formulate the problem as fully stochastic, it is generally accepted to treat the growth of normal cells deterministically (Crump et al., 2005).

We formulate the model as follows. Let $X(t)$ be the number of normal cells at time t, $Y(t)$ the number of initiated cells (also called a intermediate cell, an initiated cell is one that has, through a genetic mutation, begun to expand clonally to form a tumor but is not yet malignant), and $Z(t)$ the number of malignant cells. We assume $Y(0) = Z(0) = 0$. Initiation is a inhomogeneous Poisson process with intensity $\mu_0(t)X(t)$, that is, it is a Poisson Process with expectation $\int_0^t \mu_0(s)X(s)\,ds$. We treat $(Y(t), Z(t))$ as a two-state Markov branching process. Initiated cells divide clonally at rate $\alpha(t)$ and die at rate $\beta(t)$. Progression (division of an initiated cell into one initiated and one malignant cell) occurs at rate $\mu_1(t)$. A schematic of the model is shown in Figure 2.2.

Let

$$P_{(j,k)} = P[Y(t) = j, Z(y) = k | Y(0) = 0, Z(0) = 0]. \tag{2.51}$$

Then, the probability generating function for the numbers of initiated and malig-

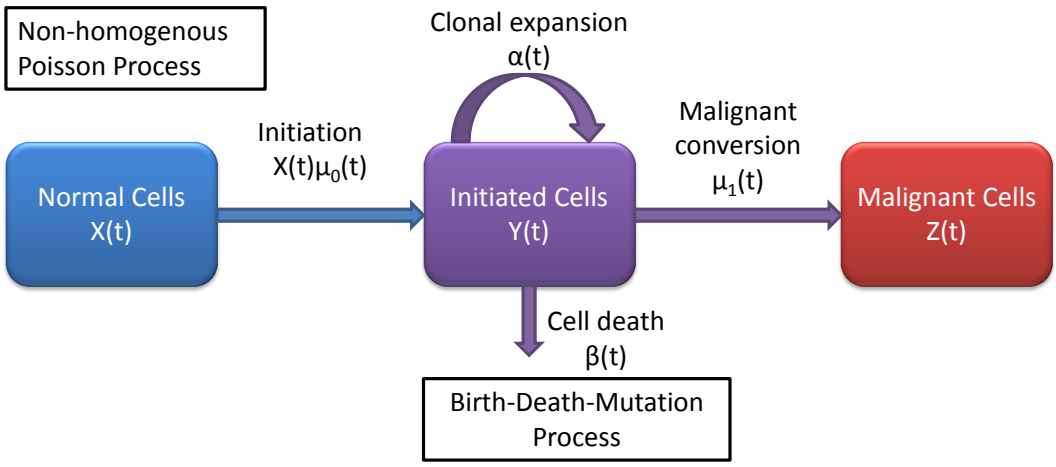

Figure 2.2: Schematic of the two-stage clonal expansion model

nant cells is

$$\begin{aligned}\Psi(y,z,t) &= E\left[y^{Y(t)}z^{Z(t)}|Y(0)=0,Z(0)=0\right], \\ &= \sum_{(j,k)} P_{(j,k)}(t)y^j z^k.\end{aligned} \tag{2.52}$$

In terms of the probability generating function, the survival and hazard functions are

$$S(t) = P[T>t] = \sum_j P_{(j,0)}(t) = \sum_{j,k} P_{(j,k)}(t)1^j 0^k = \Psi(1,0,t), \tag{2.53}$$

$$h(t) = -\frac{\Psi'(1,0,t)}{\Psi(1,0,t)}. \tag{2.54}$$

As with the Armitage–Doll model (we do not yet need our theory of inhomogeneous continuous time Markov chains), we may write the Kolmogorov forward equations:

$$\begin{aligned}\frac{d}{dt}P_{(j,k)}(t) = &\left[(j-1)\alpha(t) + X(t)\mu_0(t)\right]P_{(j-1,k)}(t) + (j+1)\beta(t)p_{(j+1,k)}(t) \\ &+ j\mu_1(t)p_{(j,k-1)} - \left[j\left(\alpha(t)+\beta(t)+\mu_1(t)\right) + X(t)\mu_0(t)\right]P_{(j,k)}(t)\end{aligned} \tag{2.55}$$

Multiplying both sides by $y^j z^k$ and summing over all j and k, we arrive at the following differential equation for the probability generating function:

$$\frac{\partial \Psi(y,z,t)}{\partial t} = (y-1)\mu_0(t)X(t)\Psi(y,z,t) + \left[(\mu_1(t)z + \alpha(t)y - (\alpha(t)+\beta(t)+\mu_1(t)))\, y + \beta(t)\right] \frac{\partial \Psi(y,z,t)}{\partial y}. \quad (2.56)$$

Since we usually assume that all cells begin as normal, the initial condition is $\Psi(y,z,0) = 1$. This partial differential equation is first-order, and thus may be solved by the method of characteristics. We choose characteristic curves $(y(\tau), z(\tau), t(\tau))$ such that the following ODEs are satisfied.

$$\begin{aligned} \frac{dy}{d\tau} &= (\alpha(t)+\beta(t)+\mu_1(t))y - \mu_1(t)zy - \alpha(t)y^2 - \beta(t), \\ \frac{dz}{d\tau} &= 0, \\ \frac{dt}{d\tau} &= 1. \end{aligned} \quad (2.57)$$

We have, then, that z is constant along characteristic curves. Further we transform our PDE into the following ODE:

$$\frac{d\Psi(y,z,t)}{d\tau} = (y-1)\mu_0(t)X(t)\Psi(y,z,t). \quad (2.58)$$

Since $\frac{d\Psi}{d\tau} = \frac{d\Psi}{dt}$, we may solve for Ψ for any characteristic:

$$\Psi(y,z,t) = \exp\left[\int_0^t (y(s)-1)\,\mu_0(s)X(s)\,ds\right]. \quad (2.59)$$

Now, we fix t. As we are seeking the survival function $S(t) = \Psi(1,0,t)$, we consider the characteristic curve through $(y(0),0,0)$ with the boundary condition $y(t) = 1$. We will need to solve for y. Along this characteristic, for $0 \le \tau \le t$, $y(\tau,t)$ satisfies

the initial value problem

$$\begin{aligned} \frac{dy}{d\tau} &= (\alpha(\tau) + \beta(\tau) + \mu_1(\tau))y - \alpha(\tau)y^2 - \beta(\tau), \\ y(t) &= 1. \end{aligned} \tag{2.60}$$

Employ the the change of variables $s = t - \tau$, and define the following system of equations:

$$\begin{aligned} x_1(s) &= y(s), \\ x_2(s) &= \frac{dy}{dt}(s), \\ x_3(s) &= \Psi(1, 0, t - s), \\ x_4(s) &= -\frac{d}{dt} \ln \Psi(1, 0, t - s). \end{aligned} \tag{2.61}$$

Then, we can write the following equations:

$$\begin{aligned} \frac{dx_1}{ds} &= \alpha(t-s)x_1^2 + \beta(t-s) - (\alpha(t-s) + \beta(t-s) + \mu_1(t-s))x_1, \\ \frac{dx_2}{ds} &= 2\alpha(t-s)x_1x_2 - (\alpha(t-s) + \beta(t-s) + \mu_1(t-s))x_2, \\ \frac{dx_3}{ds} &= \mu_0(t-s)X(t-s)\left[x_1 - 1\right]x_3, \\ \frac{dx_4}{ds} &= -\mu_0(t-s)X(t-s)x_2, \\ x_1(0) &= 1, \\ x_2(0) &= -\mu_1(t), \\ x_3(0) &= 1, \\ x_4(0) &= 0. \end{aligned} \tag{2.62}$$

Then $S(t) = x_3(t)$ and $h(t) = x_4(t)$.

If the parameters α, β, μ_0, and μ_1 are constant (or piecewise constant (Heidenreich et al., 1997)), there are closed form solutions for the survival and hazard. The

solutions for constant parameters are

$$S(t) = \left(\frac{q-p}{qe^{-pt} - pe^{-qt}} \right)^r, \tag{2.63}$$

and

$$\begin{aligned} h(t) &= \frac{rpq(e^{-qt} - e^{-pt})}{qe^{-pt} - pe^{-qt}}, \\ &= \frac{-rpq\left(e^{(q-p)t} - 1\right)}{(-q-p) + q\left(e^{(q-p)t} + 1\right)} \end{aligned} \tag{2.64}$$

where

$$\begin{aligned} p, q &= \frac{1}{2}\left(-(\alpha - \beta - \mu_1) \mp \sqrt{(\alpha - \beta - \mu_1)^2 + 4\alpha\mu_1} \right) \\ r &= \frac{\mu_0 X(0)}{\alpha} \end{aligned} \tag{2.65}$$

It is useful to note that $\lim_{t\to\infty} h(t) = -rp$, $p + q = -(\alpha - \beta - \mu_1)$, and $pq = -\alpha\mu_1$. In the general case of age-dependent parameters, numerical solutions can be found (Little et al., 2002; Crump et al., 2005).

2.4.4.2 Two-stage clonal expansion model: Backward derivation

The clonal expansion model formulation may be extended to three stages and other more complex models (Hazelton et al., 2006; Jeon et al., 2006, 2008; Luebeck and Moolgavkar, 2002; Luebeck et al., 2008; Little, 1995; Little et al., 2002; Meza et al., 2005, 2008, 2010a,b; Dewanji et al., 2011). Unfortunately, although the method of using the forward equations to derive the probability generating function for multistage models is valid, the results must typically solved by numerical methods that may accrue a significant amount of error (Meza, 2006). Thus, the backward equations are used for large multistage models. Here, we demonstrate how this would be done for the two-stage model, using the theory we previously developed for inhomogeneous continuous-time Markov chains and Markov branching processes.

This exposition, although it concerns known results (Crump et al., 2005) and is informed by the work of Bill Hazelton and Jihyoun Jeon, is my own.

Let $\Psi(y, z, \tau, t)$ be the generating function for the numbers of intermediate and malignant cells given that there are none at time τ. Let $\Phi(y, z, \tau, t)$ and $\Theta(y, z, \tau, t)$ be the generating functions for the numbers of intermediate and malignant cells given that there is, for Φ, one initiated and no malignant cells and, for Θ, no initiated and one malignant cell. That is,

$$\begin{aligned}
\Psi(y, z, \tau, t) &= \sum_{(j,k)} P[Y(t) = j, Z(k) = 0 | Y(\tau) = 0, Z(\tau) = 0] y^j z^k, \\
&= E[y^{Y(t)} z^{Z(t)} | Y(\tau) = 0, Z(\tau) = 0], \\
\Phi(y, z, \tau, t) &= \sum_{(j,k)} P[Y(t) = j, Z(k) = 0 | X(\tau) = 0, Y(\tau) = 1, Z(\tau) = 0] y^j z^k, \\
&= E[y^{Y(t)} z^{Z(t)} | Y(\tau) = 1, Z(\tau) = 0], \\
\Theta(y, z, \tau, t) &= \sum_{(j,k)} P[Y(t) = j, Z(k) = 0 | X(\tau) = 0, Y(\tau) = 0, Z(\tau) = 1] y^j z^k, \\
&= E[y^{Y(t)} z^{Z(t)} | Y(\tau) = 0, Z(\tau) = 1].
\end{aligned} \tag{2.66}$$

The inclusion of $X(\tau) = 0$ in the definition of Φ_1 and Φ_2 is a subtle point usually not pointed out in derivations of the MSCE, but it is important because we are including the inhomogeneous Poisson process for initiation.

We find the form of $\Psi(y, z, t)$ using the backward equation for the transition probability:

$$\begin{aligned}
\frac{\partial P_{(0,0),(j,k)}}{\partial \tau}(\tau, t) &= \nu_{(0,0)}(\tau) P_{(0,0),(j,k)}(\tau, t) - \sum_{(i,\ell) \neq (j,k)} q_{(0,0),(i,\ell)}(\tau) P_{(i,\ell),(j,k)}(\tau, t), \\
&= \mu_0(\tau) X(\tau) P_{(0,0),(j,k)}(\tau, t) - \mu_0(\tau) X(\tau) P_{(1,0),(j,k)}(\tau, t).
\end{aligned} \tag{2.67}$$

Multiply both side by $y^j z^k$ and sum over j and k. If we had not drawn attention to the conditioning on $X(\tau) = 0$ in the definition of Φ, it would be tempting to write the result as $\frac{\partial}{\partial \tau} \Psi = \mu_0(\tau) X(\tau)(\Psi - \Phi)$. This is, however, not correct. Rather,

observe, because this is a Markov branching process,

$$\begin{aligned}
&\sum_{(j,k)} P[Y(t)=j, Z(t)=k | Y(\tau)=1, Z(\tau)=0] y^j z^k \\
&= E[y^{Y(t)} z^{Z(t)} | Y(\tau)=1, Z(\tau)=0], \\
&= E[y^{Y(t)} z^{Z(t)} | Y(\tau)=0, Z(\tau)=0] E[y^{Y(t)} z^{Z(t)} | X(\tau)=0, Y(\tau)=1, Z(\tau)=0], \\
&= \Psi(y,z,\tau,t)\Phi(y,z,\tau,t).
\end{aligned} \tag{2.68}$$

so that, suppressing dependence on y and z, we have, with initial condition,

$$\begin{aligned}
\frac{\partial \Psi}{\partial \tau}(\tau,t) &= \mu_0(\tau) X(\tau) \Psi(\tau,t) \left[1 - \Phi(\tau,t)\right], \\
\Psi(y,z,t-0,t) &= y^0 z^0 = 1.
\end{aligned} \tag{2.69}$$

Because we do not need to worry about $X(t)$ and the inhomogeneous Poisson process driving initiation when considering the backward equations for Φ and Θ, we may directly use the theory we developed in section 2.4.3. We have that, in the notation of that section,

$$\begin{aligned}
\eta_\Phi(y,z,t) &= \frac{\beta(t)}{\alpha(t)+\beta(t)+\mu_1(t)} + \frac{\alpha(t)}{\alpha(t)+\beta(t)+\mu_1(t)} y^2 + \frac{\mu_1(t)}{\alpha(t)+\beta(t)+\mu_1(t)} yz \\
\eta_\Theta(y,s,t) &= 0 \\
\nu_\Phi(t) &= \alpha(t)+\beta(t)+\mu_1(t) \\
\nu_\Theta(t) &= 0
\end{aligned} \tag{2.70}$$

Thus, suppressing the dependence on y and z,

$$\begin{aligned}\frac{\partial\Phi}{\partial\tau}(\tau,t) &= \left[\alpha(\tau)+\beta(\tau)+\mu_1(\tau)\right]\Phi_1(\tau,t)-\beta(\tau)\\ &\quad -\alpha(\tau)\Phi_1^2(\tau,t)-\mu_1(\tau)\Phi_1(\tau,t)\Phi_2(\tau,t)\\ \frac{\partial\Theta}{\partial\tau}(\tau,t) &= 0\end{aligned} \tag{2.71}$$

with initial conditions

$$\begin{aligned}\Phi(y,z,t-0,t) &= y^1z^0 = y,\\ \Theta(y,z,t-0,t) &= y^0z^1 = z.\end{aligned} \tag{2.72}$$

Now, let $'$ denote derivative with respect to t. Then we have

$$\begin{aligned}\frac{\partial\Psi}{\partial\tau}(\tau,t) &= \mu_0(\tau)X(\tau)\Psi(\tau,t)\left[1-\Phi(\tau,t)\right]\\ \frac{\partial\Psi'}{\partial\tau}(\tau,t) &= \mu_0(\tau)X(\tau)\left[\Psi'(\tau,t)\left(1-\Phi(\tau,t)\right)+\Psi(\tau,t)\Phi'(\tau,t)\right]\\ \frac{\partial\Phi}{\partial\tau}(\tau,t) &= \left[\alpha(\tau)+\beta(\tau)+\mu_1(\tau)\right]\Phi(\tau,t)-\beta(\tau)-\alpha(\tau)\Phi^2(\tau,t)-\mu_1(\tau)\Phi(\tau,t)\Theta(\tau,t)\\ \frac{\partial\Phi'}{\partial\tau}(\tau,t) &= \left[\alpha(\tau)+\beta(\tau)+\mu_1(\tau)\right]\Phi'(\tau,t)-2\alpha(\tau)\Phi(\tau,t)\Phi'(\tau,t)\\ &\quad -\mu_1(\tau)\left(\Phi'(\tau,t)\Theta(\tau,t)+\Phi(\tau,t)\Theta'(\tau,t)\right)\\ \frac{\partial\Theta}{\partial\tau}(\tau,t) &= 0\\ \frac{\partial\Theta'}{\partial\tau}(\tau,t) &= 0\end{aligned} \tag{2.73}$$

The initial conditions are derived from the fact that $\frac{\partial}{\partial t}\Psi = -\frac{\partial}{\partial\tau}\Psi$ at $\tau = t$, and similarly for Φ and Θ. Thus,

$$\begin{aligned}\Psi'(y,z,t-0,t) &= -\mu_0(t)X(t)(1-y),\\ \Phi'(y,z,t-0,t) &= -\left[\alpha(t)+\beta(t)+\mu_1(t)\right]y+\beta(t)+\alpha(t)y^2+\mu_1(t)yz,\\ \Theta'(y,z,t-0,t) &= 0.\end{aligned} \tag{2.74}$$

From these equations, it is clear that $\Theta'(y,z,\tau,t) \equiv 0$ and $\Theta(y,z,\tau,t) = z$.

With an eye toward writing an equation for the hazard function, let

$$\Gamma(y,z,\tau,t) = -\ln \Psi(y,z,\tau,t), \tag{2.75}$$

so that

$$\begin{aligned}
\frac{\partial \Gamma}{\partial \tau}(\tau,t) &= -\mu_0(\tau)X(\tau)\left[1-\Phi(\tau,t)\right], \\
\frac{\partial \Gamma'}{\partial \tau}(\tau,t) &= \mu_0(\tau)X(\tau)\Phi'(\tau,t), \\
\Gamma'(y,z,t-0,t) &= \mu_0(t)X(t)(1-y).
\end{aligned} \tag{2.76}$$

Our goal is to solve for $S(t) = \Psi(1,0,0,t)$ and $h(t) = -\Psi'(1,0,0,t)/\Psi(1,0,0,t)$. We want, then, to fix t and solve these Kolmogorov backward equations from $\tau = t$ to $\tau = 0$. This is done with the change of variables $s = t - \tau$ (so that $ds = -d\tau$). Since we are interested only in solutions with $y = 1$ and $z = 0$, we simplify notation by defining the following variables. Let $x_1(s) = \Phi(1,0,t-s,t)$, $x_2(s) = \Phi'(1,0,t-s,t)$, $x_3(s) = \Psi(1,0,t-s,t)$, and $x_4(s) = \Gamma'(1,0,t-s,t)$. We have the initial value problem

$$\begin{aligned}
\frac{\partial x_1}{\partial s}(s) &= -\left[\alpha(t-s)+\beta(t-s)+\mu_1(t-s)\right]x_1 + \beta(t-s) + \alpha(t-s)x_1^2(s,t), \\
\frac{\partial x_2}{\partial s}(s) &= -\left[\alpha(t-s)+\beta(t-s)+\mu_1(t-s)\right]x_2 + 2\alpha(t-s)x_1x_2, \\
\frac{\partial x_3}{\partial s}(s) &= -\mu_0(t-s)X(t-s)x_3(1-x_1), \\
\frac{\partial x_4}{\partial s}(s) &= -\mu_0(t-s)X(t-s)x_2, \\
x_1(0) &= 1, \\
x_2(0) &= -\mu_1(t), \\
x_3(0) &= 1, \\
x_4(0) &= 0.
\end{aligned} \tag{2.77}$$

where $S(t) = x_3(t)$ and $h(t) = x_4(t)$. This set of differential equations matches the one we derived from the forward equations earlier (eq. 2.62).

2.4.4.3 Two-stage clonal expansion model: Identifiability analysis

We now consider the non-identifiability of the system, which was considered by Heidenreich et al. (1997) and, in a more general framework, by Little et al. (2009). Here, we present an alternative derivation based on a differentiable algebra approach (Saccomani et al., 2001; Audoly et al., 2001; Meshkat et al., 2009; Eisenberg et al., 2013; Eisenberg, 2013), which has not previously been brought to bear on this class of models. This approach has some advantages over previous methods (e.g. Heidenreich et al. (1997); Little et al. (2009)) because it demonstrates that approaches for identifiability in dynamical systems can be used in Markov branching processes and, more generally, continuous-time Markov processes. It also has the advantage that it also generalizes to other multistage clonal expansion models, as we will see in Chapter VI, but the two-stage model provides a more tractable example.

Assuming we are matching to age-specific incidence curves (e.g. as are available in the Surveillance, Epidemiology and End Results (SEER) cancer registries), we have that, in eqs. 2.77, the survival x_3 and hazard x_4 are known to us.

Proposition 2.4.1. *If the survival and hazard functions are known, the two-stage clonal expansion model (eqs. 2.77) is unidentifiable, with identifiable combinations $\mu X/\alpha$, $\alpha - \beta - \mu_1$, and $\alpha\mu_1$. Further, parameters r, p, and q (eq. 2.65) are identifiable.*

Proof. From eqs. 2.77, we solve for x_2 using the $\dot{x}_4$ equation,

$$x_2 = -\frac{1}{\mu_0 X}\dot{x}_4. \tag{2.78}$$

Then, we plug this into the $\dot{x}_2$ equation,

$$\begin{aligned} \dot{x}_2 &= (\alpha+\beta+\mu_1)\frac{1}{\mu_0 X}\dot{x}_4 - 2\alpha x_1 \frac{1}{\mu_0 X}\dot{x}_4, \\ -\frac{1}{\mu_0 X}\ddot{x}_4 &= (\alpha+\beta+\mu_1)\frac{1}{\mu_0 X}\dot{x}_4 - 2\alpha x_1 \frac{1}{\mu_0 X}\dot{x}_4, \end{aligned} \tag{2.79}$$

simplify,

$$\ddot{x}_4 = \dot{x}_4\left(2\alpha x_1 - (\alpha+\beta+\mu_1)\right), \tag{2.80}$$

and solve for x_1,

$$x_1 = \frac{1}{2\alpha}\left(\frac{\ddot{x}_4}{\dot{x}_4} + (\alpha+\beta+\mu_1)\right). \tag{2.81}$$

Plugging this into the $\dot{x}_1$ and $\dot{x}_3$ equations will leave both with only x_3, x_4, and their derivatives.

$$\begin{aligned} \dot{x}_1 &= -(\alpha+\beta+\mu_1)x_1 + \beta + \alpha x_1^2, \\ \frac{1}{2\alpha}\left(\frac{\dddot{x}_4\dot{x}_4 - \ddot{x}_4^2}{\dot{x}_4^2}\right) &= -(\alpha+\beta+\mu_1)\frac{1}{2\alpha}\left(\frac{\ddot{x}_4}{\dot{x}_4} + (\alpha+\beta+\mu_1)\right) + \beta \\ &\quad + \alpha\left(\frac{1}{2\alpha}\left(\frac{\ddot{x}_4}{\dot{x}_4} + (\alpha+\beta+\mu_1)\right)\right)^2, \\ 2\left(\frac{\dddot{x}_4\dot{x}_4 - \ddot{x}_4^2}{\dot{x}_4^2}\right) &= -(\alpha+\beta+\mu_1)^2 + 4\alpha\beta + \left(\frac{\ddot{x}_4}{\dot{x}_4}\right)^2, \\ 0 &= 2\dddot{x}_4\dot{x}_4 - 3\ddot{x}_4^2 + \dot{x}_4^2\left((\alpha-\beta-\mu_1)^2 + 4\alpha\mu_1\right), \end{aligned} \tag{2.82}$$

$$\begin{aligned} \dot{x}_3 &= -(\mu_0 X)x_3(1-x_1), \\ \dot{x}_3 &= -(\mu_0 X)x_3\left(1 - \frac{1}{2\alpha}\left(\frac{\ddot{x}_4}{\dot{x}_4} + (\alpha+\beta+\mu_1)\right)\right), \\ \dot{x}_3 &= -\frac{1}{2}\left(\frac{\mu_0 X}{\alpha}\right)x_3\left((\alpha-\beta-\mu_1) - \frac{\ddot{x}_4}{\dot{x}_4}\right), \\ 0 &= 2\dot{x}_3\dot{x}_4 + \left(\frac{\mu_0 X}{\alpha}\right)\left(x_3\dot{x}_4(\alpha-\beta-\mu_1) - x_3\ddot{x}_4\right). \end{aligned} \tag{2.83}$$

Thus, we have the following input–output equations, which are monic as 2 is unit

in our field $\mathbb{R}$,

$$\begin{aligned} 0 &= 2\dddot{x}_4\dot{x}_4 - 3\ddot{x}_4^2 + \dot{x}_4^2\left((\alpha-\beta-\mu_1)^2 + 4\alpha\mu_1\right), \\ 0 &= 2\dot{x}_3\dot{x}_4 + \left(\frac{\mu_0 X}{\alpha}\right) x_3\left(\ddot{x}_4 + \dot{x}_4(\alpha-\beta-\mu_1)\right). \end{aligned} \tag{2.84}$$

We see that there are three distinct coefficients but five unknown parameters, so that the model is unidentifiable. We observe the following identifiable parameter combinations: $\mu_0 X/\alpha$, $(\alpha-\beta-\mu_1)$, and $\alpha\mu_1$. Since these combinations are r, $-(p+q)$, and $-pq$, we see that r, p, and q, the parameters of the hazard, are identifiable from age-specific incidence data. □

This approach is later used in Chapter VI to assess the identifiability of multistage models of cancers with infectious disease origins.

2.4.5 APC–MSCE models

In a general APC model, the age effects are not constrained, but, if we are working within the TSCE framework, we can restrict the age effects to have the shape of the TSCE hazard:

$$\log\lambda = \beta_0 + \log\left[h(t,r,p,q)\right] + \beta_P(P) + \beta_C(C). \tag{2.85}$$

This added constraint theoretically resolves the non-identifiability problem in the full APC model (Holford, 1991; Luebeck et al., 2013). In the case of constant parameters, the multiplicative assumption of the model translates to an assumption that the period and cohort effects are on the rate of initiation μ_0 since $r = \mu_0 X(0)/\alpha$ and $X(0)$ and α are considered fixed:

$$\lambda = -\left[f(P,C)\cdot r\right]\left(\frac{pq(e^{-qt}-e^{-pt})}{qe^{-pt}-pe^{-qt}}\right). \tag{2.86}$$

Previous studies have only considered the above models. However, depending on the mechanism of carcinogenesis for a given cancer and the nature of the risk fac-

tors captured by the temporal trends, it is possible that effects on promotion or malignant conversion rates rather than initiation rates are more realistic. Thus, by considering slightly different models with period or cohort effects acting on the promotion or malignant conversion parameters, one can investigate the impact of period and cohort on different stages of carcinogenesis. In Chapter V we will consider models of the form

$$\lambda = h(t, \mathbf{r}(P, C), \mathbf{p}(P, C), \mathbf{q}(P, C)). \tag{2.87}$$

Here $\mathbf{r}(P, C) = r \cdot \theta_P(P) \cdot \theta_C(C)$ where θ_P and θ_C are natural splines, r is the value of $\mathbf{r}$ at the reference period and cohort, and $\mathbf{p}$ and $\mathbf{q}$ are defined similarly. This consideration of period and cohort effects on promotion and malignant conversion is a new contribution.

2.4.6 Other cancer models

Although not the subject of this dissertation, many other modeling techniques have been brought to bear on the subject of cancer. In general, all models must consider trade-offs between biological realism and mathematical tractability, and a range of models across the spectrum have been developed for cancer (Kopp-Schneider, 1997). One popular modeling paradigm for cancer growth incorporates spatial components, taking into account the intracellular matrix and movement by chemotaxis and haptotaxis. These models can focus on the movement of cancer cells themselves or angiogenesis, the growth of blood cells toward a tumor. Such models typically involve partial differential equations for concentration in time and sometimes agent-based models (with cells as agents) as well. Examples include Anderson and Chaplain (1998), Anderson et al. (2012), Eisenberg et al. (2011), Jackson and Zheng (2010, 2012), and Friedman and Jain (2013). Another popular modeling framework, especially in the health economics community, is Markov state transition modeling. This class of models, though not mechanistic, is often used for

chronic disease history models, especially cancer (Siebert et al., 2012). In these models, each person resides in a compartment that defines some health state and transitions occur after a defined time interval according to Markov transition properties that may be dependent on the person's age, sex, or chronic disease status. Examples include Goldie et al. (2004) and Lansdorp-Vogelaar et al. (2012).

2.5 Literature review of HPV models

2.5.1 Parameter estimation from observational studies

In order to simulate a dynamical infectious disease model, certain parameters must be known (or perhaps estimated from data). Here we discuss some relevant parameters that may be estimated from the literature.

Several studies have attempted to estimate clearance rates of female genital infections (Ho and Bierman, 1998; Franco et al., 1999; Molano et al., 2003; Moscicki et al., 1998). A review of the studies concluded that 70% of new genital HPV infections clear within one year, and 91% clear within two years; the median duration was eight months (Gerberding, 2004). Under the assumption that clearance is exponentially distributed—a strong assumption given that there is some evidence that if an infection does not clear within the first year, the probability of it resolving in the next six months is significantly reduced (Ho and Bierman, 1998)—the yearly rate of clearance γ for women is in the range 1.0–1.2. For men, a smaller, prospective investigation for the HPV in Men (HIM) study estimated median duration of HPV infection to be 5.9 months, while the full HIM study reported a median of 7.5 (Lu et al., 2009; Giuliano et al., 2011). These values give a parameter range of γ between 1.1–1.4, suggesting genital clearance is faster in men than in women. For both men and women, clearance appears to be dependent on genotype, with oncogenic types lasting longer, and, to a lesser extent, on the person's age at infection (Franco et al., 1999; Giuliano et al., 2011).

For clearance of oral HPV, various studies have reported a median duration of 6.9 months (Kreimer et al., 2013) for men, 72% clearance in four months for men (Edelstein et al., 2012), and 61% clearance in three months for a co-ed sample (Pickard et al., 2012). Small samples size or long duration before follow up have introduced a good deal of uncertainty into these numbers. Nevertheless, we may estimate a clearance parameter of γ in the range 1.2–3.8. Again, we are probably seeing bimodal behavior where most infections clear very quickly, but those that do not clear quickly take a long time to clear.

In women, 87% of anal infections were found to clear in one year (Goodman et al., 2010), which corresponds to $\gamma = 2$ under an exponential assumption.

Several studies have looked at transmission of HPV between heterosexual couples (Hernandez et al., 2008; Burchell et al., 2011; Mbulawa et al., 2013; Widdice et al., 2013), reporting transmissions per 100 person-months. Unfortunately, these units do not easily translate into a differential equations framework. It is worth noting that some studies found significantly higher transmission from female to male (Hernandez et al., 2008; Widdice et al., 2013) while others found them roughly equal (Burchell et al., 2011).

Little is known about autoinoculation rates, particularly between oral and genital. What research has been done has largely focused on sequential cervical and anal infection in the absence of anal sex (Hernandez et al., 2005, 2008; Goodman et al., 2010). In particular, Goodman et al. (2010) found that "48% of cases of incident cervical HPV infection occurring after anal HPV infection and 63% of cases of incident anal HPV infection occurring after cervical HPV infections developed in the absence of a self-reported history of anal sex."

2.5.2 Vaccination models

Nearly all models of HPV—both those focusing on transmission models of an infectious disease and those concentrating on progression to cancer—have primarily

been concerned with estimating the impact of prophylactic vaccination against HPV, both on various public health outcomes (cervical cancer, genital warts, etc.) and economically (i.e. their cost-effectiveness). These models typically address some of the following questions:

- Should the entire population be vaccinated or just high risk groups?
- Should both men and women be vaccinated, or just women?
- What is the disease burden or economic impact under different vaccination strategies?

Of course, questions of optimal vaccination strategy will be highly dependent on the outcome of interest, be it burden of infection by any strain or only oncogenic strains, burden of cervical cancer, burden of any HPV associated cancer, or simply the economic cost–benefit ratio.

Myers et al. (2000) developed a nineteen stage Markov model to model a cohort of women between ages 18–85. The model did not include transmission but rather age-specific incidence of HPV. Once infected, individuals could progress and regress between precancerous stages (low- and high-grade squamous intraepithelial lesions (SIL)) and stages of invasive cervical cancer (ICC) and ultimately to death by cancer or other causes. The model predicted age-specific incidence of cervical cancer and connected incidence of HPV to incidence of cervical cancer.

Hughes et al. (2002) developed a simple ODE dynamical systems model on the SIR framework of susceptibles, infectious, and recovered/immune by adding compartments for vaccinated and vaccinated-but-infected persons (to account for the possibility of only reduced susceptibility and loss of immunity). This model considered three sexual activity levels and distinguished between female-to-male and male-to-female transmission. Under the assumptions of 90% vaccination coverage, 75% vaccination efficacy, and a ten year mean immunity, Hughes et al. found that vaccinating both sexes would lead to a 44% reduction in prevalence while vaccinating women alone would only result in a 30% reduction.

Further, Hughes et al. (2002) coupled their dynamical transmission model to an ODE model of cancer that took into account age-specific risk of disease development. The models together allowed the authors to estimate the effect of different vaccination strategies on cervical cancer incidence. In addition to the result of their transmission model described above, the authors determined that reducing HPV prevalence would result in a smaller reduction in cancer incidence and that targeting core groups only would not be an effective vaccination strategy.

Sanders and Taira (2003) and Taira et al. (2004) developed a transmission model for HPV 16 and 18 that used four sexual activity groups, nine age divisions, and age-based mixing patterns. Basic economic considerations were taken into account to assess cost per quality-adjusted life-year (QALY). The authors recommended achieving at least 70% vaccination coverage to achieve significantly reduce cohort lifetime cervical cancer cases. The cost-effectiveness of vaccinating men and boys was questioned but depended upon vaccination coverage among women.

Barnabas et al. (2006) created a compartment deterministic transmission model for HPV 16 and progression to cervical cancer and calibrated it to period data of Finnish seroprevalence. Groups were stratified by age, and regression/progression rates were combined into estimated transmission probabilities. The authors found that reported data about sexual activity and number of partner changes did not account for the seroprevalence of HPV 16 even with a theoretical maximum of 100% transmission probability. Assuming an under-reporting rate, they derived a transmission probability of 0.6 per partnership. The results for vaccination impact were similar to other modeling reports in that high vaccination coverage was necessary and that vaccinating men as well as women had only a small additional impact.

Brisson et al. (2007b) and Van de Velde et al. (2007) developed a deterministic cohort model of the natural history of HPV to estimate the number of people that would need to be vaccinated and to quantify the impact of uncertainty in model parameters. This model was later used to determine the cost-effectiveness of vaccination in Canada (Brisson et al., 2007a). The authors have also looked at the

cost effectiveness of vaccination in developed countries (Brisson et al., 2009), understanding differences in vaccine effectiveness predictions (Van de Velde et al., 2010), understanding the impact of vaccinating boys (Brisson et al., 2011), and considering different vaccination valencies (bi-, quadra-, and nonavalent) (Van de Velde et al., 2012).

Elbasha et al. (2007) developed a heterosexual transmission model for the United States with age and sexual activity with outcomes of cervical intraepithelial neoplasia, cervical cancer, and genital warts. The analysis suggested that vaccination would reduce incidence of all three outcomes, improve quality of life and survival, and be cost effective. A cost effectiveness analysis for the U.K. was also done (Dasbach et al., 2008). Catch-up vaccination was considered in Elbasha et al. (2009). The model was expanded by Elbasha and Dasbach (2010) to include health outcomes for men as well as women. Up to this point, the health outcome of interest was primarily incidence of cervical cancer. This study took all anogenital cancers, condylomas, and head and neck cancers into account by using crude assumptions about the natural history and incidence of these outcomes. Under this framework, the authors determined vaccination of men and boys to provide significant public health benefits and likely be cost effective. This is the model developed and used by Merck, the manufacturer of the vaccine Gardisil™.

Günther et al. (2008) developed a deterministic compartmental model of HPV transmission and progression to cervical cancer including progression subcompartments for loss of immunity, treatment, and progression to cervical cancer. An important addition of this model was the complex model of sexual behavior and mixing underlying the transmission process. The authors focused on the optimal age to vaccinate girls as a function of duration of immunity.

Kim and Goldie (2008) developed a hybrid dynamic transmission model to simulate transmission of HPV 16 and 18 and a stochastic model of progression to cervical cancer. The authors used likelihood methods to calibrate parameters to demographic and epidemiological data in the US. They additionally incorporated a

detailed cost-effectiveness analysis to determined cost of QALY for different strategies. They concluded that cost-effectiveness is maximized by focusing on vaccinating preadolescent girls and recommended that strategies for screening be updated. This paper was followed up by analyses looking at the cost effectiveness of vaccinating boys as well as girls (Kim and Goldie, 2009) or just men who have sex with men (MSM) (Kim, 2010).

Jit et al. (2008) performed another primarily economic evaluation of vaccination, this time targeted to the United Kingdom. Their model, a dynamic compartmental model similar to those previously discussed, also included genotypes 6 and 11 as condylomas have a treatment cost associated with them. Cost parameters were drawn from probability distributions by Monte Carlo Latin-hypercube sampling over a series of simulations. The study found vaccination of young girls to be likely cost effective and that the bivalent and quadrivalent vaccines were of comparable cost-effectiveness.

Cost effectivess studies were done for a number of other countries not yet mentioned including Australia (Kulasingam and Myers, 2003; Kulasingam et al., 2007), which has a national screening program, France (Bergeron et al., 2008), and the Netherlands (Bogaards et al., 2011).

Baussano et al. (2013) implemented an ad-hoc dynamic model of HPV transmission to demonstrate that a catch-up vaccination is likely to be beneficial in medium- to low-income countries.

2.6 Conclusion

In this chapter I have discussed the concepts underlying dynamical infectious disease models, age–period–cohort models, and mechanistic models of cancer. I have also presented an in-depth derivation of the two-stage clonal expansion model of carcinogenesis, including the relevant theory of continuous time Markov chains.

Finally, I considered the state of HPV modeling in the literature. Although wide-ranging, this chapter is the foundation on which the next four chapters stand.

CHAPTER III

Trends in HPV cervical and seroprevalence and analysis of multisite (oral, genital, sero) concurrence and type-concordance in NHANES 2003–2012

3.1 Introduction

The human papillomavirus (HPV) infects multiple mucosal sites in the epithelium and is the etiological agent for over 90% of anogenital cancers and an increasing fraction of oropharyngeal cancers (Jemal et al., 2013). Although the progression from cervical HPV infection to cancer has been well documented because of access to tissue during gynecological exams, very little is understood about the progression to cancer in the head and neck. Further, the association between infection at different sites and their relation to seroconversion is not well characterized. Ideally, a single test, such as for seropositivity of certain HPV strains, could act as a biomarker for the risk of genital and oropharyngeal/nasopharyngeal (OP/NP) cancer (Kreimer, 2014). The National Health and Nutrition Examination Survey (NHANES), a US-wide biennial survey conducted by the CDC, samples approximately 10,000 people each year. NHANES offers an opportunity to assess not only associations between oral and genital HPV infection and seropositivity for certain genotypes, but HPV prevalence and seroprevalence trends as well. Most knowledge of the natural history of HPV comes from case-control and cohort studies, which,

although relevant, do not give information about patterns and trends at the population level. Additionally, although testing for HPV at cervical sites has been standard for some time, characterization of oral prevalence has only recently begun.

There are many strains of HPV, and these are typically classified according to their oncogenic risk. Genotypes 16, 18, 26, 31, 33, 35, 39, 45, 51, 52, 53, 56, 58, 59, 66, 68, 73, 82 are considered to be high risk, that is have the potential for oncogenesis, and genotypes 6, 11, 40, 42, 54, 55, 61, 62, 64, 67, 69, 70, 71, 72, 81, 82 subtype IS39, 83, 84, 89[CP6108] are low risk for oncogenesis but may cause other complications such as condylomas (genital warts) (Muñoz et al., 2003). (Classification into low- and high-risk types can very slightly between studies. We are using a classification consistent with Gillison et al. (2012a)). HPV infection is associated with nearly every cervical cancer, 90% of anal cancers, 60–90% of some subsites of head and neck cancers, and 40% of other genital cancers (Jemal et al., 2013; Walline et al., 2013). HPV 16 causes about 70% of genital cancers and together 16 and 18 are responsible for 90% (Jemal et al., 2013). HPV 6 and 11 cause 90% of anogenital warts (Jemal et al., 2013). HPV 16 is also found in 90% of HPV-positive squamous cell carcinomas (SCCs) in the head and neck (Gillison et al., 2012a). Most HPV infections clear within a year or two (Ho and Bierman, 1998; Franco et al., 1999; Molano et al., 2003; Moscicki et al., 2012), but some infections may persist for decades and result in oncogenesis.

Vaccines have been developed to target certain strains of HPV. Two vaccines are currently approved by the FDA: GlaxoSmithKline Biologicals's bivalent (16, 18) Cervarix®, and Merck's quadravalent (6, 11, 16, 18) Gardisil® (Kreimer, 2014). Merck's nonavalent (6, 11, 16, 18, 31, 33, 45, 52, 58) vaccine has been shown to be effective in trials (Joura et al., 2015). Vaccination against HPV is targeted at females ages 11–12 but is recommended in the US for both men and women with minimal sexual activity under the age of 26. Vaccine coverage in the US has been low, though increasing, especially among boys. The CDC reported that vaccination coverage for at least one dose (all three doses) among women ages 13–17 was 53.0% (34.8%),

53.8% (33.4%), and 57.3% (37.6%) in 2011, 2012, and 2013, respectively (Centers for Disease Control and Prevention, 2012, 2013, 2014a). Among males of the same age, coverage for at least one dose (all three doses) increased from 8.3% (1.3%) in 2011 to 20.8% (6.8%) in 2012 to 34.6% (13.9%) (Centers for Disease Control and Prevention, 2013, 2014a). Concerns that administering a vaccine for an STI to young girls would give them license to be sexually active were recently refuted (Mayhew et al., 2014), and the President's Panel on Cancer called for urgent acceleration of vaccine uptake (Rimer et al., 2014). It remains to see what effect these developments will have on future vaccination coverage.

Few studies have thus far considered multiple-site concurrence or type-concordance. Steinau et al. (Steinau et al., 2014) reported that, in the 2009–2010 NHANES survey, oral HPV infection was five-fold higher in women ages 18–59 with a current genital infection, and that type-specific concordance was low. The Hawaii cohort study reported a relative risk of 20.5 for acquiring a type-concordant anal infection after a cervical infections and a relative risk of 8.8 for acquiring a type-concordant cervical infection after an anal infection (Goodman et al., 2010). Data from the HPV in Men (HIM) study have suggested that seroconversion in men differs by anatomical site for some genotypes, with anal infections more likely to result in seroconversion than genital infections (Lu et al., 2012). To our knowledge, no studies have been published considering seroconversion due to oral infections.

Like many sexually transmitted diseases, prevalence of HPV varies widely by demographic group in the US, possibly because of sexual assortativity and differences in sexual behavior patterns. Prevalence among non-Hispanic blacks, for instance, is significantly higher at both oral and genital sites of infection than for non-Hispanic whites and Hispanics. Further, prevalence varies significantly with age. However, no attempt has yet been made to disentangle the effects of age, birth cohort, and time period for trends in HPV prevalence. One way to differentiate these effects is by the use of age–period–cohort (APC) models (Holford, 1983, 1991; Clayton and Schifflers, 1987a,b). APC models have been used for myriad public health issues

including mortality (Meza et al., 2010c), smoking histories (Holford et al., 2014), and the incidence of several cancers (Holford et al., 2006; Luebeck and Moolgavkar, 2002; Jeon et al., 2006; Kilfoy et al., 2009; Anfinsen et al., 2011; Chaturvedi et al., 2013).

In this chapter, we analyze patterns of HPV infection and seropositivity in NHANES 2003–2010. We characterize trends of genital infection in women, the concurrence and type-concordance of genital and oral infections in women, trends of seroprevalence for both men and women, and the concurrence of seropositivity with genital and oral infections.

3.2 Methods

3.2.1 Data

The CDC's National Center for Health Statistics (NCHS) administers the NHANES survey, a series of studies combining physical examinations in a mobile examination center (MEC) and interviews (both in-home and audio-assisted in-MEC) of a representative sample of the non-institutionalized, civilian population of the US. Each survey is conducted over a two-year period and is used to assess the health and nutritional well-being of the US (Centers for Disease Control and Prevention, 2014b). Study design, weighting, and collection of samples have been previously described (Dunne et al., 2007; Markowitz et al., 2009; Hariri et al., 2011; Gillison et al., 2012b).

Self-collected cervicovaginal swabs were collected and typed for women ages 14–59 in five NHANES iterations (2003–2012) for 37 genotypes. Serum samples were collected and seropositivity of HPV types 6, 11, 16, and 18 recorded for both men and women ages 14–59 for the same surveys, although the 2011–2012 data is not yet available. Oral rinses were administered to both men and women ages 14–69 in the 2009–2010 and 2011–12 surveys with 37 genotypes. The numbers of

individuals sampled by demographic group are reported in Table 3.1.

3.2.2 Statistical analysis

Statistical analyses were performed in SAS (version 9.2). Estimates were made using two year MEC exam weights (Botman et al., 2000). We analyzed overall prevalence, concurrent prevalence (defined as a positive result for at least one HPV type at two sites) for each pair of sites (cervix, oral cavity, and serum), and type–concordant prevalence (defined as at least one positive result of the same type at two sites) for each pair of sites by demographic group. Survey participants self-identified as Mexican American, Other Hispanic, Non-Hispanic White, Non-Hispanic Black, or Other Race - Including Multiracial (and, in 2011-2012, Non-Hispanic Asian). Because of small sample sizes, we considered only the first four groups and, where indicated, combined Mexican American and Other Hispanic into one Hispanic category. In an effort to estimate vaccine efficacy and avoid confounding, seroprevalence for women in 2007–2008 and 2009–2010 was broken down by vaccine status. Women reporting having had at least one dose of an HPV vaccine were considered to be vaccinated.

3.2.3 Age–period–cohort modeling

Age–period–cohort (APC) models are epidemiologic models used to disentangle effects of age, period (factors affecting all people at a given time), and birth cohort (factors affecting all people born in a given time period) on prevalence (e.g. HPV prevalence) or incidence (e.g. incidence of oral cancer) (Holford, 1983, 1991; Holford et al., 2014; Clayton and Schifflers, 1987a,b). The traditional model posits that incidence rates λ are described by a multiplicative model with age (A), period (P), and birth cohort (C). This is usually treated in the logarithmic form, in which the

Table 3.1: Numbers of people conclusively tested for HPV or HPV antibodies at each site in the 2003–04, 2005–06, 2007–08, 2009–10, and 2011–2012 National Health and Nutrition Examination Surveys (NHANES). *=does not include ages 14–17.

	Genital					Serum								Oral			
	Women					Women				Men				Women		Men	
Demographic	03–04	05–06	07–08	09–10	11–12	03–04	05–06	07–08	09–10	03–04	05–06	07–08	09–10	09–10	11–12	09–10	11–12
All	1982	2168	2044	2209	1767*	1706	2357	2101	2356	1586	2109	2084	2295	2755	2481	2747	2517
Mexican American	459	532	432	472	190*	366	608	438	505	341	542	438	517	583	275	606	313
Other Hispanic	62	78	269	248	188*	65	86	289	261	56	71	252	234	329	275	295	236
White	844	861	810	950	573*	797	927	846	1010	727	844	876	978	1150	762	1134	810
Black	543	591	461	403	505*	416	617	440	423	387	568	412	432	517	720	563	692
14–17	424	440	261	254	*	0	479	264	279	0	464	291	339	294	286	362	302
18–24	452	479	303	367	351	493	524	319	387	444	444	330	381	392	363	400	404
25–29	175	228	183	231	193	191	277	188	248	188	179	201	204	255	190	209	201
30–34	183	206	211	222	206	216	214	227	244	180	168	198	215	227	211	209	228
35–39	155	158	235	235	204	170	174	239	252	158	185	234	223	236	219	225	214
40–44	174	196	221	256	206	188	204	222	277	184	187	200	243	266	213	229	203
45–49	157	178	230	253	202	169	188	228	266	162	189	204	228	256	202	226	188
50–54	155	162	214	224	236	161	174	220	226	166	174	258	245	227	235	247	201
55–59	107	121	186	167	169	118	123	194	177	104	119	168	207	173	181	208	174

following generalized linear model is fit:

$$\log \lambda = \beta_0 + \beta_A(A) + \beta_P(P) + \beta_C(C). \tag{3.1}$$

A model for prevalence P is

$$\text{logit } P = \beta_0 + \beta_A(A) + \beta_P(P) + \beta_C(C). \tag{3.2}$$

We use this model formulation for genital HPV prevalence in women, oral HPV prevalence in men, and oral HPV prevalence in women, all by race. One drawback of APC models is their inherent unidentifiability: $p = A + C$. In practice, the identifiability problem can be resolved by considering only two-effects models, typically age–period or age–cohort. In this study, age and cohort effects are modeled using splines, using five degrees of freedom/knots for both age and cohort effects, corresponding to one knot for every nine and eight years respectively. APC models were fitted using the Epi package in the statistical software R.

3.3 Results

3.3.1 Oral–genital concurrence

Figure 3.1 presents oral prevalence for women who were tested conclusively for both oral and genital HPV. Oral prevalence is broken into three categories: infections that are not concurrent with a genital infection, infections that are concurrent with a genital infection but not type-concordant, and type-concordant infections. A large percentage of oral infections in every demographic category are concurrent with a genital infection (Figure 3.1). In 2009–10, 3.7% (95%CI: 2.5–4.9) women ages 14–59 had oral infections and 2.8% (95%CI: 1.8–3.9) had genital–oral concurrence, i.e., 76.7% of oral infections in women were accompanied by a concurrent genital infection. In 2011–12, 3.2% (95%CI: 2.0–4.3) women ages 18–59 had oral

infections and 2.4% (95%CI: 1.4–3.5) had genital–oral concurrence, i.e., 78.2% of oral infections in women were accompanied by a concurrent genital infection.

In contrast, the vast majority of women with a genital infection do not have a concurrent oral infection. In 2009–10, genital prevalence was 40.7% (95%CI: 37.6–43.7), with only 7.0% of those concurrent with an oral infection. In 2011–12, genital prevalence was 39.5% (95%CI: 35.0–44.0), with only 6.3% of those concurrent with an oral infection. Table 3.2 presents oral HPV prevalence for women ages 14–59 by genital status as well as the relative risk of oral HPV for +/- genital HPV status in 2009–10 by age and race.

Type-concordance is notably different for the 18–24 age group in that the vast majority of their oral infections are type-concordant. The most prevalent oral genotypes in 2009–2010 among females 18–24 are types 84 (1.4 %), 81 (0.6%), 54 (0.6%), and 16 (0.5%), and the most prevalent genital genotypes among the same group are 51 (11.2%), 84 (10.6%), 66 (10.4%), 16 (10.1%), 39 (9.3%), and 54 (8.2%). In 2011–2012, the more prevalent oral genotypes in this demographic are types 84 (1.1%), 83 (1.0%), 59 (0.6%), and 89 (0.4%), while the most prevalent genital genotypes were 53 (12.0%), 84 (8.5%), 42 (8.4%), 89 (7.9%), 51 (7.8%), and 66 (7.6%).

3.3.2 Seroprevalence and concurrence

HPV serostatus (for types 6, 11, 16, and 18) by age and race is presented in Figure 3.2, with concurrence and type-concordance with genital infections for women. Here, concurrence means detection of 6, 11, 16, or 18 antibodies and a genital infection of any genotype, and type-concordance means that an antibody serotype matches a genital genotype. Prevalence of genital infections is not available for men in this survey, and thus concurrence and type-concordance in men cannot be assessed. Prevalence of concurrence for women overall has remained just under 60% (2003–04: 58.2% (95%CI: 48.9–69.3), 2005–2006: 59.6% (95%CI: 51.0–69.6),

2007–2008: 56.0% (95%CI: 49.7–63.0), 2009–2010: 53.6% (95%CI: 48.1–59.7)) and type-concordance around 10% (2003–04: 10.4% (95%CI: 7.8–14.3), 2005–2006: 11.1% (95%CI: 8.1–15.0), 2007–2008: 10.3% (95%CI: 7.9–13.6), 2009–2010: 8.4% (95%CI: 7.1–9.9)).

Oral HPV prevalence by age and race is presented in Figure 3.3, with serotype-concordance, for both men and women. Serotype-concordance is defined as an oral infection of type 6, 11, 16, or 18 with serum antibodies of the same type. Prevalence of serotype-concordant oral infections is very low overall (men and women ages 14–59: 0.5% (95%CI: 0.2–0.8), and almost nonexistent for women (0.2% (95%CI: 0.0–0.8) vs 0.8% (95%CI: 0.4–1.3) for men). For men, this concordance remains around 10% of the total oral infection, which varies with age; over all ages 14–59, concordance is 8.6% of the oral prevalence (9.8% (95%CI: 7.9–11.7)) Additionally, we found that the relative risk of an oral infection given seropositivity is 2.9 (95%CI: 2.0–4.1) for men but only 1.0 (95%CI: 0.6–1.9) for women. Similarly, the relative risk of being seropositive given an oral infection is 2.8 (95%CI: 2.2–3.7) for men and 1.0 (95%CI: 0.7–1.4) for women.

3.3.3 Seroprevalence and vaccination

Seroprevalence for women in 2007–2008 and 2009–2010 by vaccination status are presented in Figure 3.4. Seroprevalence among unvaccinated people for each age category is roughly the same between 2007–2008 and 2009–2010 but shows a large increase in seroprevalence among vaccinated 14–17 and 18–24 year old women. Genital HPV prevalence (all, oncogenic, and vaccine genotypes) was also analyzed by vaccine status in 2009–2010 and 2011–2012 (Table 3.3). Vaccination was associated with significant reduction in risk for genital infection by genotypes 6, 11, 16, and 18 in the 14–17 and 18–24 age groups. Vaccination was not associated with either an increase or decrease in risk for infection when considering all genotypes or only oncogenic genotypes. The data were insufficient to be conclusive for the impact vaccination has on the risk of oral infection.

3.3.4 Age-period-cohort models

Age–cohort models fit the data better than age–period models. Figure 3.5 shows age and cohort effects (relative to the 1980 birth cohort) of APC models for genital prevalence (women) and seroprevalence (men/women) by race. Here the Mexican American and Other Hispanic race categories were collapsed to Hispanic. The age-specific prevalence for Hispanic and white females is similar to that of the overall trend: peaking at 25 and decreasing with age. For black women, however, prevalence is 10–40% greater than the average. Prevalence for this demographic group also peaks slightly later. For cohort effects, the relative prevalence for all demographic groups has been decreasing since the 1940 birth cohort, although that of black women has been increasing again since the 1980 birth cohort. Seroprevalence for women increases dramatically between ages 20–30, after which it largely stays constant, except for Hispanic women for whom it continues to increase with age. For men, the trend is a more steady increase over the lifetime. There are strong effects on seroprevalence for birth cohorts after 1980 for women. Excluding vaccinated women in the genital analysis does not substantially affect either the age or cohort effects; excluding vaccinated women from the serum analysis does not substantially affect the age effects but does, as expected, significantly reduce the cohort effects after 1980 (results not shown).

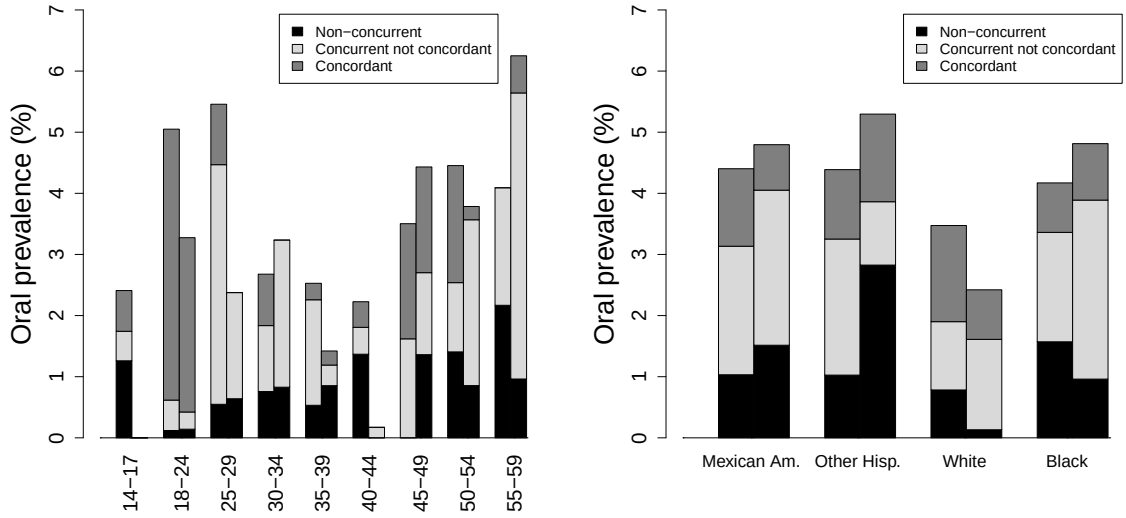

(a) By age.

(b) By race.

Figure 3.1: Oral HPV prevalence with genital concurrence and type-concordance a) by age and b) by race for women ages 14–59 in 2009–2010 and ages 18–59 in 2011–2012. Type-concordant oral infections have a simultaneous genital infection of the same type, and concurrent oral infections have a simultaneously genital infection, not necessarily of the same type. The two bars in each group represent 2009–2010 and 2011–2012 respectively.

Table 3.2: Oral HPV prevalence for women ages 14–59 by genital status with relative risk of oral HPV for +/- genital HPV status in 2009–2010. Here, $\%+$ gives the weighted HPV oral prevalence among the the N people in the given population. Bold relative risks do not contain 1.

	Oral Prevalence Among Genital +			Oral Prevalence Among Genital –			Relative Risk	
Demographic	N	$\%+$	S.E.	N	$\%+$	S.E.	RR	95%CI
All	890	7.0	1.2	1166	1.4	0.4	4.8	**2.6–9.0**
Mexican American	161	9.0	1.8	276	1.6	1.1	5.5	**1.4–21.2**
Other Hispanic	94	8.0	2.2	139	1.8	0.6	4.5	**1.9–10.5**
White	366	7.2	2.1	514	1.3	0.6	5.7	**2.0–16.1**
Black	220	4.3	1.5	156	3.9	1.5	1.1	0.4–3.0
14–17	49	6.3	1.8	195	1.5	0.8	4.1	**1.3–12.9**
18–24	195	8.6	3.3	154	0.3	0.3	30.4	**3.9–236**
25–29	123	9.5	3.4	98	1.1	0.2	8.4	**4.0–17.8**
30–34	81	4.9	2.3	113	1.2	0.9	3.9	0.7–21.7
35–39	99	5.0	2.6	117	0.9	0.6	5.6	**1.1–29.6**
40–44	93	2.4	1.3	145	2.1	1.5	1.2	0.2–6.1
45–49	107	8.1	3.7	126	0	0	—	—
50–54	80	9.2	3.4	128	2.1	1.4	4.3	0.9–20.0
55–59	63	5.2	3.2	90	3.4	2.0	1.5	0.3–8.1

Table 3.3: Genital HPV prevalence by all, oncogenic, and vaccine genotypes for women ages 14–17 and 18–24 and relative risk by vaccination status in 2009–2010 and 2011–2012. Here, $\%+$ denotes the weighted genital HPV prevalence of the listed genotypes among the N people in the population.

			Unvaccinated			Vaccinated			Relative risk	
Age	Year	Genotypes	N	$\%+$	S.E.	N	$\%+$	S.E.	RR	95%CI
14–17	2009–10	All	145	16.4	2.1	103	20.9	5.0	1.3	0.7–2.2
	2009–10	Oncogenic	145	13.0	1.7	103	17.3	5.4	1.3	0.7–2.6
	2009–10	6, 11, 16, 18	145	5.7	2.3	103	1.1	0.8	0.2	0.0–1.0
18–24	2009–10	All	251	57.8	5.1	109	59.4	4.6	1.0	0.8–1.3
	2009–10	Oncogenic	251	44.8	4.6	109	47.0	5.5	1.0	0.8–1.4
	2009–10	6, 11, 16, 18	251	19.9	3.7	109	3.5	1.0	0.2	0.1–0.3
18–24	2011–12	All	197	57.4	4.4	132	55.0	5.2	1.0	0.8–1.2
	2011–12	Oncogenic	197	43.8	5.7	132	38.8	5.5	0.9	0.6–1.3
	2011–12	6, 11, 16, 18	197	12.9	3.5	132	1.9	0.9	0.1	0.1–0.4

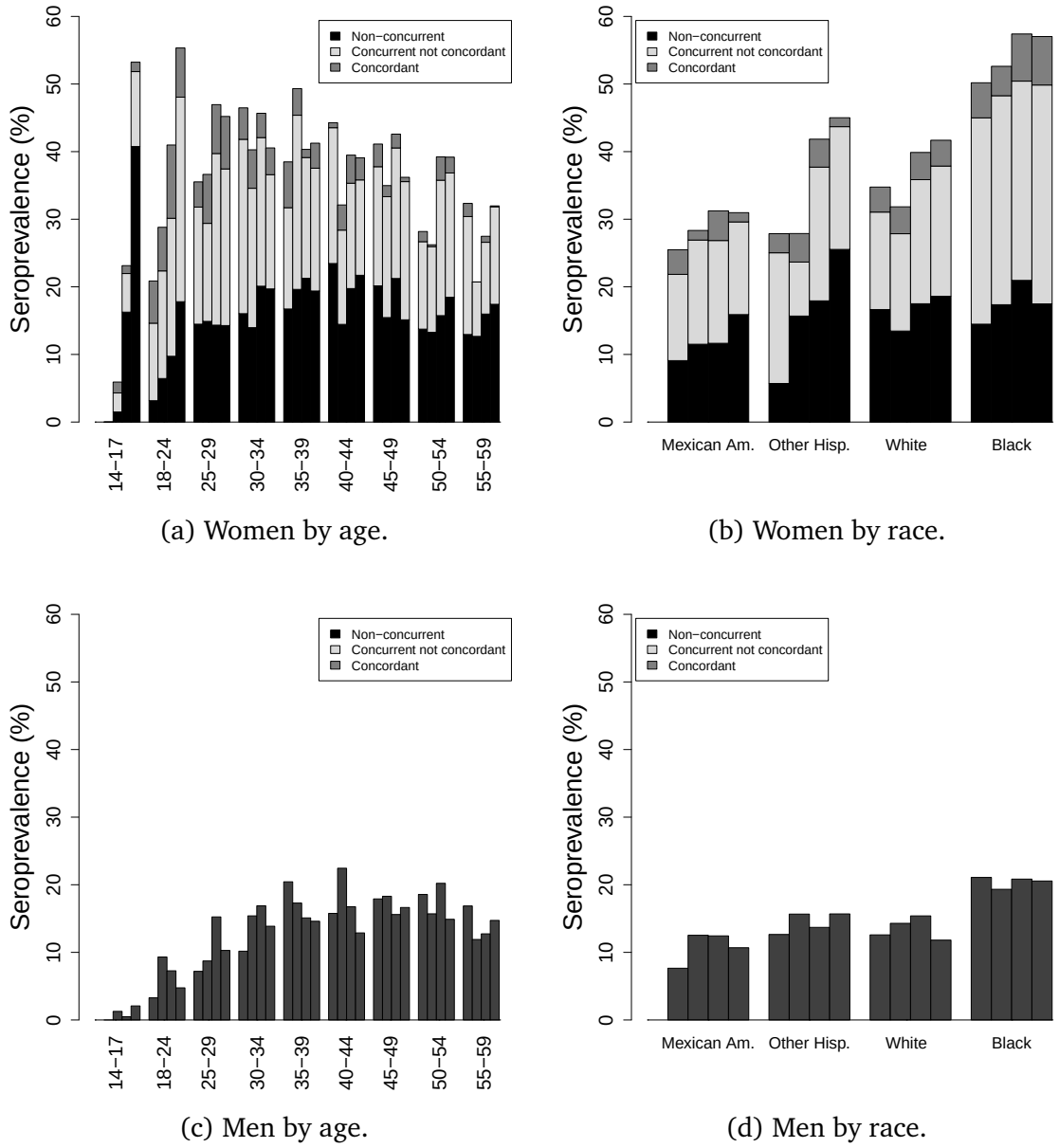

(a) Women by age.

(b) Women by race.

(c) Men by age.

(d) Men by race.

Figure 3.2: HPV seroprevalence for women with genital concurrence and type-concordance, and HPV seroprevalence for men, both ages 14–59. Concurrence means a positive serum result for 6, 11, 16, or 18 and a genital infection of any genotype, and concordance means that the antibody serotype matches the genotype of the genital infection. The four bars in each group are 2003–2004, 2005–2006, 2007–2008, and 2009–2010 respectively. Note: data for 14-17 year old men and women is not available in 2003–2004.

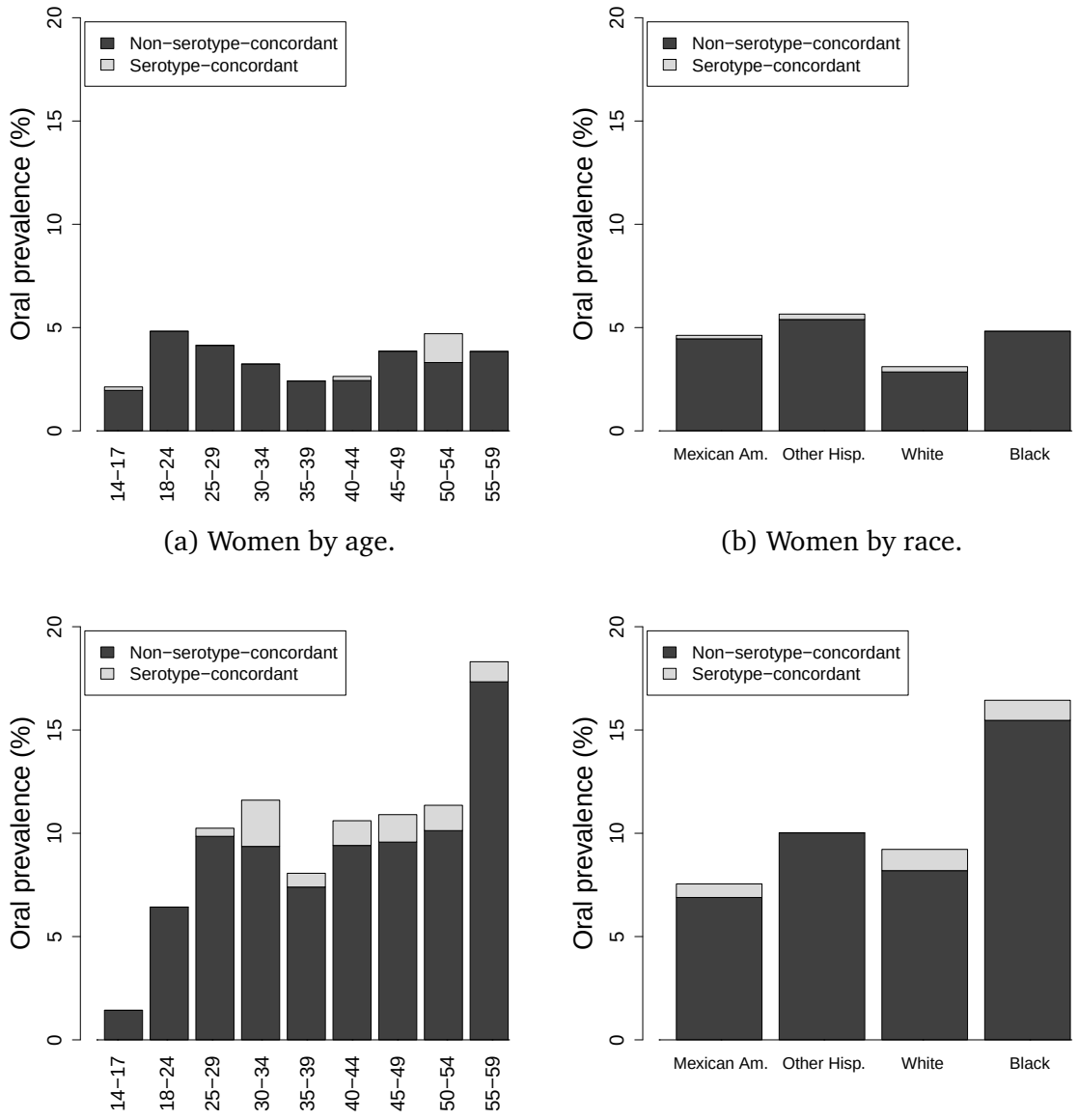

(a) Women by age.

(b) Women by race.

(c) Men by age.

(d) Men by race.

Figure 3.3: Oral HPV prevalence with serotype-concordance for men and women by age and race in 2009–2010. Serotype-concordance defined as an oral infection of type 6, 11, 16, or 18 with serum antibodies of the same type.

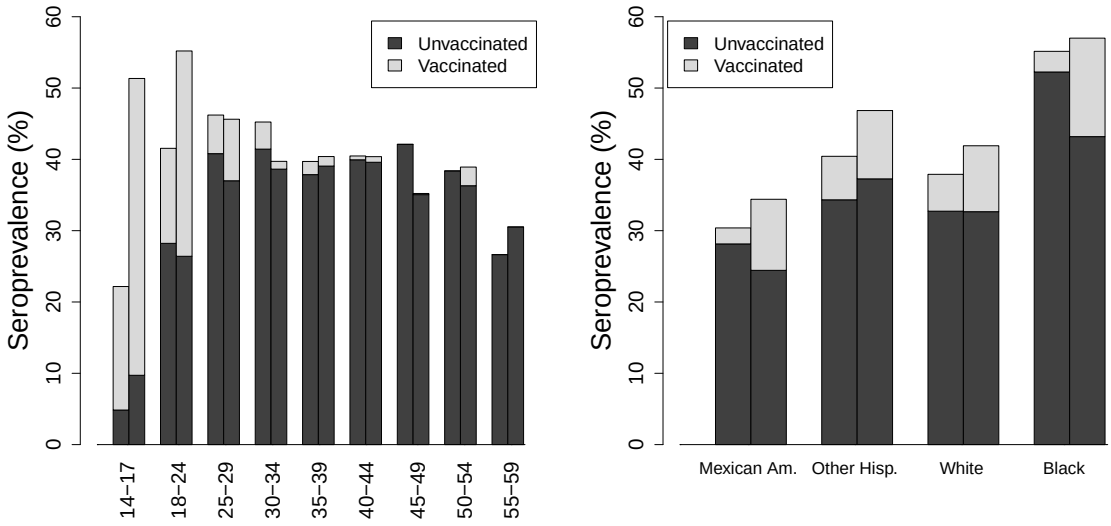

(a) By age.

(b) By race.

Figure 3.4: HPV seroprevalence by vaccination status a) by age and b) by race for women ages 14–59. The two bars in each group represent 2007–2008 and 2009–2010 respectively.

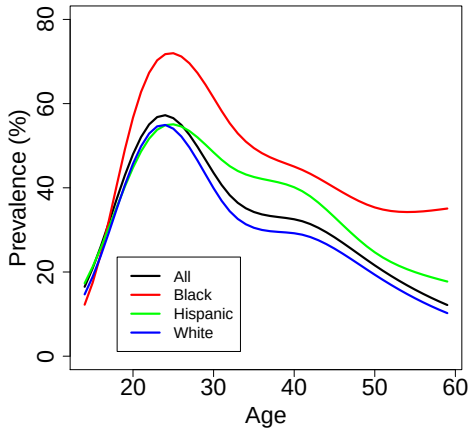

(a) Female genital prevalence by age.

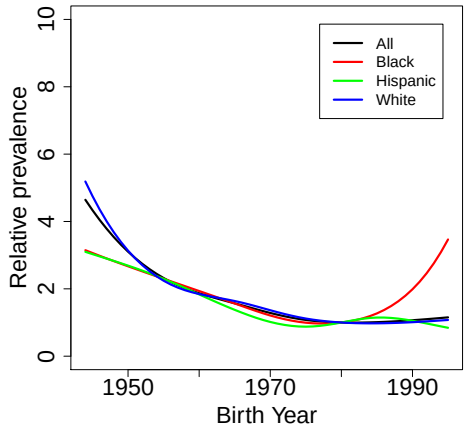

(b) Relative female genital prevalence by cohort.

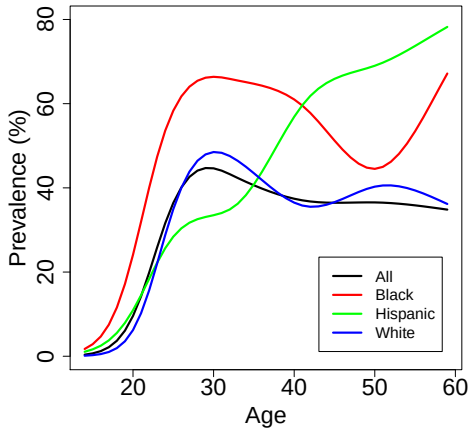

(c) Female seroprevalence by age.

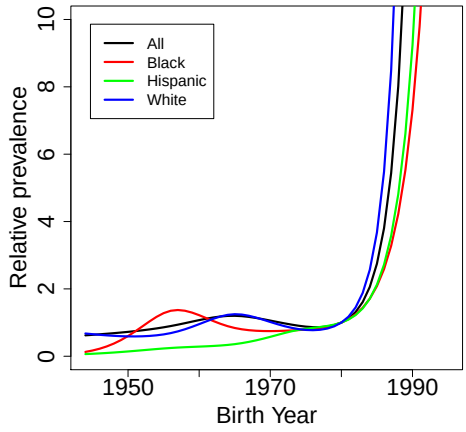

(d) Relative female seroprevalence by cohort.

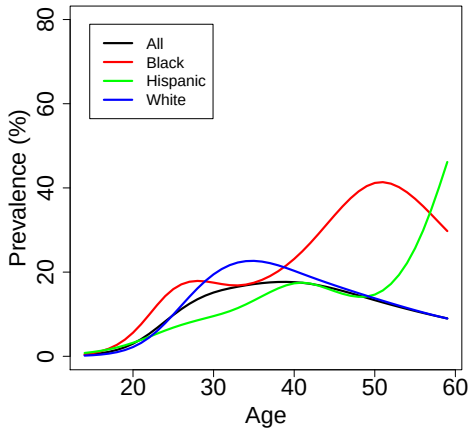

(e) Male seroprevalence by age.

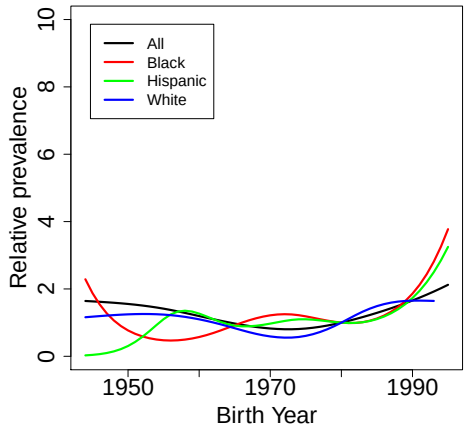

(f) Relative male seroprevalence by cohort.

Figure 3.5: APC models of genital HPV prevalence among women, seroprevalence among women, and seroprevalence among men by age and cohort and by race.

3.4 Discussion

Oral prevalence and oral–genital concurrence vary dramatically with age. Just under half of oral infections among 14–17 year olds are concurrent with a genital infection, but, between ages 18–40, more than 70% of oral infections are concurrent. This concurrence peaks for women ages 18–24, for whom nearly all oral infections are concurrent, over 90% of which are type-concordant (Figure 3.1). This may suggest that many 18–24 year olds are experiencing their first oral infection and that it is either caused by autoinoculation from their genital infection or that both infections are from the same sexual partner. That we do not see the same pattern among ages 14–17 may be indicative of different sexual norms and practices between the two groups, a possibility that warrants further study. There is another age span, 45–54, with both higher overall prevalence and higher concurrence. This may be indicative of a second sexual debut.

The differences in genotype prevalence between the two sites for the 18–24 year old group lend evidence to the theory that certain genotypes are strongly tropic—have an inclination toward certain tissue. Genotype 84 is more than twice as prevalent as the next most common genotype for oral infections in women ages 18–24 in 2009–10 and is still the most common in 2011–2012. Although NHANES has not tested for HPV genital infections in men, there is evidence that genotype 84 is at least as common as type 16 among male genital infections (Skiest and Margolis, 2008). It may be that most genotypes have a great inclination toward cervical tissue while certain genotypes, such as 84 and 16, are more likely to infect both. The high level of type-concordance among 18–24 year olds might then be explained by uneven distribution of genotypes caused by selection of sexual partners with similar ages. This theory, as well as the geographical and demographic distribution of genotypes, is a matter for future study.

Overall oral–genital concurrence and type-concordance was previously examined by Steinau et al. (2014), who reported that the relative risk for women ages 18–59

for having an oral infection given a genital infection was 4.86 in 2009–2010. However, the relative risk for having an oral infection given a genital infection changes dramatically with age, as seen in Table 3.2, although the high relative error for some estimates makes strong conclusions difficult. Women ages 18–24 with a genital infection have a notably higher relative risk of also having an oral infection. The relative risks for Mexican Americans, other Hispanics, and non-Hispanic whites are all similar but that for non-Hispanic blacks, who have lower than average oral prevalence among those with genital infections and a higher oral prevalence than average among those without genital infections, is much lower. In contrast, the relative risk of a genital infection given an oral infection is 2.0 and does not vary as dramatically by race or age (supplement).

The relatively low oral–genital type–concordance overall, noted by Steinau et al. (2014) and others, suggests that, although not independent, the sites have differences in natural history (e.g. time to clearance). However, because oral infection is relatively uncommon among women, the actual number of infected women sampled is also relatively low, and the *age-specific* concurrence and type-concordance results must be seen as suggestive and not necessarily conclusive. In terms of race, white women have the lowest oral prevalence but the highest type-concordance. Hispanic women have the highest overall oral prevalence but genital prevalence comparable to white women, who have the lowest prevalence for both sites. The differences by race may be indicative of assortativity of sexual networks (Morris et al., 2009) and racial heterogeneity of sexual behaviors.

About half of women who are seropositive do not have an accompanying genital infection. Among those who are seropositive and have a concurrent genital infection, type-concordant prevalence is low and decreases with age, as might be expected since older individuals are more likely to have already seroconverted during previous infections. For racial demographics, seroprevalence more closely follows the genital rather than oral profile. This finding may simply be a result of genital infections being much more common than oral ones for women, but it also raises

the possibility that seroconversion may occur more readily following cervical rather than oral infection. Combined with the different relative risk of being seropositive given an oral infection for men and women (Figure 3.3), this observation lends evidence to the theory that seroconversion is strongly site-specific and occurs primarily at mucosal epithelia. Cervical infections appear to often lead to seroconversion, which, based on the lack of sero–oral type-concordance in women, may provide a defense against oral infection. Men are less likely to seroconvert from genital infections (Lu et al., 2012), and so may be more vulnerable to oral infections, resulting in a higher oral prevalence.

Seroprevalence increases dramatically for 14–17 and 18–24 year old women over the period studied. Since the aim of the vaccine is seroconversion, it is likely that this increase is largely caused by the introduction of the vaccine (Figure 3.4). If one does not control for age, overall genital prevalence and prevalence of oncogenic types is higher in the vaccinated population than in the unvaccinated, and prevalence of the genotypes targeted by the vaccine is only slightly lower among the vaccinated group. Because the vaccine is relatively new, it may be being given to previously infected individuals. If we restrict our attention to either 14–17 or 18–24 year olds, as in Table 3.3, the relative risk for any and oncogenic HPV drops to near 1, and that of the vaccine types drops to about 0.2. Our results refine those reported by Markowitz (2013) (Markowitz et al., 2013), who found that, in NHANES 2007-2010, prevalence of vaccine types was 12.6% among unvaccinated 14–19 year olds but 3.1% among those vaccinated. These results suggests that the vaccine has been highly effective at preventing infections by the targeted types. The current data neither support nor refute the possibility that other genotypes may move in to fill the niche left by the vaccine genotypes.

Non-Hispanic black men and women have consistently high prevalence at genital and oral sites and seroprevalence, which is consistent with previous work (Steinau et al., 2014; Markowitz et al., 2009). The APC cohort trends for female geniral prevalence (Figure 3.5) suggest that this high prevalence relative to the other racial

groups has not changed much between the 1955 and 1980 birth cohorts and has, in fact, been increasing since the 1980 birth cohort. Sexual assortativity patterns and other contributing factors may have been relatively consistent between the 1970s and 1990s, the times that people from these birth cohorts would have been mostly sexually active. The relative prevalence among women of all demographics decreased after the 1940 birth cohort, the cohort that experienced the sexual revolution of the 1960s. For women of all races, cohort effects for seroprevalence for women are dominated by a large increase for those born after 1980, most likely a consequence of vaccine-induced seroconversion. That age–cohort models fit better than age–period is not surprising, both as trends in STI prevalence tend to be driven by cohort sexual norms and as the NHANES time span is limited.

One strength of this study is the large sample size in the NHANES survey, which allowed analysis at a relatively fine demographic stratification. NHANES is the only population data source for oral infections and also allows for analysis of multiple sites in one individual. Additionally, the use of APC models allows for the analysis of temporal trends in the data separate from the age effects. Limitations of the NHANES data set include the relatively limited time span, especially for oral infections, and the lack of genital prevalence for men and anal prevalence for men/women. Anal infections may play an important role in seroconversion, especially for men (Lu et al., 2012). Further, the relatively low numbers of infected in some demographic categories precludes strong conclusions about age-related patterns of concurrence/type-concordance.

This study follows the analysis by Steinau et al. (2014) and provides a deeper look at genital–oral concurrent and type-concordant infections. This study is the first to analyze seroprevalence in NHANES after 2003–2004 (Markowitz et al., 2009) and the first to look at concurrence/concordance between serpositivity and oral/genital infections. Our results demonstrate that, in the presence of vaccination, seroprevalence alone is neither a good biomarker for oral infections nor a sufficient one for genital infections in women. Although not independent, genital and oral infection

and seropositivity appear insufficiently correlated to be predictive of each other. Conducting studies where sampling is done at all three sites for both men and women is paramount to fully characterize the natural history of HPV and its transmission dynamics.

3.5 Appendix

Given an incidence I and at-risk population N, it is straightforward to model $\lambda = I/N$. If, alternatively, one wishes to model prevalence P, one may convert as follows.

$$\log \lambda = \log \frac{I}{N} = \log \frac{\frac{I}{I+N}}{\frac{N}{I+N}} = \log \frac{P}{1-P} = \text{logit } P \tag{3.3}$$

Confidence intervals for prevalence ratios were calculated by a log transformation. The standard errors of the natural log of prevalence ratios were approximated as follows:

$$SE(\ln \hat{p}_1/\hat{p}_0) = \sqrt{\frac{\hat{\sigma}^2_{\hat{p}_1}}{\hat{p}_1^2} + \frac{\hat{\sigma}^2_{\hat{p}_0}}{\hat{p}_0^2}} \tag{3.4}$$

Table 3.4: Genital HPV prevalence for women ages 14–59 by oral status with relative risk of genital HPV for +/- oral HPV status in 2009–2010. Here, $\%+$ gives the weighted HPV genital prevalence among the the N people in the given population. Bold relative risks do not contain 1.

	Genital Prevalence Among + Oral			Genital Prevalence Among - Oral			Relative Risk	
Demographic	N	$\%+$	S.E.	N	$\%+$	S.E.	RR	95%CI
All	86	76.7	5.1	1970	39.3	1.4	2.0	**1.7–2.3**
Mexican American	20	76.6	12.9	417	35.5	2.2	2.2	**1.5–3.1**
Other Hispanic	10	76.6	7.1	223	40.7	2.5	1.9	**1.5–2.3**
White	35	77.4	8.3	845	36.2	1.7	2.1	**1.7–2.7**
Black	16	62.3	9.5	360	59.8	3.0	1.0	0.8–1.4
14–17	8	47.7	14.4	236	17.4	2.6	2.7	**1.4–5.3**
18–24	16	97.6	2.5	333	55.4	4.3	1.8	**1.5–2.1**
25–29	13	89.9	2.9	208	49.3	3.4	1.8	**1.6–2.1**
30–34	8	71.7	22.6	186	38.3	3.9	1.9	1.0–3.6
35–39	7	78.9	15.2	209	39.1	4.1	2.0	**1.3–3.1**
40–44	7	38.6	22.3	231	35.0	3.2	1.1	0.3–3.5
45–49	8	100	0.0	225	41.2	4.4	2.4	**2.0–3.0**
50–54	12	68.4	14.7	196	31.7	5.2	2.2	**1.3–3.7**
55–59	7	47.0	22.2	146	36.4	5.4	1.3	0.5–3.4

CHAPTER IV

Transmission heterogeneity and autoinoculation in a multisite infection model of HPV

4.1 Introduction

The *basic reproduction number* R_0 is an important quantity in infectious disease systems epidemiology, defined as the average number of secondary cases arising from an typical primary case in an entirely susceptible population (Diekmann et al., 1990; Anderson and May, 1991; Diekmann and Heesterbeek, 2000). The basic reproduction ratio has a threshold value that controls the stability of the disease-free equilibrium: if $R_0 < 1$, an emergent disease will die off quickly, while if $R_0 > 1$, the disease will become epidemic (Diekmann and Heesterbeek, 2000; van den Driessche and Watmough, 2002). The values of R_0 vary greatly by disease (Anderson and May, 1991), ranging from close to 1 for seasonal influenza to 5–7 for smallpox and polio to 12–18 for measles and pertussis. Mathematical modeling is used to estimate the basic reproduction number and other relevant quantities. In practice, R_0 is calculated as a threshold parameter that may not precisely correspond to the number of secondary cases per infection, especially in the case of an environmentally transmitted disease (van den Driessche and Watmough, 2002). For example, virus shed into the environment may contribute to additional infections not directly attributable to a specific infected person. In practice, R_0 is typically calculated as the spectral radius of the next generation matrix (van den Driessche and Watmough,

2002).

The basic reproduction number also has implications for infection control. If a fraction of the population greater than $1 - \frac{1}{R_0}$ is permanently protected from infection, such as through immunization at birth, the infection cannot become epidemic (Anderson and May, 1991; Diekmann and Heesterbeek, 2000; Roberts and Heesterbeek, 2003). The concept of the basic reproduction number, at least in these infection control terms, can be extended to the type and target reproduction numbers (Roberts and Heesterbeek, 2003; Heesterbeek and Roberts, 2007; Shuai et al., 2013). If there are multiple host types, the *type reproduction number* for host type i is denoted T_i, and the infection can be controlled by protecting a greater fraction than $1 - \frac{1}{T_i}$ of host type i, provided no other host acts as a reservoir for the infection. The type reproduction number is especially of interest for vector-borne and other multiple-species infections, and it can be extend to consider any subset of host types (Roberts and Heesterbeek, 2003; Heesterbeek and Roberts, 2007). The *target reproduction number* is a further generalization, in which specific pathways are targeted for control. This corresponds to considering only certain entries of the next generation matrix, instead of whole rows as is the case of the type reproduction number (Shuai et al., 2013).

Here, we consider a class of diseases that may infect multiple sites in a host. Our motivating example is the Human Papillomavirus (HPV); it is well documented that oral and anogenital sites, although not completely independent, can become infected or clear the virus whether or not the other sites are infected and that autoinoculation may be an important pathway (Steinau et al., 2014). The analysis of oral–genital concurrence in Chapter III lends further weight to the relevance of HPV to this model. However, this model is also relevant to other sexually transmitted infections that affect multiple sites, such as the herpes simplex virus (HSV) (genital, oral, anal), chlamydia (genital, ocular), and yeast infections (genital, oral, etc.). It can also be used to consider multisite infections not typically spread by sexual interaction, such as *Trichophyton* (athlete's foot) or conjunctivitis.

Deviation from the average, or heterogeneity, in various aspects of infectious disease models is important to the study of the basic reproduction number. Heterogeneity of populations, whether in terms of behavior, spatial distribution, or other characteristics, has been widely studied (May and Anderson, 1987; Adler, 1992; Diekmann and Heesterbeek, 2000; Neri et al., 2011) and has led to the development of such tools as mulitgroup modeling. Although the contexts are quite different, like Robertson et al. (2013) we will consider heterogeneity among multiple transmission pathways. While Robertson et al. (2013) considered heterogeneity in the direct and indirect pathways of waterborne cholera transmission, we consider differences within same-site and cross-site transmission of a multisite infectious agent.

In this chapter we first develop and explore the dynamics of a multisite model with homogeneous contacts (homo- or pansexual population or a nonsexual infection), including analysis of the reproduction numbers and the effects of heterogeneity in the transmission pathways. We then extend this multisite model to one with heterogeneous contacts (heterosexual population) and see how the additional complexity translates into the reproduction numbers.

4.2 Two-site model with homogeneous contacts

We first consider a model of a two-site sexually transmitted infection assuming that contacts are homogeneous in order to explore the dynamics of a two-site system without the complication of heterosexual contact. We assume that clearance of the infection does not induce immunity (SIS framework). We denote, without loss of generality, the infection sites as oral and genital. Denote the fraction of the population that is uninfected by S, the fraction infected at site X by I^X for $X \in \{O, G\}$, and the fraction infected at both sites by I^{OG}. Let μ be the birth/death rate, γ^X the recovery rate of infection at site X, ν^{XY} the rate of autoinoculation from site X to site Y, and β^{XY} the transmission rate from site X on one individual to site Y on a second individual. The probability of two simultaneous events is assumed to be

zero. A model schematic is presented in Figure 4.1, a summary of model parameters may be found in Table 4.1, and the following equations define our system:

$$\begin{aligned}
\dot{S} &= \mu + \gamma^G I^G + \gamma^O I^O - S\mu \\
&\quad - S\big((\beta^{OO} + \beta^{OG})(I^O + I^{OG}) + (\beta^{GO} + \beta^{GG})(I^G + I^{OG})\big), \\
\\
\dot{I}^O &= S\big(\beta^{OO}(I^O + I^{OG}) + \beta^{GO}(I^G + I^{OG})\big) + \gamma^G I^{OG} \\
&\quad - I^O\big(\nu^{OG} + \gamma^O + \mu + \beta^{OG}(I^O + I^{OG}) + \beta^{GG}(I^G + I^{OG})\big) \\
\\
\dot{I}^G &= S\big(\beta^{OG}(I^O + I^{OG}) + \beta^{GG}(I^G + I^{OG})\big) + \gamma^O I^{OG} \\
&\quad - I^G\big(\nu^{GO} + \gamma^G + \mu + \beta^{OO}(I^O + I^{OG}) + \beta^{GO}(I^G + I^{OG})\big) \\
\\
\dot{I}^{OG} &= I^O\big(\nu^{OG} + \beta^{OG}(I^O + I^{OG}) + \beta^{GG}(I^G + I^{OG})\big) \\
&\quad + I^G\big(\nu^{GO} + \beta^{OO}(I^O + I^{OG}) + \beta^{GO}(I^G + I^{OG})\big) \\
&\quad - I^{OG}(\gamma^O + \gamma^G + \mu).
\end{aligned} \tag{4.1}$$

A key feature of this class of models is autoinoculation. Here, we consider autoinoculation to be the infection of a new site on a host who currently has at least one infected site in the absence of contact with another infected individual. As noted in van den Driessche and Watmough (2002), it is not always mathematically fixed whether particular terms—in this case, autoinoculation—should be considered *new* infections in the context of the next generation matrix. However, we argue that it is epidemiologically correct to consider autoinoculation to be a stage progression (incorporated in the V matrix) rather than a new infection (reflected in the F matrix). Consider an arbitrary individual, patient zero, with single-site infection who is introduced into a fully susceptible population. The basic reproduction number quantifies the number of secondary people infected by this initial infection over patient zero's whole infective period. If we consider autoinoculation to be a new infection, autoinoculation might cause one secondary infection (at patient zero's

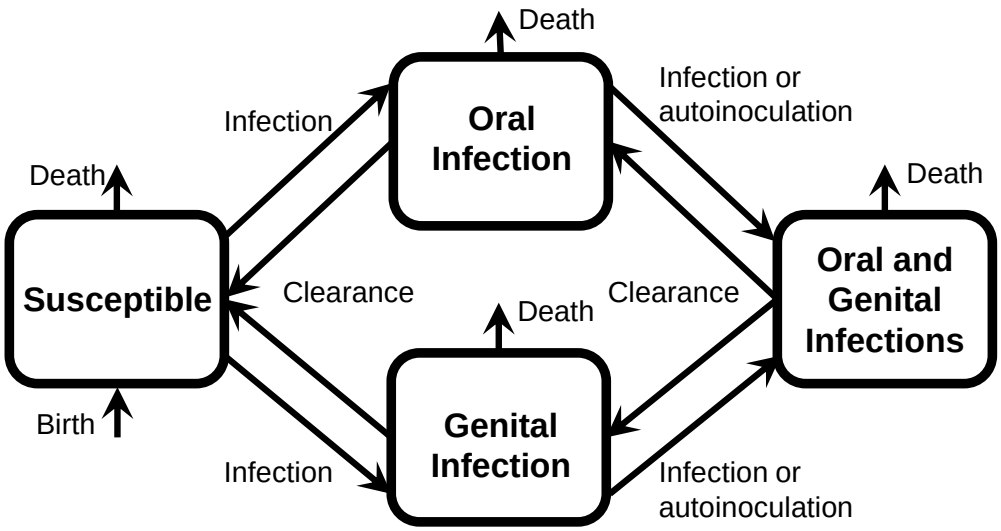

Figure 4.1: Multisite model schematic.

Table 4.1: List of parameters in the two-site infectious disease model with homogeneous contacts.

Symbol	Parameter
μ	Population birth/death rate
β^{OG}	Transmission from oral site to genital site on another person
β^{GO}	Transmission from genital site to oral site on another person
γ^{O}	Clearance of an oral infection
γ^{G}	Clearance of a genital infection
ν^{OG}	Autoinoculation of a genital site from the oral site
ν^{GO}	Autoinoculation of an oral site from the genital site

second site) but result in no new infected people. If we consider it to be a stage transfer, the infection at the new site may also contribute to secondary infections. The second interpretation gives a more epidemiologically meaningful R_0.

4.2.1 Basic Reproduction Number

We begin with a derivation and analysis of the reproduction number for this model (eq. 4.1). We construct the next generation matrix $K = FV^{-1}$ as in van den Driessche and Watmough (2002). The F matrix of new infections is

$$F = \begin{bmatrix} \beta^{OO} & \beta^{GO} & \beta^{OO} + \beta^{GO} \\ \beta^{OG} & \beta^{GG} & \beta^{OG} + \beta^{GG} \\ 0 & 0 & 0 \end{bmatrix}, \tag{4.2}$$

and the V matrix of comparment transfer is

$$V = \begin{bmatrix} \nu^{OG} + \gamma^{O} + \mu & 0 & -\gamma^{G} \\ 0 & \nu^{GO} + \gamma^{G} + \mu & -\gamma^{O} \\ -\nu^{OG} & -\nu^{GO} & \gamma^{O} + \gamma^{G} + \mu \end{bmatrix}. \tag{4.3}$$

Then it is easy to show that V^{-1} has the form

$$V^{-1} = \frac{1}{1 - p^O q^O - p^G q^G} \begin{bmatrix} \tau^O(1 - p^G q^G) & \tau^O p^G q^O & \tau^O q^O \\ \tau^G p^O q^G & \tau^G(1 - p^O q^O) & \tau^G q^G \\ \tau^{OG} p^O & \tau^{OG} p^G & \tau^{OG} \end{bmatrix}, \tag{4.4}$$

where the τ are average waiting times in the compartments, neglecting further

infection as we are considering behavior near the disease-free equilibrium, i.e.

$$\begin{aligned} \tau^O &= \frac{1}{\gamma^O + \nu^{OG} + \mu}, \\ \tau^G &= \frac{1}{\gamma^G + \nu^{GO} + \mu}, \\ \tau^{OG} &= \frac{1}{\gamma^O + \gamma^G + \mu}, \end{aligned} \tag{4.5}$$

and the p and q are probabilities that the next compartment transfer will be to I^{OG} or from I^{OG}, respectively, i.e.

$$\begin{aligned} p^O &= \frac{\nu^{OG}}{\gamma^O + \nu^{OG} + \mu}, \\ p^G &= \frac{\nu^{GO}}{\gamma^G + \nu^{GO} + \mu}, \\ q^O &= \frac{\gamma^G}{\gamma^O + \gamma^G + \mu}, \\ q^G &= \frac{\gamma^O}{\gamma^O + \gamma^G + \mu}. \end{aligned} \tag{4.6}$$

It should be noted that $1 - p^O q^O - p^G q^G > 0$ as long as V is not identically 0. We can heuristically understand the form of V^{-1} in the following way (as in van den Driessche and Watmough (2002)). In compartment I^{OG}, the probability of returning to that compartment in two moves is $p^O q^O + p^G q^G$ by going either to I^O and back or I^G and back. The average amount of time spent in I^{OG}, assuming we start in, say, I^O, is

$$\tau^{OG}\left[p^O + p^O(p^O q^O + p^G q^G) + p^O(p^O q^O + p^G q^G)^2 + \cdots\right] = \frac{\tau^{OG} p^O}{1 - (p^O q^O + p^G q^G)}. \tag{4.7}$$

We can put this heuristic approach in more formal terms: consider the adjacency matrix A of the infected components of the directed graph depicted in Figure 4.2, where entry $a_{m,n}$ is probability of entering component m from component n, for

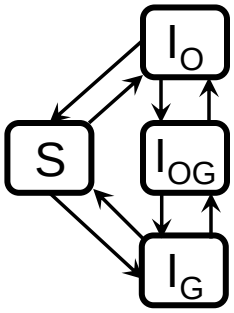

Figure 4.2: Multisite model graph.

$m, n \in \{I^O, I^G, I^{OG}\}$. Thus

$$A = \begin{bmatrix} 0 & 0 & q^O \\ 0 & 0 & q^G \\ p^O & p^G & 0 \end{bmatrix}. \tag{4.8}$$

Then

$$I + A + A^2 + \cdots = \frac{1}{1 - p^O q^O - p^G q^G} \begin{bmatrix} 1 - p^G q^G & p^G q^O & q^O \\ p^O q^G & 1 - p^O g^O & q^G \\ p^O & p^G & 1 \end{bmatrix}. \tag{4.9}$$

This expression, with the inclusion of the τ parameters, leads directly to V^{-1}.

The next generation matrix $K = FV^{-1}$ thus has the form

$$K = \begin{bmatrix} K^{O|O} & K^{G|O} & K^{OG|O} \\ K^{O|G} & K^{G|G} & K^{OG|G} \\ 0 & 0 & 0 \end{bmatrix}, \tag{4.10}$$

where

$$
\begin{aligned}
K^{O|O} &= \frac{\beta^{OO}\tau^{O}(1-p^{G}q^{G}) + \beta^{GO}\tau^{G}p^{O}q^{G} + (\beta^{OO}+\beta^{GO})\tau^{OG}p^{O}}{1-p^{O}q^{O}-p^{G}q^{G}},\\
K^{G|O} &= \frac{\beta^{OO}\tau^{O}p^{G}q^{O} + \beta^{GO}\tau^{G}(1-p^{O}q^{O}) + (\beta^{OO}+\beta^{GO})\tau^{OG}p^{G}}{1-p^{O}q^{O}-p^{G}q^{G}},\\
K^{OG|O} &= \frac{\beta^{OO}\tau^{O}q^{O} + \beta^{GO}\tau^{G}q^{G} + (\beta^{OO}+\beta^{GO})\tau^{OG}}{1-p^{O}q^{O}-p^{G}q^{G}},\\
K^{O|G} &= \frac{\beta^{OG}\tau^{O}(1-p^{G}q^{G}) + \beta^{GG}\tau^{G}p^{O}q^{G} + (\beta^{OG}+\beta^{GG})\tau^{OG}p^{O}}{1-p^{O}q^{O}-p^{G}q^{G}},\\
K^{G|G} &= \frac{\beta^{OG}\tau^{O}p^{G}q^{O} + \beta^{GG}\tau^{G}(1-p^{O}q^{O}) + (\beta^{OG}+\beta^{GG})\tau^{OG}p^{G}}{1-p^{O}q^{O}-p^{G}q^{G}},\\
K^{OG|G} &= \frac{\beta^{OG}\tau^{O}q^{O} + \beta^{GG}\tau^{G}q^{G} + (\beta^{OG}+\beta^{GG})\tau^{OG}}{1-p^{O}q^{O}-p^{G}q^{G}}.
\end{aligned}
\tag{4.11}
$$

The elements of the next generation matrix have a straightforward biological interpretation: $K^{X|Y}$ is the expected number of secondary cases of infection at site Y produced by one individual originally infected at site X, assuming an otherwise susceptible population. Because two events cannot happen simultaneously, all terms of the form $K^{X|OG}$ are zero. It is important to note here that $K^{O|O} \neq R_0^O$ and $K^{G|G} \neq R_0^G$, where $R_0^O = \beta^{OO}\tau^O$ and $R_0^G = \beta^{GG}\tau^G$ are the basic reproduction numbers of the single site SIS models, *except in the case of no autoinoculation*. In this model, without loss of generality, an individual with only a genital infection originally can autoinoculate their oral site and spread infection from either, which adds significant complexity to the terms of the next generation matrix.

We find that the spectral radius of the next generation matrix (eq. 4.10) is

$$
R_0 = \frac{1}{2}\left(K^{O|O}+K^{G|G}\right) + \frac{1}{2}\sqrt{\left(K^{O|O}+K^{G|G}\right)^2 + 4\left(K^{G|O}K^{O|G} - K^{O|O}K^{G|G}\right)}.
\tag{4.12}
$$

It is helpful here to think of $K^{O|O}+K^{G|G}$ as the R_0 of the system under the balance condition that $K^{O|O}K^{G|G} = K^{O|G}K^{G|O}$, that is when the product of the same-site transmission terms of the next generation matrix is equal to the product of the analogous cross-site terms. Hence, more generally, R_0 is $K^{O|O}+K^{G|G}$ modified

by a term that accounts for how balanced same-site and cross-site infections are, which naturally leads us to the question of heterogeneity. The balance term is, in fact, a measure of balance in same-site and cross-site transmission rates, not just in the expectations of number of infected as a cursory inspection of eq. 4.12 would suggest:

$$\begin{aligned} K^{O|G}K^{G|O} - K^{O|O}K^{G|G} &= \frac{\left(\beta^{OG}\beta^{GO} - \beta^{OO}\beta^{GG}\right)\left(\tau^{O}\tau^{G} + p^{O}\tau^{G}\tau^{OG} + p^{G}\tau^{O}\tau^{OG}\right)}{1 - p^{O}q^{O} - p^{G}q^{G}} \\ &= \frac{\left(\beta^{OG}\beta^{GO} - \beta^{OO}\beta^{GG}\right)\tau^{O}\tau^{G}\left(1 + (\nu^{OG} + \nu^{GO})\tau^{OG}\right)}{1 - p^{O}q^{O} - p^{G}q^{G}}. \end{aligned} \tag{4.13}$$

Although all parameters affect the value of R_0, it is the relationship between the transmission parameters that affects the structure of R_0, e.g. whether R_0 is taking the maximum of the same site terms, the geometric average of the cross-site terms, or some sort of intermediate behavior. Hence, understanding the effects of heterogeneity in the transmission parameters is necessary to understand the dynamics of the model.

4.2.2 Limiting cases and transmission heterogeneity

The basic reproduction number displays some interesting limiting behavior. As either $K^{G|O}$ or $K^{O|G}$, but not necessarily both, go to 0, R_0 goes to $\max\left(K^{O|O}, K^{G|G}\right)$. As both $K^{O|O}$ and $K^{G|G}$ go to 0, R_0 goes to $\sqrt{K^{G|O}K^{O|G}}$. Hence, the basic reproduction number can be thought of as occupying a space between taking the maximum and taking a geometric average, displaying behavior more similar to one or the other depending on the type and strength of transmission pathways. Note that these limiting cases are already suggestive of the effect of heterogeneity on the same-site and cross-site terms, which we will explore further below. Considering a different limiting case, we note that as the autoinoculation parameters ν^{GO} and ν^{OG} go to

zero, the basic reproduction number becomes

$$\frac{1}{2}\left(\beta^{OO}\tau^{O}+\beta^{GG}\tau^{G}\right)+\frac{1}{2}\sqrt{(\beta^{OO}\tau^{O}+\beta^{GG}\tau^{G})^{2}+4\tau^{O}\tau^{G}(\beta^{GO}\beta^{OG}-\beta^{OO}\beta^{GG})}, \tag{4.14}$$

which is a significant reduction in complexity.

Without making these significantly simplifying assumptions, we can still consider heterogeneity, as noted above, in the same-site and cross-site terms of the next generation matrix. Heterogeneity can be seen as a kind of weakly limiting case.

Proposition 4.2.1. *For a fixed total $K^{O|G}+K^{G|O}$, R_0 is largest when $K^{O|G}=K^{G|O}$. For a fixed total $K^{O|O}+K^{G|G}$, R_0 is smallest when $K^{O|O}=K^{G|G}$.*

This proposition is clear by basic calculus on eq. 4.12. For a fixed sum $K^{O|G}+K^{G|O}$, the product $K^{O|G}K^{G|O}$ is largest when $K^{O|G}=K^{G|O}$, meaning that R_0 is largest when the two sites have the same expected number of secondary cross-site infections. So, R_0 is large when the cross-site terms are similar and is small when they are different. Similarly, in the formula for R_0 (eq. 4.12), the product $K^{O|O}K^{G|G}$ has the opposite sign from $K^{O|G}K^{G|O}$, meaning that, for a fixed sum $K^{O|O}+K^{G|G}$, heterogeneity in the terms increase R_0. That is, R_0 is large when the expected number of same-site infections is very different for the oral and genital sites and small when they are similar. Heterogeneity in the expected site-specific secondary infections, i.e. elements of the next generation matrix, thus, has a very different effect for same-site than for cross-site infection.

To better understand the effect of heterogeneity in the biological transmission parameters, we derive some analytic results for a special limiting case—identical sites—and then consider, through simulation, how the general model deviates from the limiting case.

4.2.2.1 Identical site model

In order to simplify the analysis, consider the scenario in which the two sites, although they may have different transmission parameters, have identical clearance and autoinoculation parameters. While a simplification for many diseases, this one is biologically realistic for infections such as athlete's foot or conjunctivitis.

For this section, $\gamma_O = \gamma_G$ and $\nu_{OG} = \nu_{GO}$. Hence, $\tau_O = \tau_G$, $p_O = p_G$, and $q_O = q_G$. We drop the subscripts for the rest of this section, except from τ_{OG}, which is distinct from $\tau_O = \tau_G = \tau$. Here

$$K^{O|O} + K^{G|G} = \frac{1}{1-2pq}\left[(\beta^{OO} + \beta^{OG} + \beta^{GO} + \beta^{GG})p\tau^{OG} \right. \\ \left. +(\beta^{OO} + \beta^{GG})\tau(1-pq) + (\beta^{GO} + \beta^{OG})\tau pq\right] \quad (4.15)$$

and

$$K^{O|G}K^{G|O} - K^{O|O}K^{G|G} = \frac{\left(\beta^{OG}\beta^{GO} - \beta^{OO}\beta^{GG}\right)\tau\left(\tau + 2p\tau^{OG}\right)}{1-2pq} \quad (4.16)$$

Proposition 4.2.2. *For a fixed total transmission $\beta^{OO} + \beta^{GO} + \beta^{OG} + \beta^{GG} = k$, the extrema of R_0 of the identical site model are on the boundary of $\left\{\beta^{OO} \geq 0,\ \beta^{GG} \geq 0, \beta^{OG} \geq 0, \beta^{GO} \geq 0\right\}$. Moreover, R_0 is constant on the planes described by $\left\{\beta^{OG} + \beta^{GG} = \frac{k}{2}\right\}$ and $\left\{\beta^{OG} + \beta^{OO} = \frac{k}{2}\right\}$. These planes partition the constrained parameter space into two regions of higher and two regions of lower R_0.*

The proof uses the method of Lagrange multipliers and is left to the appendix (4.5). These partitioning planes contain three lines of interest: $\left\{\beta^{OO} = \beta^{GG},\ \beta^{OG} = \beta^{GO}\right\}$, $\left\{\beta^{OO} = \beta^{GO}, \beta^{GG} = \beta^{OG}\right\}$, and $\left\{\beta^{OO} = \beta^{OG}, \beta^{GG} = \beta^{GO}\right\}$. Along these lines the following are true respectively: $K^{O|O} = K^{G|G}$ and $K^{O|G} = K^{G|O}$; $K^{O|O} = K^{G|O}$ and $K^{G|G} = K^{O|G}$; and $K^{O|O} = K^{O|G}$ and $K^{G|G} = K^{G|O}$.

We wish to visualize the values of R_0 on the surface $\beta^{OO} + \beta^{GO} + \beta^{OG} + \beta^{GG} = k$ in the four dimensional transmission parameter space. In Figure 4.3, we plot slices of

two three-dimensional projections of this surface, with and without the partitioning planes. In this case, the values of R_0 are symmetric in the β^{OG} and β^{GO} coordinates as well as in the β^{OO} and β^{GG} coordinates.

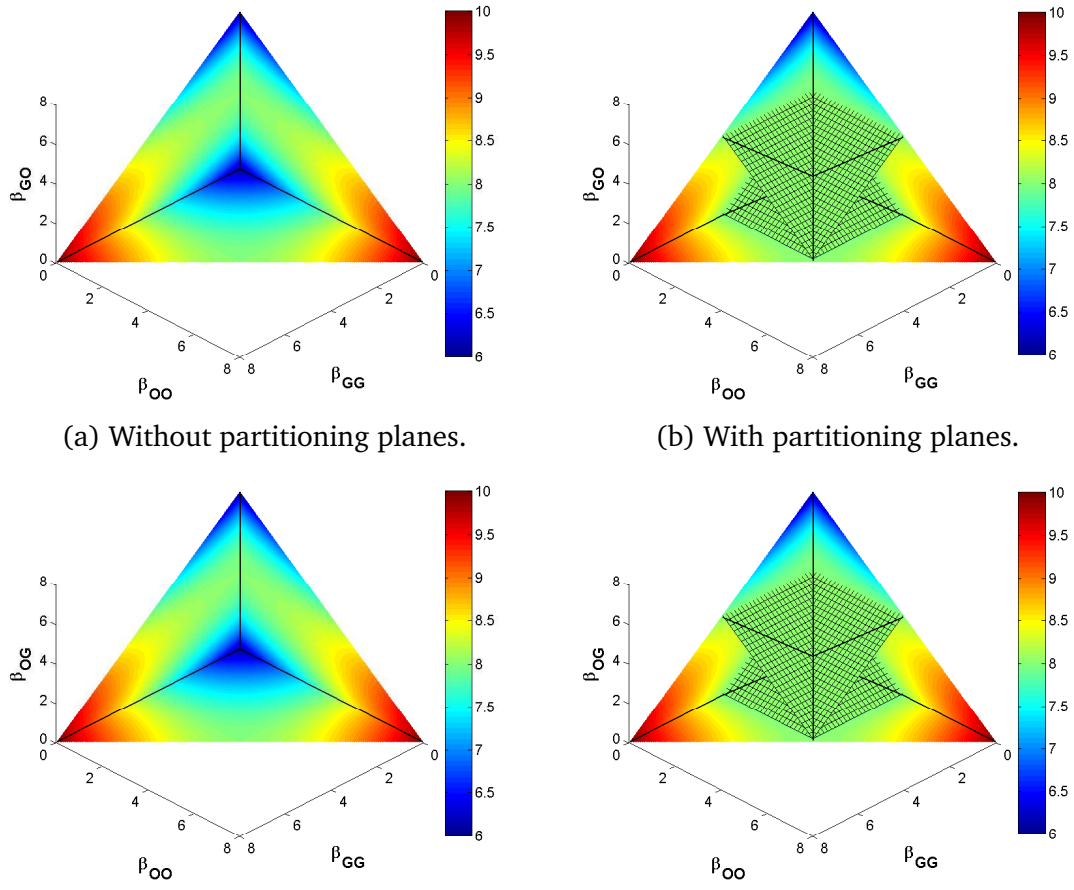

(a) Without partitioning planes.

(b) With partitioning planes.

(c) Without partitioning planes.

(d) With partitioning planes.

Figure 4.3: Heat map of R_0 under the identical site assumptions.

We see that, in the (β^{OO}, β^{GG})-plane (the lower boundary of the figure), R_0 has a minimum, and, in the (β^{OG}, β^{GO})-plane (the z-axis in the figure) R_0 has a maximum. These results are consistent with our analysis above of the impact of heterogeneity of the same-site and cross-site terms of the next generation matrix, highlighting the fact that R_0 is maximized by heterogeneity in same-site transmission and homogeneity in cross-site transmission.

In fact, the planes partition the space into four regions, two of which have larger R_0 (toward primarily same-site transmission) and two of which have smaller R_0

(toward primarily cross-site transmission). The global extrema of R_0 are achieved when there is only one transmission pathway. Indeed, if all transmission is in one pathway with rate k, then eq 4.12 simplifies (via eqs 4.15 and 4.16) to

$$R_0 = \frac{k(p\tau^{OG} + (1-pq)\tau)}{1-2pq} \tag{4.17}$$

if that pathway is same-site and

$$R_0 = \frac{k(p\tau^{OG} + pq\tau)}{1-2pq} \tag{4.18}$$

if that pathway is cross-site. On the partitioning planes of Proposition 4.2.2, we have

$$R_0 = \frac{k(p\tau^{OG} + \tau/2)}{1-2pq}. \tag{4.19}$$

4.2.2.2 Deviations from the identical site model

The equations to solve for the partitioning planes in the general case are intractable. However, numerical simulation gives a reasonably clear picture as to how R_0 behaves under deviations from the identical site model. We examine the effect that changing the autoinoculation and recovery parameters has on the values of R_0 in the constrained transmission parameter space.

Increasing $\frac{\gamma^G}{\gamma^O}$ from 1 (while keeping $\nu^{OG} = \nu^{GO}$ constant) moves the intersection of the three lines of partitioning planes so that $\beta^{OO} < \beta^{OG} = \beta^{GO} < \beta^{GG}$ as seen in Figure 4.4, which has the same parameters as Figure 4.3 except for a larger γ^G. Here, the values of R_0 are symmetric in the β^{OG} and β^{GO} coordinates, but, unlike the identical site model, the values are not symmetric in β^{OO} and β^{GG}. The planes move to balance the faster clearance in the compartment with a higher transmission rate. Note that by increasing one clearance parameter relative to Figure 4.3, R_0 is reduced overall. Increasing both parameters but not changing their ratio would have rescaled the values of R_0 in Figure 4.3 but not broken its symmetries.

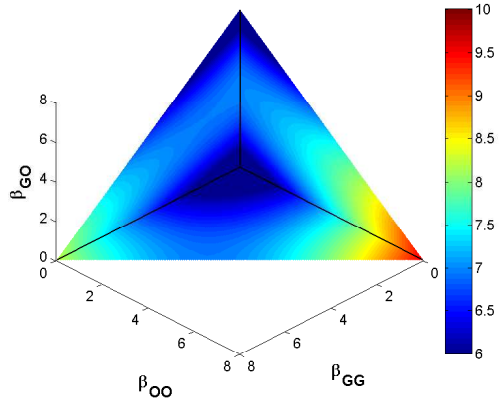

(a) Without partitioning planes.

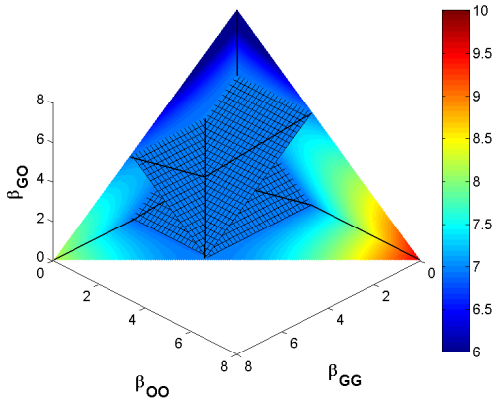

(b) With partitioning planes.

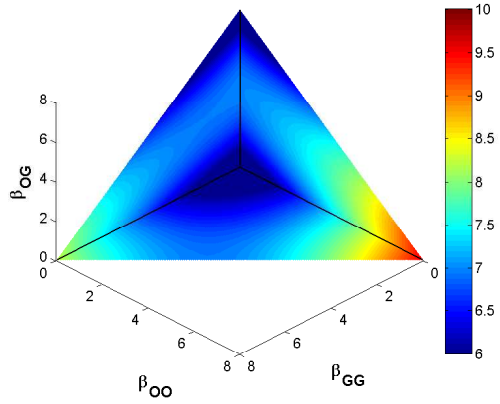

(c) Without partitioning planes.

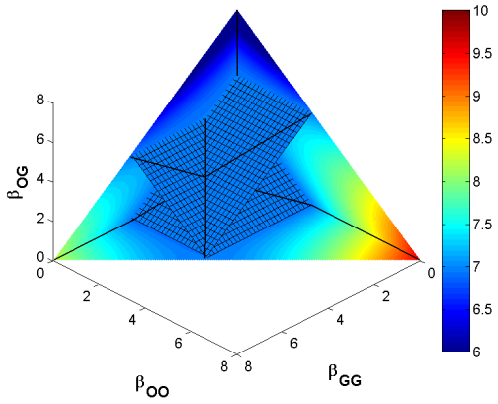

(d) With partitioning planes.

Figure 4.4: Heat map of R_0 for $\gamma_G > \gamma_O$.

Increasing $\frac{\nu^{OG}}{\nu^{GO}}$ from 1 and keeping the recovery parameters constant, moves moves the intersection of the three lines of the partitioning planes so that $\beta^{OG} < \beta^{GG} = \beta^{OO} < \beta^{GO}$ as in Figure 4.5. Now, the values of R_0 are symmetric in β^{OO} and β^{GG} but no longer in β^{OG} and β^{GO}. Here, the surface moves to balance the movement in either direction along the infection cycles; that is, we compensate for an increased ν^{OG} by also increasing its complement in the cycle, β^{GO}, and similarly for the other direction. In Figure 4.5, we see that, as we have only increased one autoinoculation parameter relative to Figure 4.3, autoinoculation acts like transmission to increase R_0 overall, which is as expected.

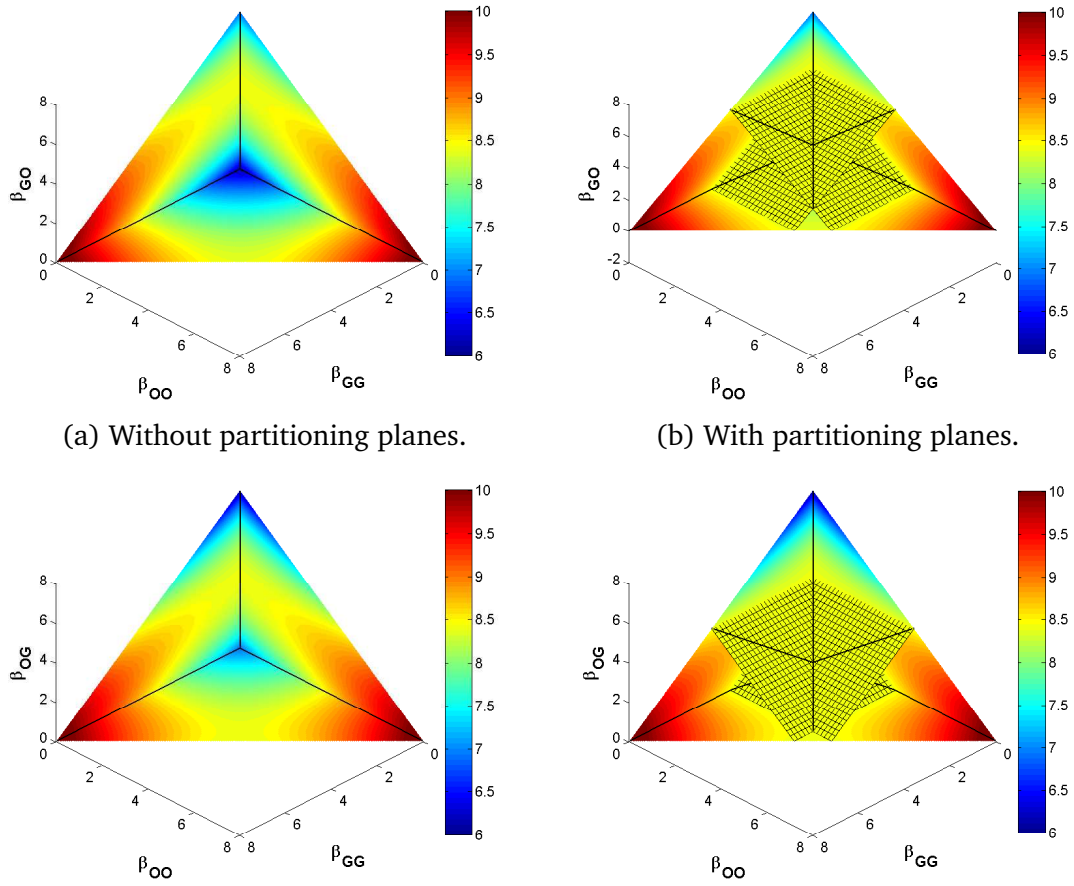

(a) Without partitioning planes.

(b) With partitioning planes.

(c) Without partitioning planes.

(d) With partitioning planes.

Figure 4.5: Heat map of R_0 for $\nu_{OG} > \nu_{GO}$.

In the identical site model, the three lines of the partitioning planes corresponded to equality of pairs of next generation matrix terms. These equalities do not hold along

the corresponding lines of the partitioning planes when $\gamma^O \neq \gamma^G$ or $\nu^{OG} \neq \nu^{GO}$.

Although the position and orientation of the partitioning planes change, the overall qualitative behavior does not. That is, regardless of the values of the recovery and autoinoculation parameters, the extrema of R_0 lie on the boundaries of the positive parameter space, and moving off the partitioning plane increases or decreases R_0 depending on which of the four regions the movement is into. Moving toward primarily same-site transmission increases R_0 while moving toward primarily cross-site transmission decreases it.

4.2.3 Type and target reproduction numbers

Let us next consider the type reproduction number for, without loss of generality, the genital site in the full two-site model (eq. 4.1), calculated as in Shuai et al. (2013). The type reproduction number for genital infections is, provided $K_{OO} < 1$,

$$\begin{aligned} T_G &= \frac{K^{O|G}K^{G|O} + K^{G|G}(1 - K^{O|O})}{1 - K^{O|O}} \\ &= K^{G|G} + \frac{K^{O|G}K^{G|O}}{1 - K^{O|O}}. \end{aligned} \tag{4.20}$$

That is, if the oral site is not an infection reservoir, here meaning that the expected number of oral infections from an oral infection is less than one, then the infection can be controlled by permanently preventing genital infection in a fraction of the population greater than

$$1 - \frac{1}{T_G} = \frac{(K^{G|G} + K^{O|O} - 1) + (K^{G|O}K^{O|G} - K^{O|O}K^{G|G})}{K^{G|G} + (K^{G|O}K^{O|G} - K^{O|O}K^{G|G})}. \tag{4.21}$$

Note the reappearance of the balance term. Further, the possible deleterious effects of model misspecification can be seen here. If one is using a model with only genital infection, one will estimate the fraction of the population in which need to prevent genital infections as $\frac{\beta^{GG}\tau^G - 1}{\beta^{GG}\tau^G}$, which may differ significantly from the true fraction.

We should be careful to realize, however, that the estimates of β^{GG} here may be biased as another result of misspecification, which makes direct comparison of the fractions under the two models difficult.

Returning to the two-site model, if we seek to control only genital-to-genital infections, perhaps through condom use, the target reproduction number is

$$T_{GG} = \frac{(1 - K^{O|O})K^{G|G}}{1 - K^{O|O} - K^{O|G}K^{G|O}}, \tag{4.22}$$

provided $K^{O|O} + K^{O|G}K^{G|O} < 1$. That is, the infection will be controlled if we prevent genital to genital infection by a fraction of more than

$$1 - \frac{1}{T_{GG}} = \frac{(K^{G|G} + K^{O|O} - 1) + (K^{G|O}K^{O|G} - K^{O|O}K^{G|G})}{K^{G|G} - K^{O|O}K^{G|G}}. \tag{4.23}$$

That this latter endeavor is more challenging is seen in the reduction in the denominator between the type and target reproduction numbers described here. The two numbers are the same only if either $K^{O|G}$ or $K^{G|O}$ is zero. That these fractions are the same when $K^{G|O}$ is zero is sensible, since all genital transmission in that case will be same-site transmission. It is not so obviously true, heuristically, in the case that $K^{O|G}$ is zero.

We also include the target reproduction number for either of the cross-site transmissions solely. The target reproduction number, provided both $K^{O|O}$ and $K^{G|G}$ are less than 1, is

$$T_{GO} = \frac{K^{G|O}K^{O|G}}{(1 - K^{O|O})(1 - K^{G|G})}, \tag{4.24}$$

so that the infection will be controlled if we prevent genital to oral transmission by more than

$$1 - \frac{1}{T_{GO}} = \frac{(K^{G|G} + K^{O|O} - 1) + (K^{G|O}K^{O|G} - K^{O|O}K^{G|G})}{K^{G|O}K^{O|G}}. \tag{4.25}$$

Again, to control only genital to oral transmission is easier than controlling all genital infections, and we see that the denominators of eqs. 4.23 and 4.25 add up to the denominator of eq. 4.21. The latter fact is a nice way of expressing that, in this case,

$$T_G = \frac{T_{GO}(T_{GG} - 1) + T_{GG}(T_{GO} - 1)}{T_{GO}T_{GG} - 1}. \tag{4.26}$$

In each of T_G, T_{GG}, and T_{OG}, $K^{O|G}$ and $K^{G|O}$ only appear as a product. That each depends upon the product instead of the sum or some other function of $K^{O|G}$ and $K^{G|O}$ cannot be easily understood without this analysis. This result has implications for disease control. For instance, a product can more effectively be reduced by reducing only one of the terms than a sum can be. Further, the trade-off structure, if one were able to reduce one term at the expense of another, is very different. That $K^{O|G}$ and $K^{G|O}$ only appear as a product also has implications for the impact of heterogeneity in the terms as it did with the basic reproduction number. In each case, heterogeneity in the cross-site terms decreases the reproduction number. The impact of heterogeneity in $K^{O|O}$ and $K^{G|G}$ is less clear for T_G and T_{GG}, though heterogeneity in these same-site terms, unlike for the basic reproduction number, decreases T_{GO}.

4.3 Two-site model with heterogeneous contacts

Here we extend the two-site model with homogeneous contacts (homo- or pansexual population or nonsexual infection) to one with heterogeneous contacts (in particular, a heterosexual population). This model has many analogous features to the model homogeneous contacts, but also has an added layer of complexity from the vector–host-like dynamics (since new infections can only occur from a member of the opposite sex). For sex $i \in \{M, F\}$ with oral (O) and genital (G) sites and

$i \neq j$, we have the following equations:

$$\begin{aligned}
\dot{S}_i &= \frac{\mu}{2} + \gamma_i^G I_i^G + \gamma_i^O I_i^O - S_i\mu \\
&\quad - S_i\big(\beta_{ji}^{OO}(I_j^O + I_j^{OG}) + \beta_{ji}^{GO}(I_j^G + I_j^{OG})\big) \\
&\quad - S_i\big(\beta_{ji}^{OG}(I_j^O + I_j^{OG}) + \beta_{ji}^{GG}(I_j^G + I_j^{OG})\big), \\
\\
\dot{I}_i^O &= S_i\big(\beta_{ji}^{OO}(I_j^O + I_j^{OG}) + \beta_{ji}^{GO}(I_j^G + I_j^{OG})\big) + \gamma_i^G I_i^{OG} \\
&\quad - I_i^O\big(\nu_i^{OG} + \gamma_i^O + \mu + \beta_{ji}^{OG}(I_j^O + I_j^{OG}) + \beta_{ji}^{GG}(I_j^G + I_j^{OG})\big), \\
\\
\dot{I}_i^G &= S_i\big(\beta_{ji}^{OG}(I_j^O + I_j^{OG}) + \beta_{ji}^{GG}(I_j^G + I_j^{OG})\big) + \gamma_i^O I_i^{OG} \\
&\quad - I_i^G\big(\nu_i^{GO} + \gamma_j^G + \mu + \beta_{ji}^{OO}(I_j^O + I_j^{OG}) + \beta_{ji}^{GO}(I_j^G + I_j^{OG})\big), \\
\\
\dot{I}_i^{OG} &= I_i^O\big(\nu_i^{OG} + \beta_{ji}^{OG}(I_j^O + I_j^{OG}) + \beta_{ji}^{GG}(I_j^G + I_j^{OG})\big) \\
&\quad + I_i^G\big(\nu_j^{GO} + \beta_{ji}^{OO}(I_j^O + I_j^{OG}) + \beta_{ji}^{GO}(I_j^G + I_j^{OG})\big) \\
&\quad - I_i^{OG}(\gamma_i^O + \gamma_i^G + \mu).
\end{aligned} \tag{4.27}$$

Here, the parameters are the same as in Table 4.1 except that we additional need to denote that transmission as originating with one of the sexes. In particular, β_{ij}^{XY} are transmission rates from site X in sex i to site Y in sex j and, as before, γ_i^X are clearance rates for sex i and site X and ν_i^{XY} are autoinoculation rates in sex i from site X to site Y. Then the matrix F has the form

$$F = \begin{bmatrix} 0 & F_{ji} \\ F_{ij} & 0 \end{bmatrix}, \tag{4.28}$$

where

$$F_{ji} = \begin{bmatrix} \beta_{ji}^{OO} & \beta_{ji}^{GO} & \beta_{ji}^{OO} + \beta_{ji}^{GO} \\ \beta_{ji}^{OG} & \beta_{ji}^{GG} & \beta_{ji}^{OG} + \beta_{ji}^{GG} \\ 0 & 0 & 0 \end{bmatrix}. \tag{4.29}$$

The V matrix has the form

$$V = \begin{bmatrix} V_i & 0 \\ 0 & V_j \end{bmatrix}, \tag{4.30}$$

where

$$V_i = \begin{bmatrix} \nu_i^{OG} + \gamma_i^O + \mu & 0 & -\gamma_i^G \\ 0 & \nu_i^{GO} + \gamma_i^G + \mu & -\gamma_i^O \\ -\nu_i^{OG} & -\nu_i^{GO} & \gamma_i^O + \gamma_i^G + \mu \end{bmatrix}. \tag{4.31}$$

Then V^{-1} has the form

$$V^{-1} = \begin{bmatrix} V_i^{-1} & 0 \\ 0 & V_j^{-1} \end{bmatrix}, \tag{4.32}$$

where

$$V_i^{-1} = \frac{1}{1 - p_i^O q_i^O - p_i^G q_i^G} \begin{bmatrix} \tau_i^O(1 - p_i^G q_i^G) & \tau_i^O p_i^G q_i^O & \tau_i^O q_i^O \\ \tau_G p_i^O q_i^G & \tau_i^G(1 - p_i^O q_i^O) & \tau_G q_i^G \\ \tau_i^{OG} p_i^O & \tau_i^{OG} p_i^G & \tau_i^{OG} \end{bmatrix} \tag{4.33}$$

and, as in the pansexual model above, the τ are average waiting times, neglecting further infection, in the compartments, and the p_i and q_i are probabilities for sex i that the next compartment transfer will be to go to I_i^{OG} or from I_i^{OG}, respectively.

The next generation matrix $K = FV^{-1}$ thus has the form

$$FV^{-1} = \begin{bmatrix} 0 & F_{ji} V_j^{-1} \\ F_{ij} V_i^{-1} & 0 \end{bmatrix}, \tag{4.34}$$

where

$$F_{ij} V_i^{-1} = \begin{bmatrix} K_{ij}^{O|O} & K_{ij}^{G|O} & K_{ij}^{OG|O} \\ K_{ij}^{O|G} & K_{ij}^{G|G} & K_{ij}^{OG|G} \\ 0 & 0 & 0 \end{bmatrix} \tag{4.35}$$

and

$$K_{ij}^{O|O} = \frac{\beta_{ij}^{OO}\tau_i^O(1-p_i^Gq_i^G) + \beta_{ij}^{GO}\tau_i^Gp_i^Oq_i^G + (\beta_{ij}^{OO}+\beta_{ij}^{GO})\tau_i^{OG}p_i^O}{1-p_i^Oq_i^O-p_i^Gq_i^G}, \tag{4.36}$$

$$K_{ij}^{G|O} = \frac{\beta_{ij}^{OO}\tau_i^Op_i^Gq_i^O + \beta_{ij}^{GO}\tau_i^G(1-p_i^Oq_i^O) + (\beta_{ij}^{OO}+\beta_{ij}^{GO})\tau_i^{OG}p_i^G}{1-p_i^Oq_i^O-p_i^Gq_i^G}, \tag{4.37}$$

$$K_{ij}^{OG|O} = \frac{\beta_{ij}^{OO}\tau_i^Oq_i^O + \beta_{ij}^{GO}\tau_i^Gq_i^G + (\beta_{ij}^{OO}+\beta_{ij}^{GO})\tau_i^{OG}}{1-p_i^Oq_i^O-p_i^Gq_i^G}, \tag{4.38}$$

$$K_{ij}^{O|G} = \frac{\beta_{ij}^{OG}\tau_i^O(1-p_i^Gq_i^G) + \beta_{ij}^{GG}\tau_i^Gp_i^Oq_i^G + (\beta_{ij}^{OG}+\beta_{ij}^{GG})\tau_i^{OG}p_i^O}{1-p_i^Oq_i^O-p_i^Gq_i^G}, \tag{4.39}$$

$$K_{ij}^{G|G} = \frac{\beta_{ij}^{OG}\tau_i^Op_i^Gq_i^O + \beta_{ij}^{GG}\tau_i^G(1-p_i^Oq_i^O) + (\beta_{ij}^{OG}+\beta_{ij}^{GG})\tau_i^{OG}p_i^G}{1-p_i^Oq_i^O-p_i^Gq_i^G}, \tag{4.40}$$

$$K_{ij}^{OG|G} = \frac{\beta_{ij}^{OG}\tau_i^Oq_i^O + \beta_{ij}^{GG}\tau_i^Gq_i^G + (\beta_{ij}^{OG}+\beta_{ij}^{GG})\tau_i^{OG}}{1-p_i^Oq_i^O-p_i^Gq_i^G}. \tag{4.41}$$

Hence, we find the basic reproduction number is

$$R_0 = \sqrt{\frac{1}{2}R^2 + \frac{1}{2}\sqrt{R^4 - 4\left(K_{FM}^{O|O}K_{FM}^{G|G} - K_{FM}^{O|G}K_{FM}^{G|O}\right)\left(K_{MF}^{O|O}K_{MF}^{G|G} - K_{MF}^{O|G}K_{MF}^{G|O}\right)}}, \tag{4.42}$$

where

$$R^2 = K_{FM}^{O|O}K_{MF}^{O|O} + K_{FM}^{G|G}K_{MF}^{G|G} + K_{FM}^{O|G}F_{MF}^{G|O} + K_{FM}^{G|O}F_{MF}^{O|G}. \tag{4.43}$$

We see that the quantity R is the R_0 of the system under the either (or both) of the balance conditions $K_{FM}^{O|O}K_{FM}^{G|G} = K_{FM}^{O|G}K_{FM}^{G|O}$ and $K_{MF}^{O|O}K_{MF}^{G|G} = K_{MF}^{O|G}K_{MF}^{G|O}$. The balance terms appearing in the form of R_0 are analogous to the one we saw in the pansexual model above, but we now have one term for each sex instead of one for the whole population.

The influence of the two-site and the heterosexual aspects of the heterosexual two-site model can be clearly seen in the form of R_0 here. The hallmark of the one-site heterosexual transmission model, similarly to vector–host models, is the geometric

average of the cross-sex elements of the next generation matrix: for the the model

$$\begin{aligned}\dot{S}_i &= \mu\left(\frac{\mu}{2} - S_i\right) + \gamma_i I_i - S_i\beta_{ji}I_j,\\ \dot{I}_i &= S_i\beta_{ji}I_j - \gamma_i I_i,\end{aligned} \tag{4.44}$$

we find

$$R_0 = \sqrt{K_{MF}K_{FM}} = \sqrt{(\beta_{FM}\tau_F)(\beta_{MF}\tau_M)}, \tag{4.45}$$

where $\tau_i = \frac{1}{\gamma_i+\mu}$. In the two-site heterosexual model, although we do not have direct geometric averaging, some patterns are preserved: in eq. 4.42, products (cycles) of the cross-sex elements replace the terms of the homogeneous-contacts model (eq. 4.12) and a square root is taken at the end, as with geometric averaging. In fact, we recover geometric averaging under certain limiting cases, as shown below.

4.3.1 Limiting cases

Here we consider two limiting cases: i) independence of sites and ii) one site is a “dead-end" infection. In the first case, we assume that there is no cross-transmission ($\beta^{OG} = \beta^{GO} = 0$) and no autoinoculation ($\nu^{OG} = \nu^{GO} = 0$). Under these assumptions, the two sites are essentially independent as $K^{O|G} = K^{G|O} = 0$, and the basic reproduction number is

$$R_0 = \max\left(\sqrt{K_{FM}^{O|O}K_{MF}^{O|O}}, \sqrt{K_{FM}^{G|G}K_{MF}^{G|G}}\right) = \max\left(R_0^O, R_0^G\right). \tag{4.46}$$

That is, since there is no autoinoculation, R_0 is the maximum of the of the basic reproduction number for the model with only oral sites R_0^O and the basic reproduction number of the model with only genital sites R_0^G.

In the second case, we assume, without loss of generality, that the oral sites are a “dead-end" infection, that is, oral sites do not transmit the infection ($\beta^{OG} = \beta^{OO} =$

$\nu^{OG} = 0$). Then $K^{O|O} = K^{O|G} = 0$, and, letting $\tau_i = \frac{1}{\gamma_i + \mu}$,

$$R_0 = \sqrt{K_{FM}^{G|G} K_{MF}^{G|G}} = \sqrt{(\beta_{FM}^{GG} \tau_F)(\beta_{MF}^{GG} \tau_M^G)} \tag{4.47}$$

under these assumptions. Thus, despite $\nu_{GO} \not\equiv 0$, R_0 is the same (c.f. eq. 4.45) as the basic reproduction number of the model with only genital sites, R_0^G. This result inintuitive, as additional time spent in compartments I^O or I^{OG} over the infective lifetime will not produce any additional infections.

4.3.2 Type reproduction number

The type reproduction number for either gender, assuming the other is not a reservoir, is the square of the basic reproduction number. This result is sensible because the system is similar to vector–host models for which similar results hold (Roberts and Heesterbeek, 2003). The type reproduction number for, without loss of generality, the genital site, as long as the oral sites are not a reservoir, that is, as long as $\sqrt{K_{FM}^{O|O} K_{MF}^{O|O}} < 1$, is

$$T_G = \frac{A}{2B} + \frac{1}{2B}\sqrt{A^2 - 4B\left(K_{FM}^{O|O} K_{FM}^{G|G} - K_{FM}^{O|G} K_{FM}^{G|O}\right)\left(K_{MF}^{O|O} K_{MF}^{G|G} - K_{MF}^{O|G} K_{MF}^{G|O}\right)}, \tag{4.48}$$

where

$$A = K_{FM}^{O|G} K_{MF}^{G|O} + K_{FM}^{G|O} K_{MF}^{O|G}, \tag{4.49}$$

$$B = 1 - K_{FM}^{O|O} K_{MF}^{O|O} \tag{4.50}$$

Although the form is similar to that of the basic reproduction number (eq. 4.42), there is no final square root because the type reproduction number considers cycles, and there is a term, $1 - K_{FM}^{O|O} K_{MF}^{O|O}$, which takes into account the strength of the infection at the other site.

4.4 Conclusion

In this chapter, I developed a model of a multisite infectious disease and derived expressions for the basic reproduction number under a number of different assumptions and limiting cases. To the best of our knowledge, it is the first analysis of such a model.

We find that autoinoculation adds considerable complexity to the analysis of two-site models. There is a possibility that neglecting autoinoculation may potentially result in severe model misspecification, that is, making incorrect estimations and conclusions as a direct result of using a model that does not fully capture the dynamics. Fortunately, the analysis of the two-site model with homogeneous contacts gives a reasonably clear picture of how the relative magnitudes of the autoinoculation parameters (and, similarly, the clearance parameters) change the impact of heterogeneity in the same-site and in the cross-site transmission parameters (Figures 4.4 and 4.5).

Regardless of the magnitudes of the autoinoculation and clearance parameters, heterogeneity in the cross-site next generation matrix terms decreases R_0 while heterogeneity in the same-site next generation matrix terms increases it. For a fixed total transmission rate, the extrema of R_0 occur when transmission is predominantly through one transmission pathway: the extremum is a maximum when that transmission pathway is same-site and a minimum when it is cross-site. Moreover, the constrained transmission parameter space is partitioned by two planes into four regions in which R_0 is either larger or smaller than its value on the partition.

That heterogeneity affects the pathways differently is surprising given that heterogeneity is classically associated with larger R_0 (Dushoff and Levin, 1995; Diekmann and Heesterbeek, 2000). Robertson et al. (2013) investigated the effect of heterogeneity in transmission pathways for a waterborne disease model, considering heterogeneity in the direct (person-to-person) and indirect (person-to-water-to-person) pathways among different communities as well as their relative contribu-

tions. They found that although it was possible to have high heterogeneity and a low R_0 by minimizing the connectendess of communities (i.e. a low indirect transmission), their measure of heterogeneity, namely the variance of the direct transmission plus twice the covariance of the direct and indirect transmission, was predictive of and increased with R_0. Our results, then, suggest that the effects of heterogeneity in transmission pathways can be very dependent on the structure of the transmission pathways and, thus, should be investigated more broadly.

We are able to comment on the effects of heterogeneity in the clearance and autoincoulation parameters as well. Heterogeneity in the clearance parameters breaks the symmetry between the two same-site transmission terms when considering R_0 on the plane $\beta_{OO} + \beta_{GG} + \beta_{OG} + \beta_{GO} = k$, and heterogeneity in the autoinoculation parameters breaks the symmetry in the cross-site transmission terms. In particular, increasing γ^G relative to γ^O (genital sites clear faster) moves the intersection of the three lines of the partitioning planes so that $\beta^{OO} < \beta^{OG} = \beta^{GO} < \beta^{GG}$. That is, for a fixed sum $\beta^{OO} + \beta^{GG}$, R_0 achieves its minimum at a point where $\beta^{OO} < \beta^{GG}$. Increasing ν^{OG} relative to ν^{GO} moves the intersection point so that $\beta^{OG} < \beta^{OO} = \beta^{GG} < \beta^{GO}$. Thus for a fixed total $\beta^{OG} + \beta^{GO}$, R_0 achieves its maximum at a point where β^{GO} is greater than β^{OG}.

The analysis of the type and target reproduction numbers for the model with homogeneous contacts gives a quantitative way to describe how much more difficult it is to control an infection by targeting a specific pathway rather than a whole site. This may be relevant in the context of HPV, when considering condom use and vaccination as controls. Further, we note the importance of the product of the cross-site infection terms to the basic, type, and target reproduction numbers, a somewhat counterintuitive result. In the pansexual model, $K^{O|G}$ and $K^{G|O}$ never appear anywhere but as the product $K^{O|G}K^{G|O}$. This structure drives the results about cross-site heterogeneity. It may also have implications for the efficacy of different control methods, since a product and a sum are affected by their terms differently and have different trade-off structures.

Although extending the pansexual two-site model to a heterosexual one adds even more complexity, we can see the contributions of the two-site aspect, which balances between taking a maximum and taking a geometric average, and the heterosexual aspect, which incorporates vector–host-like dynamics by taking a square root of transmission cycles between the two sexes. Further, the behavior of the model near limiting cases is clear. However, further analysis is needed to fully flesh out the dynamics of the model more generally.

These results could be generalized to models with more than two sites. Because of the shape of the F matrix, the R_0 of an n-site model will be the largest eigenvalue of the $n \times n$ submatrix of $K = FV^{-1}$ containing only those rows and columns corresponding to infection at a single site. Thus, combinatorial tools might be helpful to study R_0 in this generalized context.

4.5 Appendix

Here, we consider potential locations for extrema of R_0 in $(\beta^{OO}, \beta^{GG}, \beta^{OG}, \beta^{GO})$ space for the identical site model using Lagrange multipliers. Under the identical site assumption, we write the following derivatives:

$$\begin{aligned}\frac{\partial R}{\partial \beta^{OO}} &= \frac{1}{2}\frac{p\tau^{OG}+\tau(1-pq)}{1-2pq} \\ &+ \frac{1}{4}\frac{1}{2R-K^{O|O}-K^{G|G}}\left(2\left(K^{O|O}+K^{G|G}\right)\left(\frac{p\tau^{OG}+\tau(1-pq)}{1-2pq}\right)\right. \\ &\left.-4\left(\frac{\beta^{GG}\tau\left(\tau+2p\tau^{OG}\right)}{1-2pq}\right)\right)\end{aligned} \tag{4.51}$$

$$\begin{aligned}\frac{\partial R}{\partial \beta^{GG}} &= \frac{1}{2}\frac{p\tau^{OG}+\tau(1-pq)}{1-2pq} \\ &+ \frac{1}{4}\frac{1}{2R-K^{O|O}-K^{G|G}}\left(2\left(K^{O|O}+K^{G|G}\right)\left(\frac{p\tau^{OG}+\tau(1-pq)}{1-2pq}\right)\right. \\ &\left.-4\left(\frac{\beta^{OO}\tau\left(\tau+2p\tau^{OG}\right)}{1-2pq}\right)\right)\end{aligned} \tag{4.52}$$

$$\begin{aligned}\frac{\partial R}{\partial \beta^{GO}} &= \frac{1}{2}\frac{p\tau^{OG}+\tau pq}{1-2pq} \\ &+ \frac{1}{4}\frac{1}{2R-K^{O|O}-K^{G|G}}\left(2\left(K^{O|O}+K^{G|G}\right)\left(\frac{p\tau^{OG}+\tau pq}{1-2pq}\right)\right. \\ &\left.+4\left(\frac{\beta^{OG}\tau\left(\tau+2p\tau^{OG}\right)}{1-2pq}\right)\right),\end{aligned} \tag{4.53}$$

$$\begin{aligned}\frac{\partial R}{\partial \beta^{OG}} &= \frac{1}{2}\frac{p\tau^{OG}+\tau pq}{1-2pq} \\ &+ \frac{1}{4}\frac{1}{2R-K^{O|O}-K^{G|G}}\left(2\left(K^{O|O}+K^{G|G}\right)\left(\frac{p\tau^{OG}+\tau pq}{1-2pq}\right)\right. \\ &\left.+4\left(\frac{\beta^{GO}\tau\left(\tau+2p\tau^{OG}\right)}{1-2pq}\right)\right).\end{aligned} \tag{4.54}$$

The method of Lagrange multipliers under the constraint that $\beta^{OO} + \beta^{GO} + \beta^{OG} + \beta^{GG} = k$ is constant, gives the system of equations in which all of the derivatives are equal. The conditions $\frac{\partial R}{\partial \beta^{OO}} = \frac{\partial R}{\partial \beta^{GG}}$ and $\frac{\partial R}{\partial \beta^{OG}} = \frac{\partial R}{\partial \beta^{GO}}$ give that $\beta^{OO} = \beta^{GG}$ and $\beta^{GO} = \beta^{OG}$ respectively. The last condition imay be found as follows:

$$\begin{aligned}
0 &= \frac{\partial R}{\partial \beta^{GG}} - \frac{\partial R}{\partial \beta^{OG}}, \\
&= \frac{1}{2}\tau + \frac{1}{4}\frac{1}{2R - K^{O|O} - K^{G|G}} \left(2\left(K^{O|O} + K^{G|G}\right)\tau \right. \\
&\qquad \left. -4\left(\beta^{GO} + \beta^{OO}\right)\frac{\tau\left(\tau + 2p\tau^{OG}\right)}{1-2pq} \right), \\
&= \left(2R - K^{O|O} - K^{G|G}\right)\tau + \left(K^{O|O} + K^{G|G}\right)\tau - 2\left(\beta^{GO} + \beta^{OO}\right)\frac{\tau\left(\tau + 2p\tau^{OG}\right)}{1-2pq}, \\
&= R - \left(\beta^{GO} + \beta^{OO}\right)\frac{\left(\tau + 2p\tau^{OG}\right)}{1-2pq}.
\end{aligned} \tag{4.55}$$

Under the assumption that $\beta^{OO} = \beta^{GG}$ and $\beta^{GO} = \beta^{OG}$, R simplifies to the following,

$$\begin{aligned}
R &= \left(\frac{(\beta^{OO} + \beta^{OG})p\tau^{OG} + \beta^{OO}\tau(1-pq) + \beta^{OG}\tau pq}{1-2pq} \right) \\
&\quad + \left[\left(\frac{(\beta^{OO} + \beta^{OG})p\tau^{OG} + \beta^{OO}\tau(1-pq) + \beta^{OG}\tau pq}{1-2pq} \right)^2 \right. \\
&\quad \left. + \frac{\left((\beta^{OG})^2 - (\beta^{OO})^2\right)\tau\left(\tau + 2p\tau^{OG}\right)}{1-2pq} \right]^{1/2} \\
&= \frac{(\beta^{OO} + \beta^{OG})p\tau^{OG} + \beta^{OO}\tau(1-pq) + \beta^{OG}\tau pq}{1-2pq} \\
&\quad + \frac{(\beta^{OO} + \beta^{GG})p\tau^{OG} + \beta^{OG}\tau(1-pq) + \beta^{OO}pq\tau}{1-2pq} \\
&= \frac{(\beta^{OO} + \beta^{GG})(\tau + 2p\tau^{OG})}{1-2pq}
\end{aligned} \tag{4.56}$$

It is clear that this condition gives no additional information. All potential interior

extrema lie on the line described by $\{\beta^{OO} = \beta^{GG}, \beta^{OG} = \beta^{GO}\}$. Along this line

$$R_0 = \frac{k(p\tau^{OG} + \tau/2)}{1 - 2pq}. \tag{4.57}$$

Setting the general identical site equation for R_0 equal to this value, we find solutions on two planes, namely $\{\beta^{OG} + \beta^{GG} = \frac{k}{2}\}$ and $\{\beta^{OG} + \beta^{OO} = \frac{k}{2}\}$.

CHAPTER V

Age effects and temporal trends in HPV-related and HPV-unrelated oropharyngeal and oral cavity squamous cell carcinoma in the United States

5.1 Introduction

In 2013, the National Cancer Institute published its Annual Report to the Nation on the Status of Cancer, 1975–2009, highlighting the trends in the burden of human papillomavirus (HPV) associated cancers in the United States. Although total cancer incidence has recently declined, incidence of HPV-positive oropharyngeal (OP) cancers have increased proportionally (Chaturvedi et al., 2011; Jemal et al., 2013), so much so as to be called an epidemic by some (Marur et al., 2010). There appear to be two major etiologies of head and neck squamous cell carcinomas (HNSCC), one with alcohol and tobacco use as predominant etiologic factors (Sturgis et al., 2004), and one related to HPV infection and subsequent HPV genome integration, each with its own prognosis, risk-factor profiles, and genetic markers (Gillison et al., 2012a). HPV-positive cancers appear to be limited to certain subsites of the head and neck, particularly in the oropharyngeal region, and, on the basis of molecular and epidemiologic data, head and neck subsites have been designated as HPV-related or HPV-unrelated (Chaturvedi et al., 2008; Brown et al., 2011, 2012). Not all cancers at HPV-related sites are HPV-positive, but the classification is useful in

the abscence of information about tumor HPV-status in cancer registries.

Analysis of HPV-related oral (oralpharyngeal and oral cavity) squamous cell carcinomas (OSCC) incidence in the Surveillance, Epidemiology, and End Results (SEER) cancer registries, have identified gender disparities but diminishing racial differences in the United States (Brown et al., 2011, 2012). Overall OSCC incidence rates for men are two to four times that of women across all races, though this varies slightly for the different cancer subsite groups (Brown et al., 2012). Racial differences between rates of OSCC in white and black women have largely disappeared. Although rates for black men have historically been higher than for white men, declining rates among black men have been met by a recent increase in incidence for white men (Brown et al., 2011). These results, however, only address overall temporal trends and neither distinguish between age, period and birth cohort trends nor make implications about the underlying biological and epidemiological causes. Multistage clonal expansion (MSCE) models, a class of Markov models, capture the initiation–promotion–progression hypothesis of tumorigenesis, in which normal cells undergo a genetic transformation that leads to clonal expansion, followed by transformations that lead to malignancy (Moolgavkar and Venzon, 1979; Moolgavkar and Knudson, 1981; Luebeck and Moolgavkar, 2002; Meza et al., 2008). Using models that account for the natural history of cancers is important because the effects of carcinogens acting as initiators or promoters results in different temporal trends in the the age-specific incidence of cancer, which can be inferred from population level data (Heidenreich et al., 1997; Meza et al., 2008). MSCE models have been shown to capture temporal patterns of cancer risk and provide insight into the underlying mechanisms leading to population level cancer incidence patterns Meza et al. (2008, 2010b); Luebeck and Moolgavkar (2002); Luebeck et al. (2013). We demonstrate that MSCE models with temporal effects for period and birth cohort separately can better identify temporal trends and place them in the context of putative underlying cancer mechanisms.

Demographic	HPV-related	HPV-unrelated	Oral tongue
White men	32634	27535	11106
Black men	4491	4668	977
White women	9072	13583	7135
Black women	1313	1561	474

Table 5.1: Number of cases of oral (oropharyngeal and oral cavity) squamous cell carcinoma among ages 0–84 between 1973–2011 by race and cancer subsite group.

5.2 Data and methods

5.2.1 Data

We consider a subset of head and neck cancers reported to the Surveillance, Epidemiology, and End Results (SEER) cancer registries. We use the International Classification of Diseases (ICD) codes, as in Chaturvedi et al. (2008); Brown et al. (2011, 2012), to group sites into HPV-related, HPV-unrelated except for oral tongue, and HPV-unrelated oral tongue. A full list of the codes and sites is provided in the supplementary information. For brevity, we will henceforth denote these subgroups as HPV-related, HPV-unrelated, and oral tongue, respectively.

We use SEER 9 data 1973–1991, SEER 13 data 1992–1999, and SEER 18 data 2000–2011, in order to leverage the increased sample size in later years. We refer to this data set as SEER max. Concerns that can arise when combining these data sets—relating to changing racial composition, urban/rural divides, and the geographical distribution of new SEER registries— are minimized in this study by performing separate analyses for white men, black men, white women, and black women. Only white and black races are considered in this analysis, and we do not stratify by Hispanic/non-Hispanic ethnicity; SEER reports incidence rates by ethnic origin only for all races combined, white, and non-white. We consider only ages 0–84, as all cases for ages 85 and over are aggregated in the database. Table 5.1 gives the total number of cases for ages 0–84 for each group between 1973 and 2011.

5.2.2 Two-stage Clonal Expansion Models

The two-stage clonal expansion (TSCE) model was developed by Moolgavkar, Venzon, and Knudson (Moolgavkar and Venzon, 1979; Moolgavkar and Knudson, 1981) to capture the initiation–promotion–progression paradigm. Moolgavkar, Venzon, and Knudson described initiation through a non-homogenous Poisson process and clonal expansion and malignant conversion through a birth–death–mutation process, the details of which are described at length elsewhere Moolgavkar and Venzon (1979); Moolgavkar and Knudson (1981); Moolgavkar and Luebeck (1990); Meza et al. (2008). There are four, possibly age dependent, parameters: initial mutation rate $\mu_0(t)$, growth rate $\alpha(t)$ and death rate $\beta(t)$ of initiated cells, and malignant mutation rate $\mu_1(t)$. In Figure 5.1, we present a schematic of the model, which includes the possible time-dependent effects of HPV or other factors on the parameters.

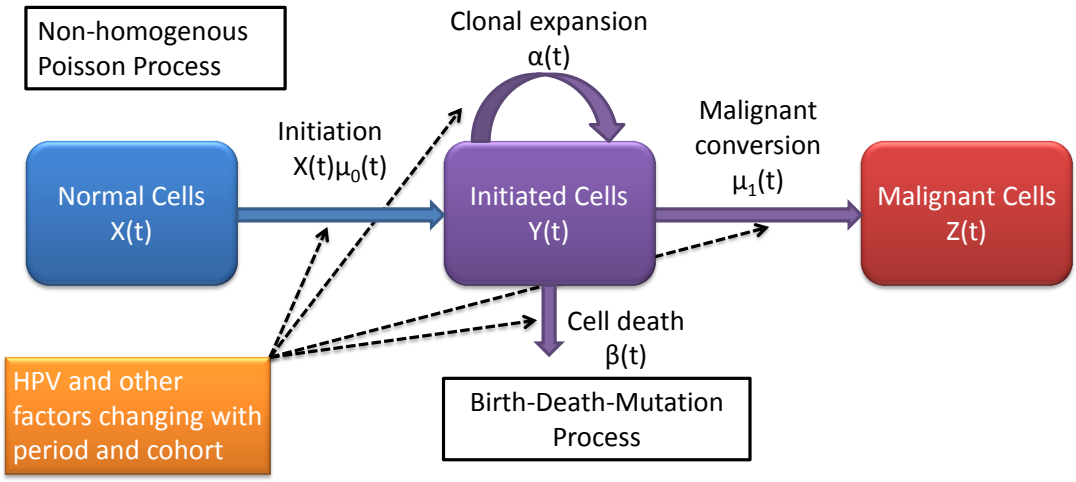

Figure 5.1: Schematic of the two-stage clonal expansion model with period and cohort dependencies.

If the parameters α, β, μ_0, and μ_1 are not age-dependent, the closed form solutions

for the survival and hazard are

$$S(t) = \left(\frac{q-p}{qe^{-pt} - pe^{-qt}} \right)^r, \tag{5.1}$$

$$h(t) = \frac{rpq(e^{-qt} - e^{-pt})}{qe^{-pt} - pe^{-qt}}, \tag{5.2}$$

where

$$r = \frac{\mu_0 X(0)}{\alpha}, \tag{5.3}$$

$$p, q = \frac{1}{2}\left(-(\alpha - \beta - \mu_1) \mp \sqrt{(\alpha - \beta - \mu_1)^2 + 4\alpha\mu_1} \right). \tag{5.4}$$

The parameters themselves are not identifiable in the model given the age-specific incidence, but r, p, and q are identifiable combinations. Note that $-(p+q)$ is the net clonal cell proliferation $\alpha - \beta - \mu_1$, and $pq = -\alpha\mu_1$. Further, $q \approx \mu_1/(1 - \frac{\beta}{\alpha})$ and $p \approx -(\alpha - \beta)$ (Moolgavkar et al., 2009). Hence, we identify (multiplicative) effects on r with effects on initiation, effects on p with effects on promotion, and effects on q with effects on malignant conversion.

Under the TSCE model, the sojourn time T_s of a tumor, the time between the time of tumor onset (first premalignant mutation) and the time of clinical detection can be approximated by

$$T_s \approx -\frac{\ln(q/(-p)}{-p} \approx -\frac{\ln\left(\alpha\mu_1/(\alpha-\beta)^2\right)}{\alpha - \beta} \tag{5.5}$$

(as long as $\mu_1 \ll 1$ and $\mu_1 < p^2/\alpha$) (Meza et al., 2008; Schöllnberger et al., 2010; Luebeck et al., 2013).

In the general case of age-dependent parameters, that is α, β, μ_0, and μ_1 are arbitrary functions of t, numerical solutions can be found (Little et al., 2002; Crump et al., 2005), although we will not consider that case in this investigation. This model formulation may be extended to three stages and other more complex models and has been applied successfully to a variety of cancer types (Hazelton et al.,

2006; Jeon et al., 2006, 2008; Luebeck and Moolgavkar, 2002; Luebeck et al., 2008; Little et al., 2002; Meza et al., 2005, 2008, 2010b,a; Dewanji et al., 2011).

5.2.3 Age–period–cohort models

Age–period–cohort (APC) models are a class of epidemiologic models used to disentangle effects of age, period (factors affecting all people alive at a given time), and birth cohort (factors affecting all people born in a given time period) given prevalence (e.g. HPV prevalence) or incidence (e.g. incidence of oral cancer). The traditional model posits that incidence rates λ are described by a multiplicative model with age (A), period (P), and birth cohort (C) (Holford, 1983, 1991; Clayton and Schifflers, 1987a,b). This is usually treated in the logarithmic form, in which we fit the model

$$\log \lambda = \beta_0 + \beta_A(A) + \beta_P(P) + \beta_C(C), \tag{5.6}$$

where β_0 is a constant and β_A, β_P, and β_C are some functions to be determined, often constained to be discrete functions or splines.

One drawback of full APC models is their inherent unidentifiability: $P = A + C$. To resolve the unidentifiability, one may consider only two effect models, typically age–period or age–cohort, or constrain the age effects to have a given shape, such as the hazard function of a MSCE model, as we do in this analysis (Holford, 1991; Luebeck and Moolgavkar, 2002; Meza et al., 2008; Luebeck et al., 2013).

Given a set of observed cases $\{x_i\}$ with corresponding population-at-risk sizes $\{n_i\}$, we derive a likelihood for the APC model in the following way. We assume that observed incident cases x_i for a given population all of age A_i at time P_i from birth cohort $C_i = P_i - A_i$ are Poisson distributed with mean $\mu_i = n_i \cdot \lambda(A_i, P_i, C_i)$, where λ is the incident rate function dependent on parameter β_0 and functions β_A, β_P, and β_C. Observations are assumed to be independent, and thus the likelihood for the

whole data set of observations $\{x_i\}$ is given by

$$L(\beta_0, \beta_A, \beta_P, \beta_C) = \prod_i \frac{e^{-\mu_i} \mu_i^{x_i}}{x_i!}. \tag{5.7}$$

5.2.4 APC–TSCE hybrid models

In a general APC model, the age effects are not constrained, but if we are working within the TSCE framework, we can restrict the age effects to have the shape of the TSCE hazard:

$$\log \lambda = \beta_0 + \log\left[h(t, r, p, q)\right] + \beta_P(P) + \beta_C(C). \tag{5.8}$$

This added constraint theoretically resolves the non-identifiability problem in the full APC model (Holford, 1991; Luebeck et al., 2013). In the case of constant parameters, the multiplicative assumption of the model translates to an assumption that the period and cohort effects are on the rate of initiation μ_0 since $r = \mu_0 X(0)/\alpha$ and $X(0)$ and α are considered fixed:

$$\lambda = -\left[f(P, C) \cdot r\right] \left(\frac{pq(e^{-qt} - e^{-pt})}{qe^{-pt} - pe^{-qt}}\right). \tag{5.9}$$

However, depending on the mechanism of carcinogenesis for a given cancer and the nature of the risk factors captured by the temporal trends, it is possible that the effects on promotion or malignant conversion rates rather than initiation rates are more realistic. Thus, by considering slightly different models with period or cohort effects acting on the promotion or malignant conversion parameters, one can investigate the impact of period and cohort on different stages of carcinogenesis. In this analysis we consider models of the form

$$\lambda = h(t, \mathbf{r}(P, C), \mathbf{p}(P, C), \mathbf{q}(P, C)). \tag{5.10}$$

Here $\mathbf{r}(P, C) = r \cdot \theta_P(P) \cdot \theta_C(C)$ where θ_P and θ_C are natural splines, r is the value

of $\mathbf{r}$ at the reference period and cohort, and $\mathbf{p}$ and $\mathbf{q}$ are defined similarly.

5.2.5 Optimization

The negative log-likelihood (NLL) for observed cases $\{x_i\}$ with corresponding population-at-risk sizes $\{n_i\}$ under these models is given by

$$\mathrm{NLL}\left(r, p, q, \{\theta_P, \theta_C\}_r, \{\theta_P\, \theta_C\}_p, \{\theta_P, \theta_C\}_q\right) = -\sum_i \left(-\mu_i + x_i \log \mu_i - x_i!\right), \quad (5.11)$$

where $\mu_i = n_i \cdot \lambda(r, p, q, P_i, C_i)$ and $\{\theta_P, \theta_C\}$ are the parameters of the natural spline functions. The negative log likelihood, under the assumptions of each model, was minimized using a Davidon-Fletcher-Powell optimization algorithm in R (v. 3.1) (Luebeck and Meza, 2013). We use the Akaike Information Criterion (AIC) as a measure of model fit. We use the formulation AIC=2(neg. log-likelihood+k) where k is the number of parameters. Hence, a more negative AIC represents a better fit, and one point gain in the negative log-likelihood is equivalent to reducing model complexity by one parameter.

5.3 Results

5.3.1 Age-adjusted incidence

We plot the age-adjusted incidence rates of oral squamous cell carcinomas (OSCCs) reported in SEER max (1973–2011) by subsite group in Figure 5.2; rates are adjusted to the population in the year 2000. For HPV-related sites, incidence rates in white and black women show little to no trend. There appears to be a slight downward trend for black men, but a clear upward trend is seen for white men. For HPV-unrelated sites, all four groups peak in the early 1980s and trend down afterward. For oral tongue sites, incidence for white men has remained relatively constant, black men and black women have trended down (slightly for women and

more strongly for men), and white women have trended slightly up.

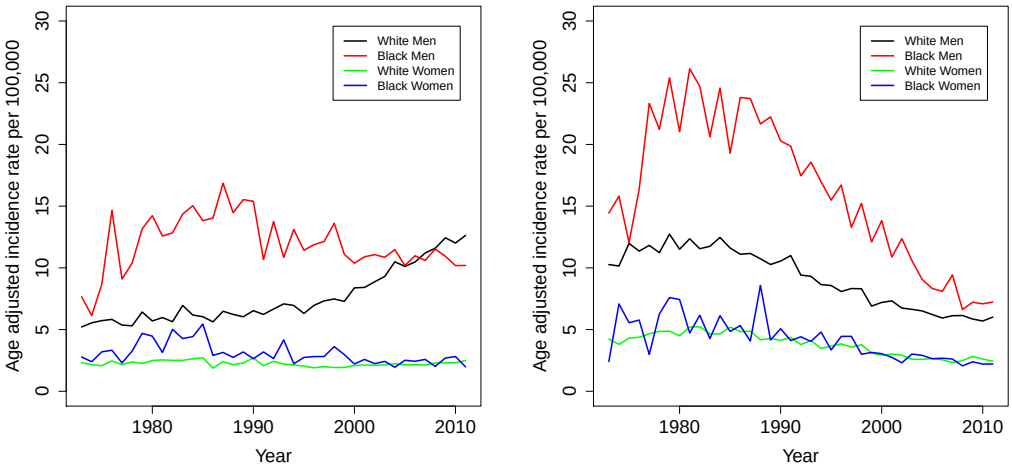

(a)

(b)

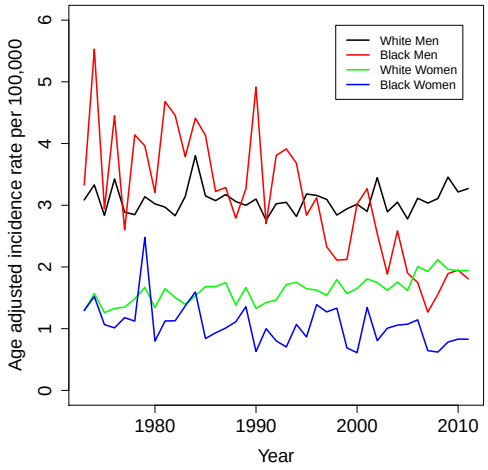

(c)

Figure 5.2: Age-adjusted incidence rates of oral squamous cell carcinoma among ages 30–84 by cancer subsite group: (a) HPV-related, (b) HPV-unrelated, and (c) oral tongue oropharyngeal. Please note the change in axes scale for the oral tongue cancer.

5.3.2 Incidence by period and cohort

In Figure 5.3a, it appears that incidence of HPV-related OSCCs increased dramatically for the birth cohorts between 1940 and 1970. When age-specific incidence is

stratified by period, we see an increasing trend after the early 1990s (Figure 5.3b). For the HPV-unrelated OSCCs, we see a decrease in incidence with each birth cohort decade as well as by period (Figure 5.3c and d). Yearly variation in incidence make interpretation of the other race–cancer-site pairs difficult, and we do not include them here.

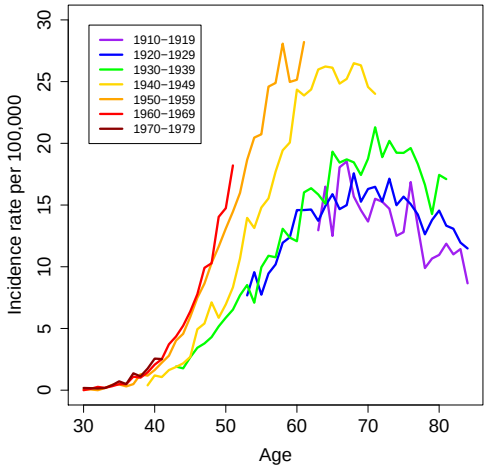

(a) HPV-related incidence by birth cohort.

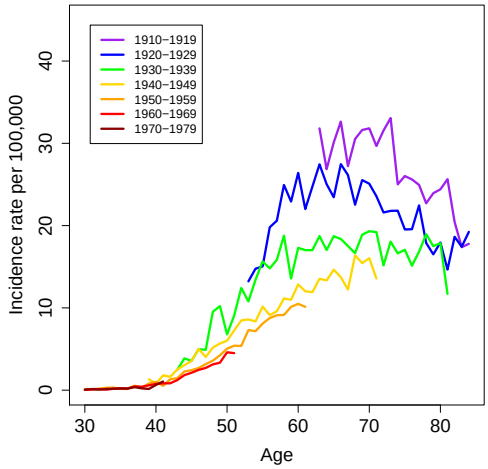

(b) HPV-unrelated incidence by birth cohort.

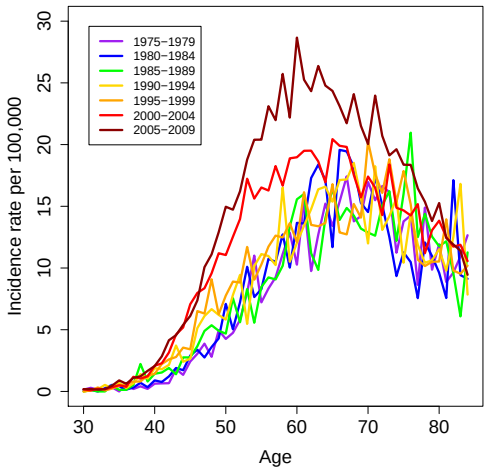

(c) HPV-related incidence by period.

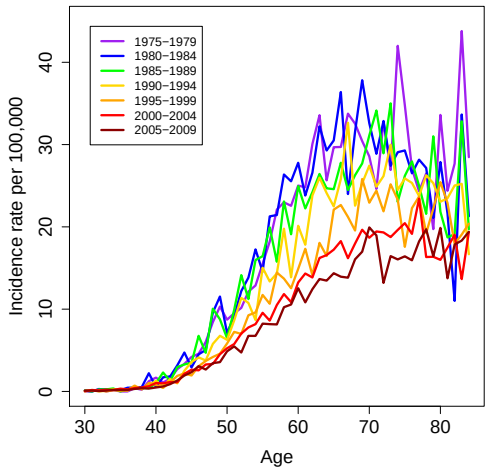

(d) HPV-unrelated incidence by period.

Figure 5.3: Incidence rates by period and cohort of oral squamous cell carcinoma among white males for HPV-related and HPV-unrelated subsites groups.

5.3.3 APC–TSCE model results

We constrain the age effects to the form of a TSCE hazard. We consider period and cohort effects on our proxies for tumor initiation r, promotion p, and malignant conversion q. Further, to force the cohort and period effects into a more realistic form, we use natural splines with eight degrees of freedom for cohort effects and five for period, corresponding to approximately one degree of freedom for twelve and eight years respectively. We choose one model for all demographics in each of the three cancer subsite groups. We determined that period and cohort effects on initiation (r) gave the best model fits for all three subsite groups as this model gave the lowest AIC for most demographics in each category. A table of AIC for the considered models is shown in the appendix. For comparison to this APC–TSCE model, we fitted the standard APC model as well; again, these results may be found in the appendix.

In Figure 5.4, we present the model hazard (age-specific cancer incidence function) for HPV-related, HPV-unrelated, and oral tongue OSCCs, for each of the four considered groups under the model that considers cohort and period effects on r. For all three OSCC subsite groups, the hazard begins to increase earlier for black men than white men and earlier for black women than white women, and the asymptotes for white and black men are higher than for white and black women. The shape of the hazard for the oral tongue sites is qualitatively different from that of the other two.

Cohort effects and period effects are also plotted for this model in Figure 5.4. The cohort and period effects are plotted on a log-scale to emphasize that, for example, an effect of 0.5 and an effect of 2 are equally different from the reference. To interpret the period and cohort effects, note that the product of the two effects gives the modeled relative incidence compared to that of the members of the reference group, here the 1930 birth cohort in 1975.

We observe that, for HPV-related OSCCs, there is a five-fold increase in relative cohort effect for white women between 1900 and 1930 followed by another five-

fold increase between 1930 and 1980, a pretty dramatic change overall. Further, the overall cohort trends for the oral tongue subsites are somewhat similar to those of HPV-related subsites, while those of the HPV-unrelated are different from the other two. Finally, all three cancer subsite groups show decreasing period trends for most demographics, though the period effects for HPV-unrelated and oral tongue OSCC incidence for white women do not follow this pattern.

The estimates of the biological parameters for initiation r, promotion p, and malignant conversion q are presented in Table 5.2. The values of the biological parameters display some clear patterns. For all three cancer subsite groups, men have a larger initiation r than women, regardless of race, and black men and women have a larger promotion p than their white counterparts. Further, the promotion p is very similar for the HPV-related and HPV-unrelated subsites. We can see the effect of the different values of the biological parameters reflected in the plot of the hazards (Figure 5.4). A larger initiation r corresponds to a higher final asymptote (with the exception of black and white women in the HPV-unrelated plot), since the asymptotic value of the hazard $h(t)$ is $r \cdot (-p)$ and the deviance in p is relatively small. Further, a larger promotion p corresponds to an earlier increase in the hazard. We estimate mean sojourn time T_s from the biological parameters: black men and women have shorter sojourn times, and, generally, the sojourn time is shorter for women than for men. White men and women for HPV-related OSCCs are the one exception.

5.4 Discussion

5.4.1 Main findings

Trends in incidence of carcinoma at the three groups of subsites of the oropharynx and oral cavity, namely HPV-related sites, HPV-unrelated sites (except for oral tongue), and oral tongue sites, appear to be primarily driven by period and birth

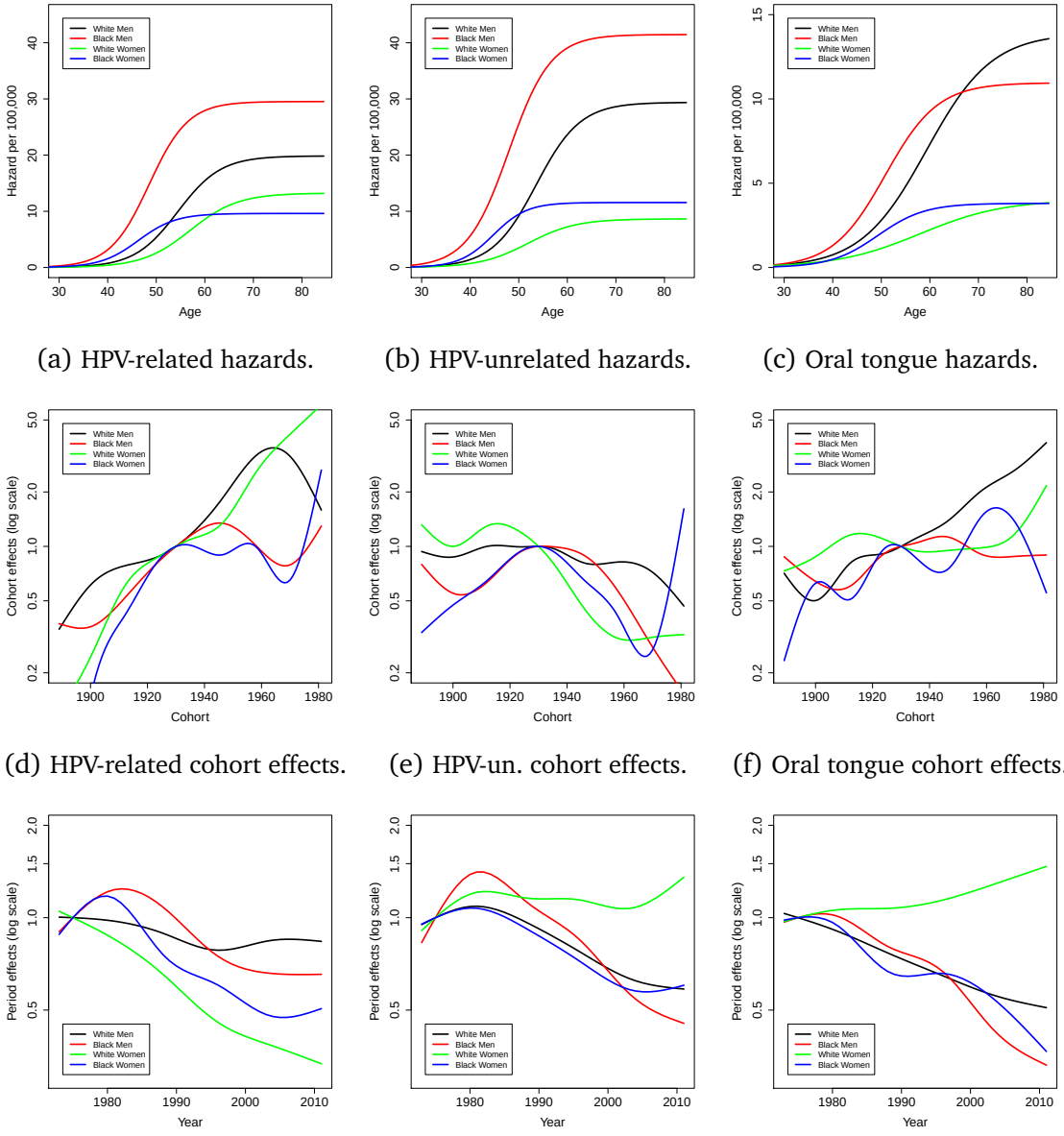

(a) HPV-related hazards. (b) HPV-unrelated hazards. (c) Oral tongue hazards.

(d) HPV-related cohort effects. (e) HPV-un. cohort effects. (f) Oral tongue cohort effects.

(g) HPV-related period effects. (h) HPV-un. period effects. (i) Oral tongue period effects.

Figure 5.4: Hazard, cohort effects, and period effects for the cohort-and-period-effects-on-r APC–TSCE models of oral squamous cell carcinoma by race and cancer subsite group.

Data	T_s	r	Low r	High r	p	Low p	High p	q	Low q	High q
HPV related										
White men	54.4	8.81E-4	7.65E-4	1.02E-3	-2.25E-1	-2.32E-1	-2.19E-1	1.07E-6	8.22E-7	1.38E-6
Black men	48.5	1.18E-3	8.76E-4	1.60E-4	-2.49E-1	-2.74E-1	-2.26E-1	1.40E-6	6.10E-7	3.19E-6
White women	57.1	6.51E-4	4.97E-4	8.53E-4	-2.03E-1	2.13E-1	-1.94E-1	1.89E-6	1.20E-6	2.97E-6
Black women	46.2	3.71E-4	2.29E-4	6.00E-4	-2.59E-1	-3.11E-1	-2.13E-1	1.57E-6	2.92E-7	8.51E-6
HPV unrelated										
White men	53.6	1.33E-3	1.17E-3	1.52E-3	-2.20E-1	-2.29E-1	-2.12E-1	1.65E-6	1.20E-6	2.26E-6
Black men	48.0	1.78E-3	1.34E-3	2.37E-3	-2.33E-1	-2.57E-1	-2.09E-1	3.32E-6	1.49E-6	7.40E-6
White women	52.0	4.28E-4	3.49E-4	5.26E-4	-2.02E-1	-2.18E-1	-1.86E-1	5.60E-6	3.10E-6	1.01E-5
Black women	44.8	4.00E-4	2.70E-4	5.94E-4	-2.89E-1	-3.50E-1	-2.34E-1	7.01E-7	8.74E-8	5.63E-6
Oral tongue										
White men	59.3	9.39E-4	6.76E-4	1.30E-3	-1.48E-1	-1.55E-1	-1.41E-1	2.28E-5	1.37E-5	3.79E-5
Black men	50.8	5.93E-4	2.74E-4	1.28E-3	-1.85E-1	-2.25E-1	-1.50E-1	1.53E-5	4.49E-6	5.24E-5
White women	58.1	3.47E-4	2.03E-4	5.91E-4	-1.16E-1	-1.27E-1	-1.06E-1	1.38E-4	6.80E-5	2.79E-4
Black women	49.3	1.84E-4	7.51E-5	4.51E-4	-2.07E-1	-2.67E-1	-1.57E-1	7.76E-6	1.10E-6	5.49E-5

Table 5.2: Biological parameters for the period-and-cohort-on-r APC–TSCE models of oral squamous cell carcinoma by race and cancer subsite group with 95% Wald confidence intervals.

cohort effects on the cancer initiation rate rather than the cancer promotion rate or malignant conversion rate. For all three subsite groups, too, men had higher estimated initiation rates than women of the same race, and black men and women had higher estimated promotion rates than white people of the same sex. Cancer at the HPV-related and HPV-unrelated sites had very similar estimated promotion rates, which were different from those of cancers of the oral tongue.

The three subsite groups have largely distinct patterns of period and birth cohort effects on their estimated initiation rates. HPV-related carcinomas, for instance, are strongly cohort driven in this analysis, a result that is consistent with other findings that prevalence of sexually transmitted infections are usually related to cohort factors (Gravitt et al., 2013). In particular, in Chapter III, we found HPV prevalence itself to be strongly cohort driven. Although the overall patterns between the subsite groups are distinct, there are some similarities. The period effects for all three sites have similar trajectories, with the notable exception of white women, which could be related to their lower incidence. Additionally, the cohort effects for the oral tongue sites are similar, if less pronounced, to those for the HPV-related sites, for all demographic groups but white women. This finding may suggest the etiology of cancer at the oral tongue sites may also be influenced by changes in sexual behavior.

The separation of cohort and period effects in this analysis reveals some trends that were not apparent from the age-adjusted incidence rates alone. In particular, the age-adjusted rates for HPV-related OSCCs in white women remain nearly constant, but this analysis suggests that this seeming lack of trend belies a combination of increasing cohort and decreasing period trends. A similar effect is seen for the age-adjusted rates of oral tongue cancer for white men. Trends in the age-adjusted incidence may be a result of factors that affect everyone in a given time period or, more subtley, be caused by changes between one birth cohort to the next. One can begin to see the effects of these factors when plotting age-specific incidence stratified by different time periods or birth cohorts, as we do for white men for the HPV-related and HPV-unrelated subsite groups in Figure 5.3. Trends in period or birth cohort for

age-specific incidence can either exaggerate trends in the age-adjusted incidence when the period and birth cohort trends align or be masked when the trends are opposing. However, the trends in period and cohort can sometimes be difficult to see in the data alone, especially for relatively rare diseases that have large variation in incidence, and so the results of the age–period–cohort models are especially valuable.

As we saw in Figure 5.4, the model hazard begins to increase earlier in life for black men and women for all of the subsite groups, which is reflected in the higher estimated cancer promotion rates for those demographics. Although one might, if looking only at the HPV-related figure, conjecture that higher oral prevalence of HPV among black Americans could be at fault, it seems more likely, taking the analysis of the other two groups into account, that it is a factor of other differences in the two populations (smoking, drinking, or other risk factors and exposures). Further, men of both races have higher hazards than the women of the same race, which is reflected, in part, in higher estimated rates of cancer initiation. Again, although this is consistent with men having higher oral prevalence of HPV than women, the consistency across the subsite groups suggests that this effect is more likely due to the underlying differences in biology.

Analysis of the estimated biological parameters for the three groups, the promotion parameter p in particular, suggests that HPV-related and HPV-unrelated cancers are distinct from the cancer of the oral tongue. Interestingly, the estimated rates of promotion p and the sojourn times are very similar between the HPV-related and HPV-unrelated OPSCCs and are quite different from those of oral tongue cancer, which seems to progress more slowly; the mean sojourn time for the oral tongue sites is about 2–5 years longer than the other two. The similarity between the HPV-related and HPV-related promotion parameter and estimated sojourn times suggest that the tumor dynamics are very similar for these sites once the tumor has been initiated, possibly through gene inactivation, whether by HPV or alcohol and tobacco use. This is in contrast with the known differences in cancer survival between HPV

related and HPV unrelated cancers (Chaturvedi et al., 2011).

5.4.2 Comparison to other literature

To better understand if the differences between the promotion parameters at the different subsite groups of the oropharynx and oral cavity are significant (HPV-related: -0.20 to -0.26; HPV-unrelated: -0.20 to -0.29; oral tongue: -0.11 to -0.21), we compare with findings from colorectal and esophogeal adenocarcinoma. Estimates of the promotion parameters for colorectal adenocarcinomas in United States (SEER) were -0.14, -0.19, and -0.20 for men for the proximal colon, distal colon, and rectum, and -0.14, -0.18, and -0.18 for women (Meza et al., 2010c). Estimates of the promotion parameter p for esophageal adenocarcinoma (SEER) in white men and women range from -0.16 to -0.20 Jeon et al. (2006). Hence, this analysis suggests that not only are we seeing significant differences between the dynamics of oral tongue carcinoma and the other sites, but also among the demographics for each subsite group.

That the promotion parameter for cancer of the oral tongue is significantly different from that of the other two is consistent with the findings of other recent studies (Saba et al., 2011; Patel et al., 2011; Brown et al., 2012) that observed age- and sex-specific incidence that seem to distinguish it from the other sites. This has led to suggestions that cancer of the oral tongue may have a different etiology from smoking and drinking (Saba et al., 2011) or HPV (Patel et al., 2011; Saba et al., 2011), possibly bacterial/viral infection or genetic abnormalities (Saba et al., 2011; Brown et al., 2012). Our analysis of period and cohort effects suggests that changes in oral tongue cancer incidence by birth cohort are somewhat similar to those for HPV, which may suggest that the etiology of oral tongue cancer is also linked to changing sexual mores and practices.

5.4.3 Strengths and limitations

As with any mathematical model, the modeling framework underlying this analysis is a simplification of the complex biological underpinnings of tumorigenesis and thus neglects a number relevant factors. Additionally, as with other SEER-based studies, our work is limited by the uncertainty in classification of sites as presumed HPV-related or HPV-unrelated. Similarly, this analysis is limited by the lack of alcohol and tobacco consumption data in SEER, which precludes the possibility of controlling for these important risk factors.

The use of a multistage model rooted in the biology of the system, a model which has been previously developed and validated, offers several advantages in this context. In particular, we are able to assess not only on trends in the data but to also pose hypotheses on the biological implications (i.e. the initiation, promotion, and malignant conversion rates and sojourn times) as well; previous studies have not included biologically motivated carcinogenesis models in their analyses. Additionally, the large sample size afforded by the SEER database allows analysis stratified by both sex and race.

5.4.4 Implications

This analysis suggests that cancer at HPV-related and HPV-unrelated sites have similar tumor growth dynamics once initiated. More work is needed to investigate these dynamics as survival rates for HPV-positive and HPV-negative tumors are drastically different. Testing for HPV in oropharyngeal carcinomas should become routine and the results recorded in cancer registries.

This study supports the hypothesis that oral tongue cancer has a different etiology from either HPV or alcohol and tobacco use. Although, there is little evidence as to what this etiology is, our analysis offers some additional information that may be useful to future studies. In particular, the birth cohort trends for oral tongue cancer appear similar to that of cancer of the HPV-related subsites, suggesting trends in

sexual behavior may be relevant. That white women have distinctly different period effect trends for HPV-related (decreasing) and oral tongue (increasing) cancer while the three other demographics have similar decreasing trends for both groups may offer additional clues, though it is not clear at this time what those might be.

Further, work is needed to understand why men have higher rates of initiation than women, for both white and black Americans, at all three subsite groups, a phenomenon that may be biologically rooted, and why black men and women have higher promotion rates than their white counterparts, a result of risk factors more likely influenced by socioeconomics and behavior than biology.

Future studies may be able to include a joint analysis of HPV prevalence and incidence HPV-related oropharyngeal squamous cell carcinomas using extensions of the two-stage carcinogenesis model. Indeed, such models may be able to shed light on the similarities and differences in initiation and growth of HPV-related and HPV-unrelated tumor as well as help quantify the additional risk for oral cancer associated with HPV infection.

5.5 Appendix

5.5.1 Subsite classification

Following Chaturvedi et al. (2008); Brown et al. (2011, 2012), we consider squamous cell carcinomas (SCC) of the head and neck at the following fourteen sites to be HPV-related: C01.9 base of tongue, NOS (not otherwise specified); C02.4 lingual tonsil; C09.0 tonsillar fossa; C09.1 tonsillar pillar; C09.8 overlapping lesion of tonsil; C09.9 tonsil, NOS; C10.0 vallecula; C10.1 anterior surface of epiglottis; C10.2 lateral wall of oropharynx; C10.3 posterior wall of oropharynx; C10.4 branchial cleft; C10.8 overlapping lesion of oropharynx; C10.9 oropharynx, NOS; C14.2 waldeyer ring.

We consider the following twenty-five sites to be HPV-unrelated: C03.0 upper gum; C03.1 lower gum; C03.9 gum, NOS; C04.0 anterior floor of mouth; C04.1 lateral floor of mouth; C04.8 overlapping lesion of floor of mouth; C04.9 floor of mouth, NOS; C05.0 hard palate; C05.1 soft palate, NOS; C05.2 uvula; C05.8 overlapping lesion of palate; C05.9 palate, NOS; C06.0 cheek mucosa; C06.1 vestibule of mouth; C06.2 retromolar area; C06.8 overlapping lesion of other and unspecified mouth; C06.9 mouth, NOS; C12.9 pyriform sinus; C13.0 postcricoid region; C13.1 aryepiglottic fold, hypopharyngeal; C13.2 posterior wall of hypopharynx; C13.8 overlapping lesion of hypopharynx; C13.9 hypopharynx, NOS; C14.0 pharynx, NOS; C14.8 overlapping lesion of lip, oral cavity and pharynx.

We consider the following six oral tongue sites to be HPV-unrelated: C02.0 dorsal surface of tongue, NOS; C02.1 border of tongue; C02.2 ventral surface of tongue, NOS; C02.3 anterior 2/3 of tongue, NOS; C02.8 overlapping lesion of tongue; C02.9 tongue, NOS.

5.5.2 APC-TSCE model fitting

In Table 5.3, we present the AIC for the models considered in this analysis.

Data	No effects	Period r	Cohort r	Both r	Period p	Cohort p	Both p	Period q	Cohort q	Both q
HPV-related										
White men	2883	582	45	0	1096	771	350	1658	1490	1042
Black men	218	166	53	0	85	49	35	87	98	61
White women	224	193	111	0	188	84	55	194	100	90
Black women	78	46	29	0	32	21	15	43	32	36
HPV-unrelated										
White men	2130	75	242	0	529	472	155	1023	916	729
Black men	1039	152	178	0	118	247	83	290	338	248
White women	1363	509	49	0	178	130	26	314	195	188
Black women	252	69	1	0	26	30	8	75	68	54
Oral tongue										
White men	32	31	14	0	33	12	18	32	10	13
Black men	84	-4	11	0	-13	16	-2	6	24	12
White women	78	24	-2	0	33	0	5	31	1	8
Black women	-4	-4	-3	0	0	-5	-3	0	1	6

Table 5.3: Akaike Information Criterion (AIC) for APC–TSCE models of incidence of oral squamous cell carcinomas by race and cancer subsite group relative to the model with both period and cohort effects on r. The absolute values are -157378, -2726, -15411, 2760, -105394, -1280, -33528, 3110, -21646, 2819, -7677, and 2029, respectively. *=optimizer did not converge

Confidence intervals (95%) are presented in Figure 5.5 for the APC–TSCE model with period and cohort effects on initiation. Markov chain monte carlo (MCMC) methods were used to estimate covariance matrices for the sixteen parameters in each case.

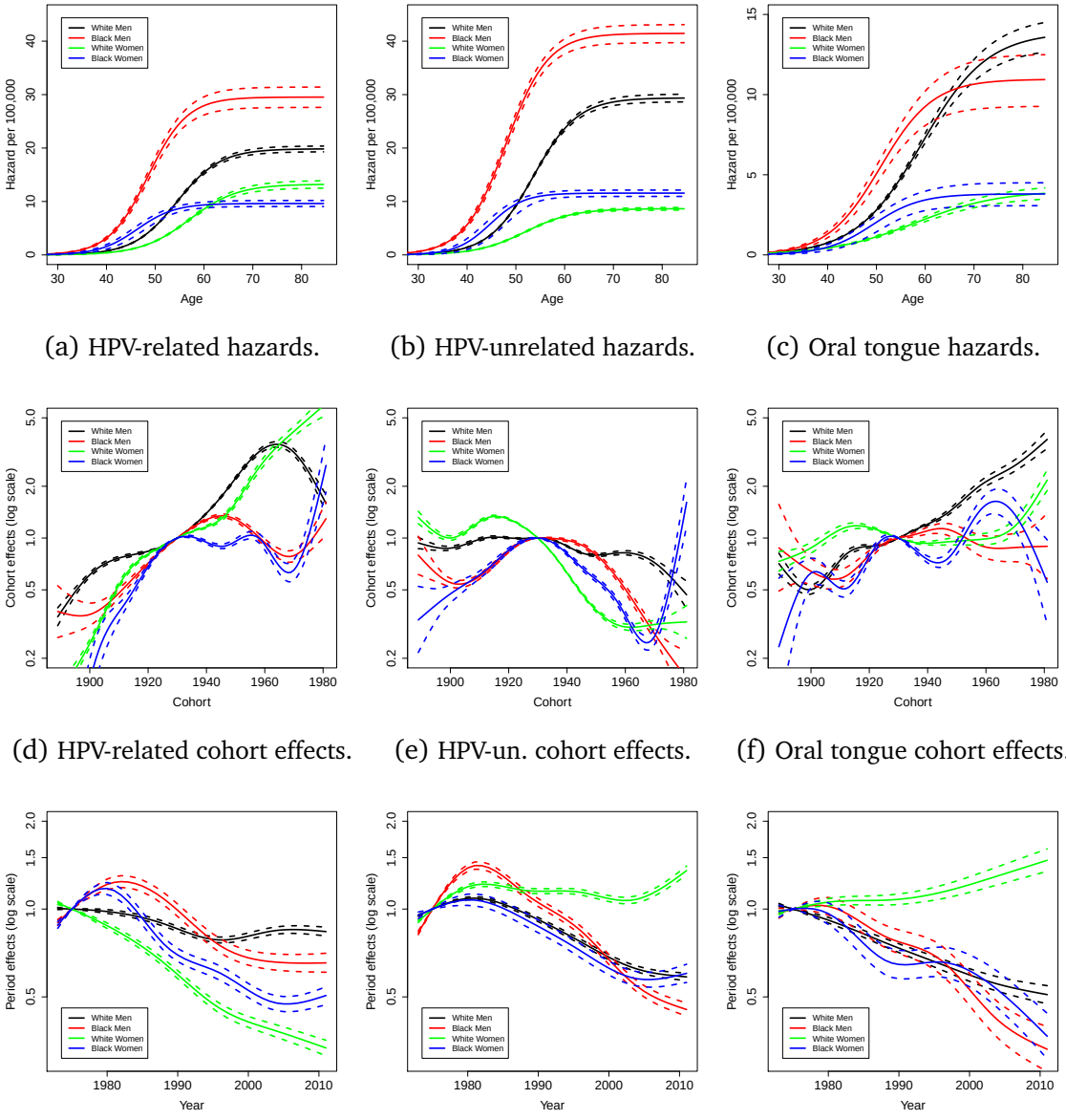

(a) HPV-related hazards. (b) HPV-unrelated hazards. (c) Oral tongue hazards.

(d) HPV-related cohort effects. (e) HPV-un. cohort effects. (f) Oral tongue cohort effects.

(g) HPV-related period effects. (h) HPV-un. period effects. (i) Oral tongue period effects.

Figure 5.5: Hazard, cohort effects, and period effects for the cohort-and-period-effects-on-r APC–TSCE models of oral squamous cell carcinoma by race and cancer subsite group with 95% confidence intervals.

5.5.3 APC Results

The residual deviance for each unconstrained APC model with natural spline effects is shown Table 5.4 for each race–gender pair. We use seven degrees of freedom for age, eight for cohort effects, and five for period, corresponding to approximately one degree of freedom for eight, twelve, and eight years respectively. Comparison of values may be made only down columns, not across rows. To avoid issues of identifiability, we use the age–cohort model. The age and cohort effects are plotted in Figure 5.6.

Model	White men Residual Dev.	Black men Residual Dev.	White women Residual Dev.	Black women Residual Dev.
HPV-related				
Age–Cohort	2300.7	2208.5	2133.6	1817.2
Age–Period–Cohort	2252.4	2176.5	2104.3	1802.5
Age–Period	2564.8	2286.7	2223.5	1844.5
HPV-unrelated				
Age–Cohort	2390.0	2209.6	2177.8	2026.5
Age–Period–Cohort	2286.7	2123.5	2119.8	2017.5
Age–Period	2352.0	2277.3	2589.6	2097.2
Oral tongue				
Age–Cohort	2466.9	1801.8	2308.6	1282.2
Age–Period–Cohort	2430.4	1785.4	2298.4	1279.3
Age–Period	2454.8	1806.0	2337.5	1294.9

Table 5.4: Residual deviance for APC model fits of oral squamous cell carcinoma incidence by race and cancer subsite group.

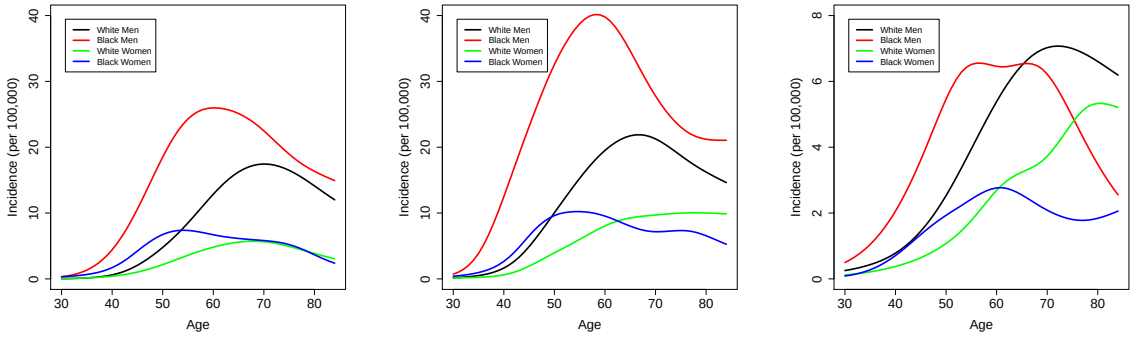

(a) HPV-related age effects. (b) HPV-unrelated age effects. (c) Oral tongue age effects.

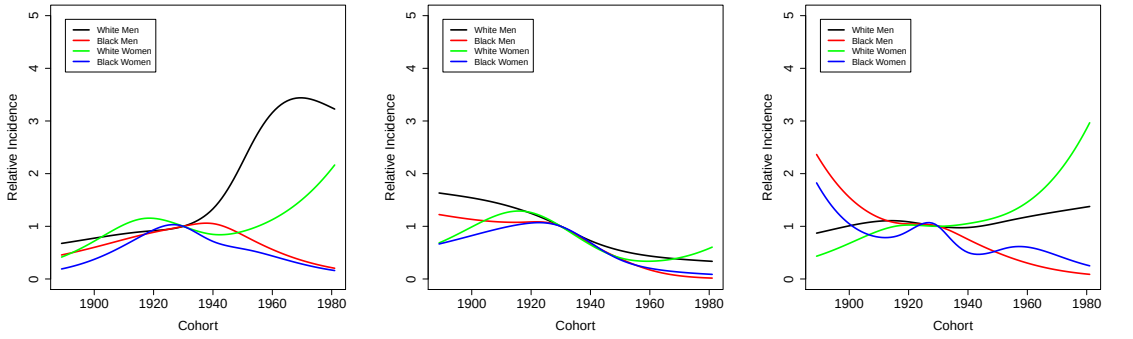

(d) HPV-related cohort effects. (e) HPV-un. cohort effects. (f) Oral tongue cohort effects.

Figure 5.6: Age and cohort effects for APC models of oral squamous cell carcinoma incidence by race and cancer subsite group.

CHAPTER VI

Multistage clonal expansion models with infection-related initation pathways

In this chapter, we outline theory that can connect the dynamics of HPV transmission, as considered in Chapters III and IV, to carcinogenesis in the head and neck, which was studied in Chapter V. This is the first attempt of which we are aware to connect infectious disease models at the population level to mechanistic models of cancer incidence at the population level. However, while we model the mechanistic process of viral carcinogenesis in a simplified form, we do not include explicit within-host viral dynamics. We will consider two related multistage clonal expansion models with infection-related initiation pathways. Given the unidentifiability we observed in the two stage clonal expansion model and the fact that these models consider a novel combination of (theoretical) data sets, the issue of identifiability is an important first step to successful parameter estimation and model inference. Thus we will address the identifiability of the models given age-specific cancer incidence and age-specific prevalence of HPV using a differential algebra approach (Eisenberg et al., 2013; Eisenberg, 2013).

As discussed in Chapter V, subsites of the head and neck where cancers are often found to be HPV-positive are designated HPV-related. However, not all cancers at these sites are HPV-positive. In this chapter, we develop models that attempt to differentiate between tumor initiation that is driven by HPV integration into the genome (IARC, 2007) from carcinogenesis independent of HPV. It is not immedi-

ately clear whether or not tumors, once initiated by these different pathways, have the same mechanistic tumor phenotype; in particular, it is not clear whether these tumors will have the same promotion and malignant conversion dynamics.

The analysis of incidence rates in Chapter V of HPV-related and HPV-unrelated subsites suggests that the dynamics of tumorigenesis may not be that different for the different pathways once a tumor is initiated. We thus derive the equations for two similar models, one in which the biology of tumors initiated through HPV-related and HPV-unrelated pathways is presumed to be the same, and one in which it is presumed to be different. Schematics of these models are presented in Figure 6.1.

We assume that initiation through HPV and through other pathways are independent. We assume the HPV pathway exists at age t with probability $P(t)$, where $P(t)$ is the prevalence of oral HPV at age t among the considered demographic group . The initiation rate associated with this pathway, then, includes both HPV integration into the host genome and initiation of tumorigenesis.

6.1 Same-phenotype model

6.1.1 Model derivation

Let $X(t) = X$ be the fixed number of normal cells, $Y(t)$ the number of initiated cells, and $Z(t)$ the number of malignant cells. Let μ_0 be the rate of initial mutation for all causes except for HPV. Let ρ be the relative risk of initiation given an HPV infection at age t. Denote

$$\nu(t) = \mu_0(1 - P(t) + \rho P(t)). \tag{6.1}$$

Let

$$\sigma = \mu_0(\rho - 1), \tag{6.2}$$

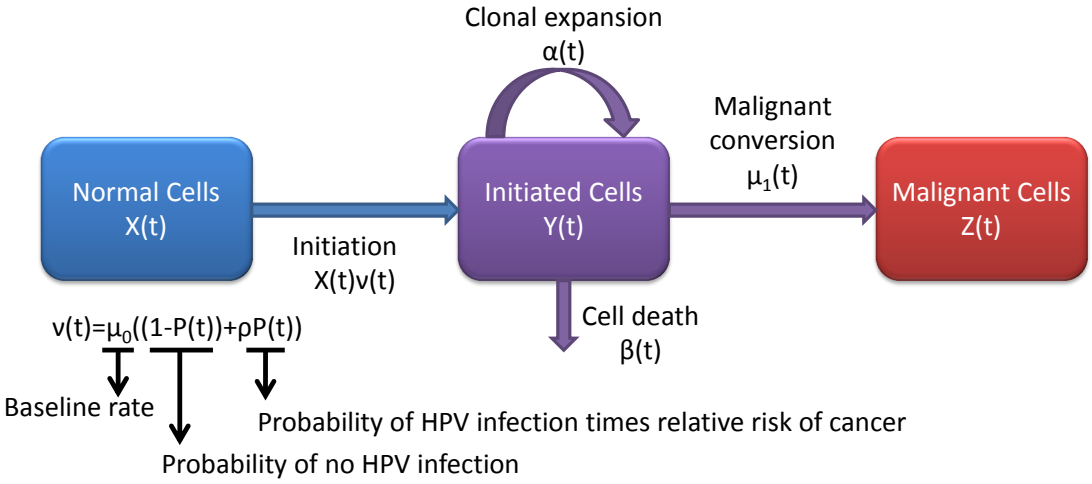

(a)

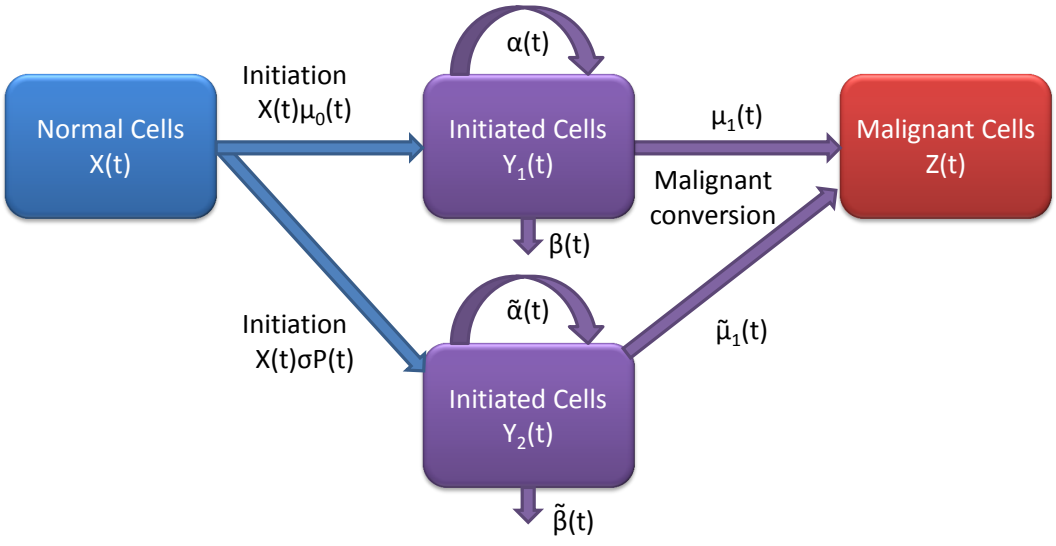

(b)

Figure 6.1: Schematics a multistage clonal expansion models with initiation driven by infectious disease prevalence assuming HPV-related and HPV-unrelated tumor have the (a) same or (b) different cancer phenotype.

so that we may write $\nu(t) = \mu_0 + \sigma P(t)$ to better compare to the model that assumes different tumorigenesis dynamics for the two pathways. Let α, β, and μ_1 be the growth rate, death rate, and malignant conversion rate as usual. A schematic of the model is shown in Figure 6.1a.

This model is in fact the two-stage clonal expansion model with age-dependent initiation rate. We derived these equations (eq. 2.77) in Chapter II. We write them here to make the dependence on the prevalence $P(t)$ explicit.

$$\begin{aligned}
\frac{\partial x_1}{\partial s}(s) &= -\left[\alpha + \beta + \mu_1\right] x_1 + \beta + \alpha x_1^2, \\
\frac{\partial x_2}{\partial s}(s) &= -\left[\alpha + \beta + \mu_1\right] x_2 + 2\alpha x_1 x_2, \\
\frac{\partial x_3}{\partial s}(s) &= -(\mu_0 + \sigma P(t-s)) X x_3 (1 - x_1), \\
\frac{\partial x_4}{\partial s}(s) &= -(\mu_0 + \sigma P(t-s)) X x_2, \\
x_1(0) &= 1, \\
x_2(0) &= -\mu_1(t), \\
x_3(0) &= 1, \\
x_4(0) &= 0.
\end{aligned} \tag{6.3}$$

Solving this set of equations for each value of t, we recover the survival $S(t) = x_3(t)$ and hazard $h(t) = x_4(t)$ functions.

6.1.2 Identifiability

Next, we examine the identifiability of the model in eq. 6.3, using the differential algebra approach discussed in Chapter II (Saccomani et al., 2001; Eisenberg, 2013). As noted there, this approach was developed for rational-function differential equation models. While eq. 6.3 has a delay term, it appears only in the (known) disease prevalence input $P(t-s)$, so that we can treat the overall function $P(t-s)$ as a function of s for any fixed t. The structure of the identifiable combinations holds for

any value of t, and so the results generalize to all t.

Assuming we have age-specific incidence data and know the prevalence of HPV by age, the observable quantities in the system of equations are the survival x_3 and hazard x_4 as well as the prevalence P.

Proposition 6.1.1. *If the survival and hazard functions are known, then the model in eq. 6.3 is unidentifiable, and $\mu_0 X/\alpha$, $\sigma X/\alpha$, $\alpha - \beta - \mu_1$, and $\alpha\mu_1$ are the identifiable combinations.*

Proof. For ease of notation denote $u(s) := P(t-s)$. Recall from Chapter II that a set of input–output equations for a system is a monic, polynomial representation of the model in terms of only the observed variables (here x_3, x_4, and u), their derivatives, and the parameters. We eliminate x_1 and x_2 as follows. Using the $\dot{x}_4$ equation,

$$x_2 = -\frac{\dot{x}_4}{\mu_0 X + \sigma X u}. \tag{6.4}$$

We plug this into the $\dot{x}_2$ equation,

$$\begin{aligned} \dot{x}_2 &= -\left[\alpha + \beta + \mu_1\right] x_2 + 2\alpha x_1 x_2, \\ 0 &= \ddot{x}_4(\mu_0 X + \sigma X u) + \dot{x}_4\left[(\mu_0 X + \sigma X u)\left((\alpha + \beta + \mu_1) - 2\alpha x_1\right) - \sigma X \dot{u}\right], \end{aligned} \tag{6.5}$$

and solve for x_1,

$$x_1 = \frac{1}{2\alpha}\left[\frac{\ddot{x}_4}{\dot{x}_4} - \frac{\sigma X \dot{u}}{\mu_0 X + \sigma X u} + (\alpha + \beta + \mu_1)\right]. \tag{6.6}$$

We now eliminate all variables but the survival x_3 and hazard x_4 by plugging x_1 into the $\dot{x}_1$ and $\dot{x}_3$ equations,

$$\begin{aligned} \dot{x}_1 &= -\left[\alpha + \beta + \mu_1\right] x_1 + \beta + \alpha x_1^2, \\ \dot{x}_3 &= -(\mu_0 + \sigma P(t-s)) X x_3 (1 - x_1), \end{aligned} \tag{6.7}$$

which, respectively, become our input–output equations,

$$\begin{aligned}
0 = \dot{x}_4^2 \Bigg[& \left((\alpha - \beta - \mu_1)^2 + 4\alpha\mu_1 \right) \left(\left(\frac{\mu_0 X}{\sigma X} \right)^2 + 2 \left(\frac{\mu_0 X}{\sigma X} \right) + u^2 \right) \\
& -2 \left(\frac{\mu_0 X}{\sigma X} \right) \ddot{u} + \dot{u}^2 - 2u\ddot{u} \Bigg] - 3 \left(\left(\frac{\mu_0 X}{\sigma X} \right)^2 + 2 \left(\frac{\mu_0 X}{\sigma X} \right) + u^2 \right) \ddot{x}_4^2 \\
& + 2 \left(\frac{\mu_0 X}{\sigma X} + u \right) \dot{u} \dot{x}_4 \ddot{x}_4 + 2 \left(\left(\frac{\mu_0 X}{\sigma X} \right)^2 + 2 \left(\frac{\mu_0 X}{\sigma X} \right) + u^2 \right) \dot{x}_4 \dddot{x}_4 \\
0 = 2\dot{x}_3 \dot{x}_4 & - \left(\frac{\mu_0 X + \sigma X u}{\alpha} \right) x_3 \ddot{x}_4 + x_3 \dot{x}_4 \left(\frac{\sigma X}{\alpha} \dot{u} + \left(\frac{\mu_0 X + \sigma X u}{\alpha} \right) (\alpha - \beta - \mu_1) \right)
\end{aligned} \tag{6.8}$$

which we note are monic under the field $\mathbb{R}$ and an appropriate ranking of variables. As noted in Chapter II, testing identifiability for the full model now reduces to testing injectivity of the map from the parameters to the coefficients of the input–output equations. We set each of the distinct coefficients to a symbolic copy of itself and solve the resulting system of equations to find the following:

$$\begin{aligned}
\frac{\sigma X}{\alpha} &= \frac{\bar{\sigma} \bar{X}}{\bar{\alpha}}, \\
\frac{\mu_0 X}{\alpha} &= \frac{\bar{\mu}_0 \bar{X}}{\bar{\alpha}}, \\
\alpha - \beta - \mu_1 &= \bar{\alpha} - \bar{\beta} - \bar{\mu}_1, \\
\alpha\mu_1 &= \bar{\alpha}\bar{\mu}_1.
\end{aligned} \tag{6.9}$$

We see that it is not possible to solve for all the parameters uniquely, which indicates that the model (eq. 6.3) is structurally unidentifiable. However, we can see that $\mu_0 X/\alpha$, $\sigma X/\alpha$, $\alpha - \beta - \mu_1$, and $\alpha\mu_1$ are a set of identifiable combinations. □

We note that by setting $u = 0$, we recover the equations derived in the proof of Proposition 2.4.1. This highlights that knowing the prevalence has actually done very little to improve the identifiability of cancer progression parameters of the model. However, since $\rho = \frac{\sigma_0 X}{\alpha} / \frac{\mu X}{\alpha} + 1$, the relative risk between individuals with

an HPV infection and those without is identifiable.

Next, we note that our proof of Proposition 6.1.1 did not depend on any knowledge of the initial conditions. Although initial conditions can provide additional identifiability information, they do not in this case. Because we assumed that we know x_3 and x_4 for all s, we know $x_3(0)$, $x_4(0)$, $\dot{x}_3(0)$, and $\dot{x}_4(0)$. However, because $x_1(0) = 1$, the $\dot{x}_3$ equation, $\dot{x}_3(0) = 0$, provides no new information. Similarly, $\dot{x}_4(0) = (\mu_0 + \sigma u)X\mu_1 = \left(\frac{\mu_0 X}{\alpha} + \frac{\sigma X}{\alpha}\right)(\alpha\mu_1)$ is a product of the previously identified combinations.

6.2 Different cancer phenotypes model

6.2.1 Model derivation

Let $X(t)$ be the number of normal cells, $Y_1(t)$ the number of cells whose initiation is unrelated to oral HPV infection, $Y_2(t)$ the number of cells whose initiation is related to oral HPV infection, and $Z(t)$ the number of malignant cells. Let μ_0 be the rate of initial mutation for all causes unrelated to oral HPV infection. For ease of notation, let

$$\sigma(t) = \sigma P(t) \tag{6.10}$$

be the rate of initiation by related to oral HPV infection. Let α, β, and μ_1 be the growth rate, death rate, and malignant conversion rate for the Y_1 cells and $\tilde{\alpha}$, $\tilde{\beta}$, and $\tilde{\mu}_1$ the analogous rates for the Y_2 cells. A schematic of the model is shown in Figure 6.1b.

For this model, we derive the equations as we did in Chapter II. For $t > \tau$,

$$\begin{aligned}
\Psi(y_1, y_2, z, \tau, t) &= E[y_1^{Y_a(t)} y_2^{Y_2(t)} z^{Z(t)} | Y_1(\tau) = 0, Y_2(\tau) = 0, Z(\tau) = 0)], \\
\Phi_1(y_1, y_2, z, \tau, t) &= E[y_1^{Y_1(t)} y_2^{Y_2(t)} z^{Z(t)} | Y_1(\tau) = 1, Y_2(\tau) = 0, Z(\tau) = 0], \\
\Phi_2(y_1, y_2, z, \tau, t) &= E[y_1^{Y_1(t)} y_2^{Y_2(t)} z^{Z(t)} | Y_1(\tau) = 0, Y_2(\tau) = 1, Z(\tau) = 0], \\
\Theta(y_1, y_2, z, \tau, t) &= E[y_2^{Y_2(t)} y_2^{Y_2(t)} z^{Z(t)} | Y_1(\tau) = 0, Y_2(\tau) = 0, Z(\tau) = 1].
\end{aligned} \tag{6.11}$$

Now, the survival and hazard functions are given by

$$S(t) = \sum_{j,k} P_{(0,0,0),(j,k,0)}(0,t) = \sum_{j,k,\ell} P_{(0,0,0),(j,k,\ell)}(0,t) 1^j 1^k 0^\ell = \Psi(1,1,0,0,t), \tag{6.12}$$

$$h(t) = -\frac{\Psi'(1,1,0,0,t)}{\Psi(1,1,0,0,t)}. \tag{6.13}$$

We may write the Kolmogorov backward equations:

$$\begin{aligned}
\frac{d\Psi}{d\tau} &= (\mu_0 X)\Psi(1-\Phi_1) + \sigma(\tau) X \Psi(1-\Phi_2), \\
\frac{d\Phi_1}{d\tau} &= \left[\alpha + \beta + \mu_1\right]\Phi_1 - \beta - \alpha\Phi_1^2 - \mu_1\Phi_1\Theta, \\
\frac{d\Phi_2}{d\tau} &= \left[\tilde{\alpha} + \tilde{\beta} + \tilde{\mu}_1\right]\Phi_2 - \tilde{\beta} - \tilde{\alpha}\Phi_2^2 - \tilde{\mu}_1\Phi_2\Theta, \\
\frac{d\Theta}{d\tau} &= 0.
\end{aligned} \tag{6.14}$$

Denote derivative with respect to t as $'$. Then

$$\begin{aligned}
\frac{d\Psi}{d\tau} &= (\mu_0 X)\Psi(1-\Phi_1) + \sigma(\tau) X \Psi(1-\Phi_2), \\
\frac{d\Psi'}{d\tau} &= -(\mu_0 X)[\Phi_1'\Psi + (\Phi_1 - 1)\Psi'] - \sigma(\tau) X[\Phi_2'\Psi + (\Phi_2 - 1)\Psi'], \\
\frac{d\Phi_1}{d\tau} &= \left[\alpha + \beta + \mu_1\right]\Phi_1 - \beta - \alpha\Phi_1^2 - \mu_1\Phi_1\Theta, \\
\frac{d\Phi_1'}{d\tau} &= \left[\alpha + \beta + \mu_1\right]\Phi_1' - 2\alpha\Phi_1\Phi_1' - \mu_1\left(\Phi_1'\Theta + \Phi_1\Theta'\right), \\
\frac{d\Phi_2}{d\tau} &= \left[\tilde{\alpha} + \tilde{\beta} + \tilde{\mu}_1\right]\Phi_2 - \tilde{\beta} - \tilde{\alpha}\Phi_2^2 - \tilde{\mu}_1\Phi_2\Theta, \\
\frac{d\Phi_2'}{d\tau} &= \left[\tilde{\alpha} + \tilde{\beta} + \tilde{\mu}_1\right]\Phi_2' - 2\tilde{\alpha}\Phi_2\Phi_2' - \tilde{\mu}_1\left(\Phi_2'\Theta + \Phi_2\Theta'\right),
\end{aligned} \tag{6.15}$$

with initial conditions

$$
\begin{aligned}
&\Psi(y_1, y_2, z, t-0, t) = 1,\\
&\Psi'(y_1, y_2, z, t-0, t) = -\mu_0(t)X(t)(1-y_1) - \sigma(t)X(1-y_2),\\
&\Phi(y_1, y_2, z, t-0, t) = y_1,\\
&\Phi_1'(y_1, y_2, z, t-0, t) = -\left[\alpha(t) + \beta(t) + \mu_1(t)\right] y_1 + \beta(t) + \alpha(t)y_1^2 + \mu_1(t)y_1 z,\\
&\Phi(y_1, y_2, z, t-0, t) = y_2,\\
&\Phi_2'(y_1, y_2, z, t-0, t) = -\left[\tilde{\alpha}(t) + \tilde{\beta}(t) + \tilde{\mu}_1(t)\right] y_2 + \tilde{\beta}(t) + \tilde{\alpha}(t)y_2^2 + \tilde{\mu}_1(t)y_2 z,\\
&\Theta(y_1, y_2, z, t-0, t) = z,\\
&\Theta'(y_1, y_2, z, t-0, t) = 0.
\end{aligned}
\tag{6.16}
$$

From these equations, it is clear that $\Theta'(y_1, y_2, z, \tau, t) \equiv 0$ and $\Theta(y_1, y_2, z, \tau, t) = z$.

Let

$$\Gamma(y_1, y_2, z, \tau, t) = -\ln \Psi(y_1, y_2, z, \tau, t), \tag{6.17}$$

so that

$$\frac{\partial \Gamma}{\partial \tau} = -(\mu_0 X)(1-\Phi_1) - \sigma(\tau)X(1-\Phi_2), \tag{6.18}$$

$$\frac{\partial \Gamma'}{\partial \tau} = (\mu_0 X)\Phi_1' + \sigma(\tau)X\Phi_2'. \tag{6.19}$$

Let $x_1(s) = \Phi_1(1, 0, t-s, t)$, $x_2(s) = \Phi_1'(1, 0, t-s, t)$, $x_3(s) = \Phi_2(1, 0, t-s, t)$, $x_4(s) =$

$\Phi_2'(1,0,t-s,t)$, $x_5(s) = \Psi(1,0,t-s,t)$, and $x_6(s) = \Gamma'(1,0,t-s,t)$. Then, we have

$$\begin{aligned}
\frac{\partial x_1}{\partial s}(s) &= -\left[\alpha+\beta+\mu_1\right]x_1 + \beta + \alpha x_1^2,\\
\frac{\partial x_2}{\partial s}(s) &= -\left[\alpha+\beta+\mu_1\right]x_2 + 2\alpha x_1 x_2,\\
\frac{\partial x_3}{\partial s}(s) &= -\left[\tilde{\alpha}+\tilde{\beta}+\tilde{\mu}_1\right]x_3 + \tilde{\beta} + \tilde{\alpha} x_3^2,\\
\frac{\partial x_4}{\partial s}(s) &= -\left[\tilde{\alpha}+\tilde{\beta}+\tilde{\mu}_1\right]x_4 + 2\tilde{\alpha} x_3 x_4,\\
\frac{\partial x_5}{\partial s}(s) &= -(\mu_0 X)x_5(1-x_1) - \sigma P(t-s)X x_5(1-x_3),\\
\frac{\partial x_6}{\partial s}(s) &= -(\mu_0 X)x_2 - \sigma P(t-s)X x_4,\\
x_1(t) &= 1,\\
x_2(t) &= -\mu_1(t),\\
x_3(t) &= 1,\\
x_4(t) &= -\tilde{\mu}_1(t),\\
x_5(t) &= 1,\\
x_6(t) &= 0.
\end{aligned} \tag{6.20}$$

6.2.2 Identifiability

Again, assuming we have age-specific incidence data and know the prevalence of HPV by age, the observable quantities in the system of equations are the survival x_5 and hazard x_6 as well as the prevalence P.

The identifiability of a model with two cancer phenotypes has not been previously considered, so we first find the identifiable combinations assuming that P is constant over all t, without loss of generality taking $P \equiv 1$. Secondly, we find the identifiable combinations of the full model with $P = P(t)$.

Proposition 6.2.1. *If the survival and hazard functions are known and $P \equiv 1$, then the model in eqs 6.20 is unidentifiable, and the identifiable combinations are $\mu_0 X/\alpha$, $\sigma X/\tilde{\alpha}$, $(\alpha-\beta-\mu_1)^2 + 4\alpha\mu_1$, and $(\tilde{\alpha}-\tilde{\beta}-\tilde{\mu}_1)^2 + 4\tilde{\alpha}\tilde{\mu}_1$.*

Proposition 6.2.2. *If the survival and hazard functions are known and the prevalence $P(t)$ is known, then the model in eqs 6.20 is unidentifiable, and the identifiable combinations are $\mu_0 X/\alpha$, $\sigma X/\tilde{\alpha}$, $\alpha - \beta - \mu_1$, $\tilde{\alpha} - \tilde{\beta} - \tilde{\mu}_1$, $\alpha\mu_1$ and $\tilde{\alpha}\tilde{\mu}_1$.*

The proofs of Propositions 6.2.1 and 6.2.2 proceed similarly to that of Proposition 6.1.1. The algebra required is extremely cumbersome, yielding input–output equations with 79 and 1949 terms respectively, and so calculations were completed in Mathematica 10. Indeed, the computations were extensive enough that standard approaches (e.g. using Gröebner bases) were computationally intractable, running for over five days without terminating. Thus, we instead used a manual simplification step similar to that used by Eisenberg et al. (2013) to eliminate particular squared terms that complicate the standard algorithms and generate input–output equations. Because the number coefficients was large, setting each coefficient equal to a symbolic copy of itself and solving for the parameters (to test injectivity of the map from the parameters to the coefficients) was also computationally intractable, and so we used a numeral point in parameter space (chosen arbitrarily) to test identifiabilty. As noted in Saccomani et al. (2001), since the identifiability results are generic, this approach will yield correct identifiability results almost always, and provides a significant increase in computational speed. We then used a Gröebner basis (or the equivalent method Solve in Mathematica) to evaluate whether each parameter could be uniquely solved to equal its numerical value. From the resulting solutions/Gröebner basis elements, we determined that the models were unidentifiable, and determined the identifiable combinations given above. The proof structure is outlined in the appendix (section 6.5).

It is worth noting that, in this model, the relative risk between individuals with an HPV infection and those without is no longer identifiable. Instead $\frac{\tilde{\alpha}}{\alpha}(\rho - 1)$, a less useful quantity, is identifiable.

6.3 Model behavior

Here, we consider the range behavior exhibited by these two models. We fix $\sigma = \mu_0$, corresponding to a relative risk of 2, so that the range behavior will be interesting but still reasonable. All simulations in this section have the following base values: $\mu_0 = 10^{-10}$, $X = 10^7$, $\alpha = 3$, $\beta = 2.8$, $\mu_1 = 10^{-7}$. These values were based on estimates in Chapter V, though they do not represent any specific cancer or demographic group.

Because prevalence is so important, we consider a number of different prevalences. We begin with base prevalence of $P(t) = (6.4825E-4)t^2e^{-10^{-3}(10+t)^2}$, which was chosen to approximately match a typical bump-shaped curve seen for infectious diseases over age. We also consider $4P(t)$, $8P(t)$, and age-independent prevalences corresponding the average values of the $P(t)$, $4P(t)$, and $8P(t)$ over ages 0 to 84: 0.05, 0.20, and 0.40, respectively. The considered prevalences are plotted in Figure 6.2.

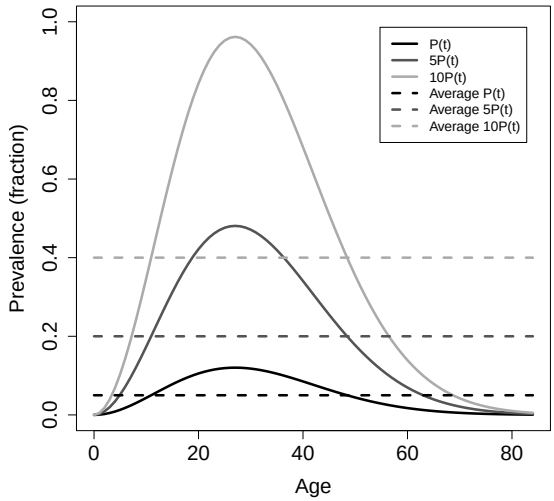

Figure 6.2: Theoretical prevalences considered for understanding the behavior of the MSCE models with infection-related initiation pathways.

For each prevalence, we vary each of the identifiable combinations: $\tilde{\alpha} - \tilde{\beta} - \tilde{\mu}_1$ (Figure 6.3), $\tilde{\alpha}\tilde{\mu}_1$ (Figure 6.4), and $\sigma X/\tilde{\alpha}$ (Figure 6.5), while keeping the other two

identifiable combinations constant. This is accomplished by setting $\sigma = \mu_0$, $\tilde{\alpha} = \sigma\alpha/(A\mu_0)$, $\tilde{\mu}_1 = B\alpha\mu_1/\tilde{\alpha}$, $\tilde{\beta} = \tilde{\alpha} - \tilde{\mu}_1 - C(\alpha - \beta - \mu_1)$ and varying parameters A, B, and C. Note that the same-phenotype and different-phenotype models align when $\tilde{\alpha} = \alpha$, $\tilde{\beta} = \beta$, and $\tilde{\mu}_1 = \mu_1$, which is represented by the black line in Figures 6.3, 6.4, and 6.5.

These simulations reveal practical identifiability issues when prevalence is low. In each of the figures with low prevalence (Figures 6.3a, 6.3b, 6.4a, 6.4b, 6.5a, 6.5b), distinguishing between the curves would be incredibly difficult given the noise of real data. Hence, because oral HPV is a low prevalence disease (10% in men and 4% in women (Gillison et al., 2012b)), it may be difficult to distinguish between the same cancer phenotype and different cancer phenotype models with the given incidence data (not differentiating between HPV-positive and HPV-negative cancers). For practical purposes then, the same phenotype model may suffice. The prevalence of genital HPV is higher, but it is thought that virtually all cervical cancers are HPV-initiated, so that these models are not applicable.

Further, these simulations demonstrate the importance of the shape of the prevalence function. In Figures 6.3, 6.4, and 6.5, the differences in shape between the left and right columns of subfigures are apparent. The differences are plainest in Figure 6.3, which controls the relative net cell proliferation $\frac{\tilde{\alpha}-\tilde{\beta}-\tilde{\mu}_1}{\alpha-\beta-\mu_1}$ between the two pathways and in which the figures with the age-dependent prevalence (left) develop a hump as the ratio increases while those with the constant prevalence (right) develop an almost step-like appearance that separates the increase in hazard related to each of the two pathways (HPV-related followed by HPV-unrelated). The hump-like shapes are reminiscent of some of the age-effects (Figure 5.6) calculated for the oral cancers in Chapter V. This suggests that, for non-negligible prevalence levels, the patterns of HPV prevalence could be inferred from cancer data.

In Figure 6.3, we see that increasing the net cell proliferation of the HPV-related pathway $\tilde{\alpha} - \tilde{\beta} - \tilde{\mu}_1$ relative to that of the HPV-unrelated pathway increases the hazard and moves the initial increase in hazard earlier in life. This observation

is biologically sensible. Decreasing the net cell proliferation decreases the hazard mildly, but only to a point. If the proliferation is very slow relative to the other pathway, the model is indistinguishable from one with only the relevant pathway.

In Figure 6.4, we see that the ratio between $\tilde{\alpha}\tilde{\mu}_1$ and $\alpha\mu_1$ is much less sensitive than the other two identifiable combinations. Here, we change the ratio by several orders of magnitude and still only effect a moderate change in the shape of the hazards. The difference between the age-dependent and constant prevalences, while still apparent, is less pronounced than in Figure 6.3.

In Figure 6.5, we change the ratio between $\sigma X/\tilde{\alpha}$ and $\mu_0 X/\alpha$. This changes essentially captures the difference in initiation rates between the two pathways. Changing the ratios is seen to change the asymptotes of the hazards but not have a significant impact on the shapes. As in Figure 6.3, reducing the relative initiation rate of the HPV-related pathway collapses the hazard onto that of the model with only the HPV-unrelated initiation pathway (not pictured).

In these figures, we see that, although the shape of the same cancer phenotype model hardly deviates from that of the TSCE model, the different cancer phenotype model can display a wide range of behavior depending on the shape of the prevalence function and the ratios of the identifiable combinations of the two pathways.

6.4 Conclusion

In Chapter II, we derived the equations of the two-stage clonal expansion model and proved that it is unidentifiable given age-specific incidence with identifiable combinations $\alpha - \beta - \mu_1$, $\alpha\mu_1$, and $\mu_0 X/\alpha$. In this chapter, we considered extensions of this model by including infection-related initiation pathways and found the identifiable combinations given age-specific incidence.

Knowing the prevalence in the same cancer phenotype model allowed identification of $\sigma X/\alpha$ in addition to the identifiable combinations already listed. The relative risk

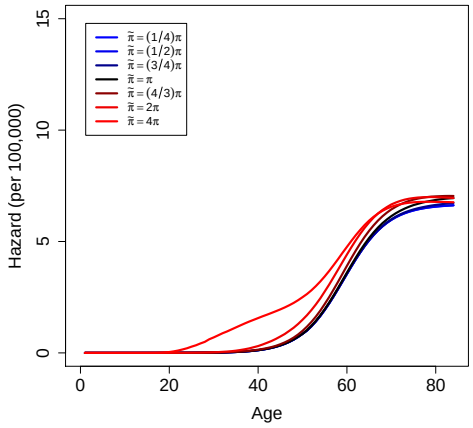

(a) Prevalence: $P(t)$.

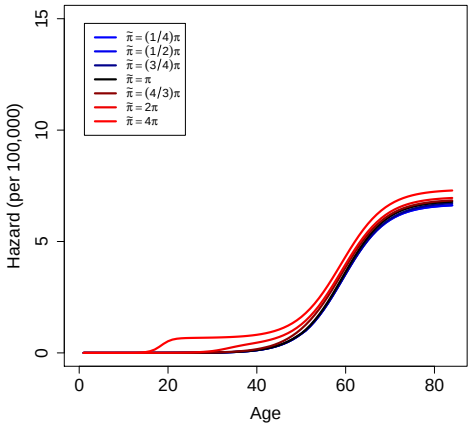

(b) Constant prevalence: average value of $P(t)$.

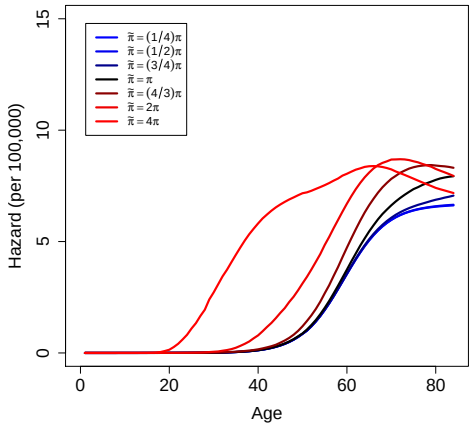

(c) Prevalence: $4P(t)$.

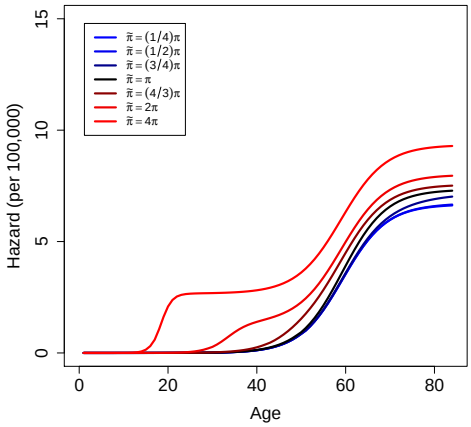

(d) Constant prevalence: average value of $4P(t)$.

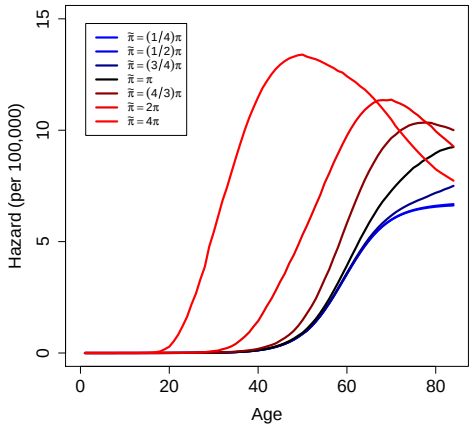

(e) Prevalence: $8P(t)$.

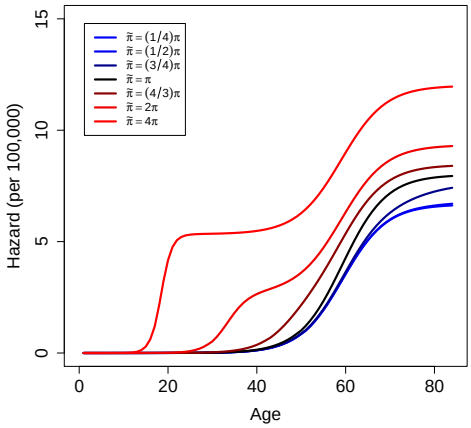

(f) Constant prevalence: average value of $8P(t)$.

Figure 6.3: Behavior of the MSCE models with infection-related initiation pathways for different values of $\tilde{\pi} = \tilde{\alpha} - \tilde{\beta} - \tilde{\mu}_1$. The hazard in black is for the same phenotype model, and the hazards in color are the different phenotype model.

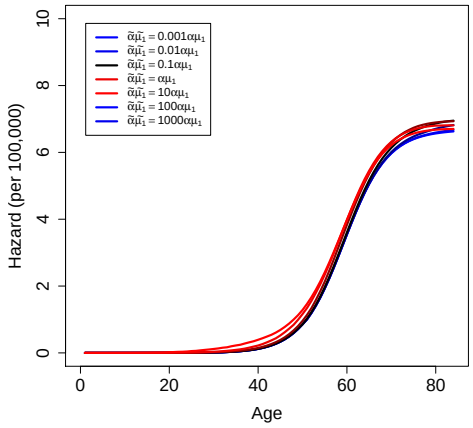

(a) Prevalence: $P(t)$.

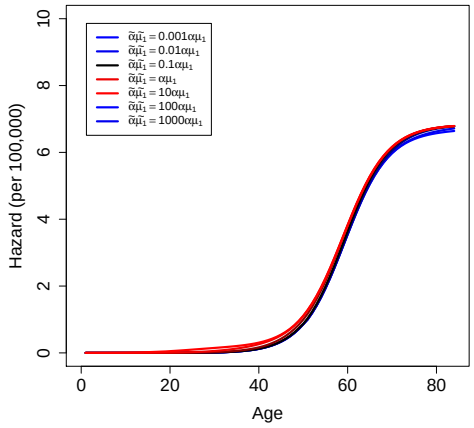

(b) Constant prevalence: average value of $P(t)$.

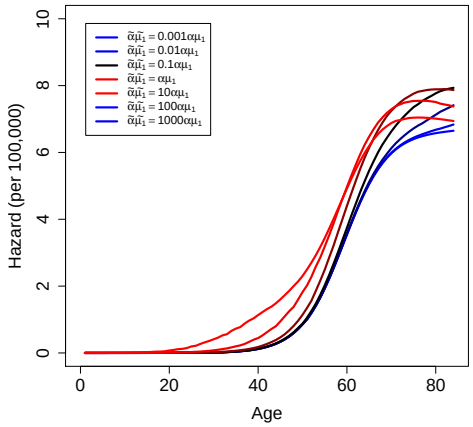

(c) Prevalence: $4P(t)$.

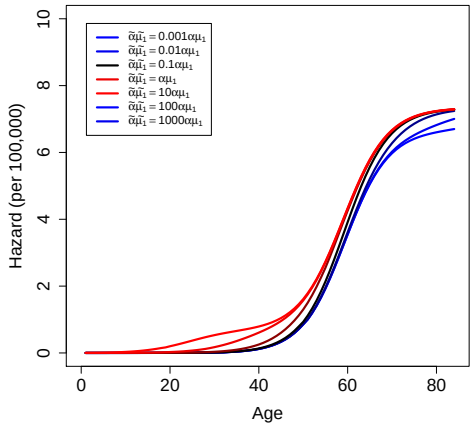

(d) Constant prevalence: average value of $4P(t)$.

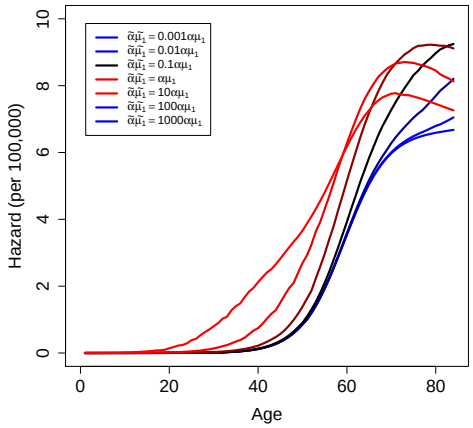

(e) Prevalence: $8P(t)$.

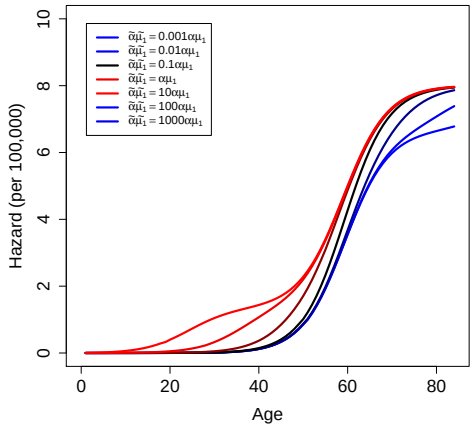

(f) Constant prevalence: average value of $8P(t)$.

Figure 6.4: Behavior of the MSCE models with infection-related initiation pathways for different values of $\tilde{\alpha}\tilde{\mu}_1$. The hazard in black is for the same phenotype model, and the hazards in color are the different phenotype model.

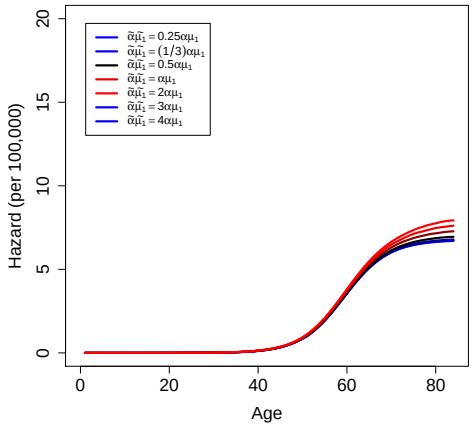

(a) Prevalence: $P(t)$.

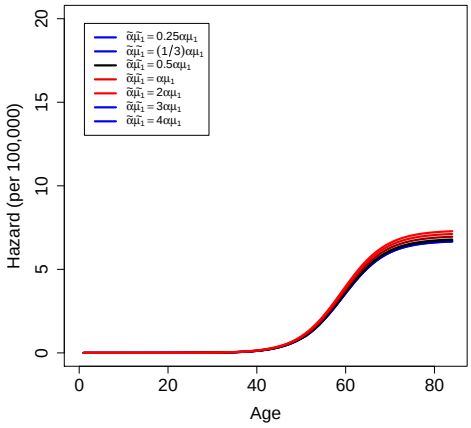

(b) Prevalence: average value of $P(t)$.

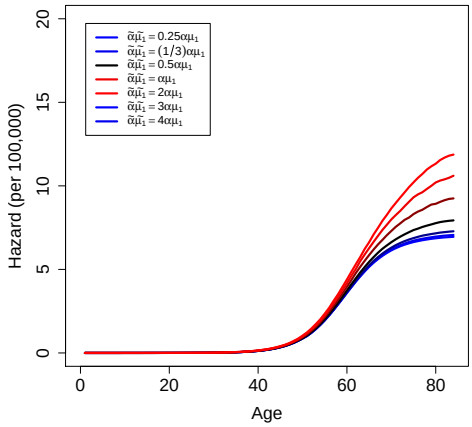

(c) Prevalence: $4P(t)$.

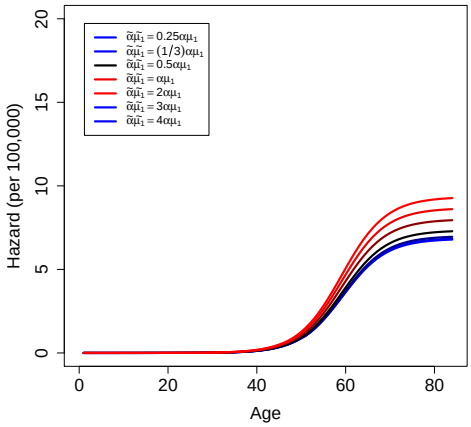

(d) Prevalence: average value of $4P(t)$.

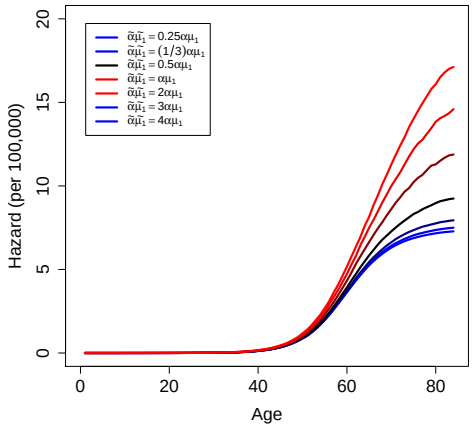

(e) Prevalence: $8P(t)$.

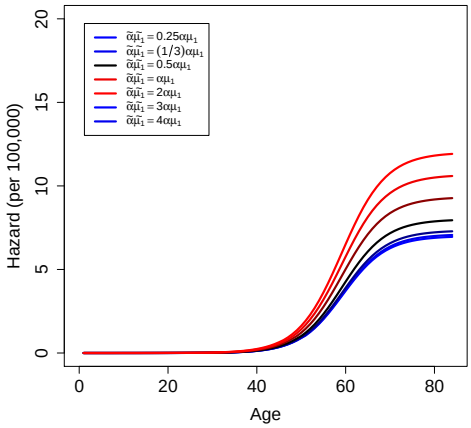

(f) Constant prevalence: average value of $8P(t)$.

Figure 6.5: Behavior of the MSCE models with infection-related initiation pathways for different values of $\sigma X/\tilde{\alpha}$. The hazard in black is for the same phenotype model, and the hazards in color are the different phenotype model.

between individuals with an HPV infection and those without was also identifiable. We also found that the shape of the hazard did not deviate significantly from the canonical shape of the TSCE model.

The model that allowed different tumorigenesis dynamics for the two types of initiation displayed a wider range of behavior; some instances of which were similar to age-effects for oral cancer that we previously estimated. In fact, it may be possible to make inferences about the prevalence of HPV from the incidence of oral cancer. The identifiable combinations related to the second pathway were analogous to those of the first pathway. However, depending on the shape of the age-specific incidence and prevalence functions, practical identifiability of these combinations may be difficult. Additionally, the relative risk between individuals with an HPV infection and those without is not identifiable in this model.

6.5 Appendix

The proofs of Propositions 6.2.1 and 6.2.2 are outlined here. Calculations were carried out in Mathematica 10.

- Solve the $\dot{x}_6$ equation for x_4. Take a derivative to find $\dot{x}_4$. Then, x_4 and $\dot{x}_4$ are functions of x_2, x_6, u, and their derivatives.
- Substitute x_4, $\dot{x}_4$, and $\dot{x}_2$ (from the $\dot{x}_2$ equation) into the $\dot{x}_4$ equation and clear the denominator. This equation now contains x_1, x_2, x_3 and various derivatives of x_6 and u.
- Solve this equation for x_2, and take a derivative to find $\dot{x}_2$. Plug these into the $\dot{x}_2$ equation. Plug in $\dot{x}_1$ and $\dot{x}_3$ (from the $\dot{x}_1$ and $\dot{x}_3$ equations). Clear the denominator. This equation now contains x_1, x_3, and derivatives of x_6 and u.
- Solve the $\dot{x}_5$ equation for x_3. Take a derivative to find $\dot{x}_3$. Plug these into the two equations that still contain x_3 and its derivative, and clear the denominators. There are now three equations containing only x_1, x_5, x_6, u, and their derivatives.
- Solve for x_1 using what was formerly the $\dot{x}_3$ equation. Then, x_1 has two solutions of the form $(p_1 \pm \sqrt{p_2})/p_3)$. Find p_1, p_2, p_3 and their derivatives.
- Plug $x_1 = (p_1 + \sqrt{p_2})/p_3$ into the $\dot{x}_1$ equation, and clear the denominator. The equation is now of the form $0 = v + w\sqrt{p_2}$ where v and w are functions of the parameters and p_1, p_2, and p_3. Multiply both sides of the equation by $v - w\sqrt{p_2}$ to clear the square roots. Plug in p_1, p_2, p_3 and their derivatives. This is now an algebraic equation only in x_5, x_6, u, and their derivatives.
- Do the same operations for the other equation (formerly $\dot{x}_2$ equation).
- The remaining two equations are algebraic equations of in x_5, x_6, u, and their derivatives.
- For $u \equiv 1$, the two equations have 23 and 56 monomials whose coefficients

have between 2 and 2936 terms. For $u = u(s)$, the equations have 424 and 1525 monomials.

- In each equation, divide by the coefficient of one of the monomials to be sure that the equations are monic. Collect all of the coefficients.
- Determine the identifiable combinations from the list of coefficients by setting the coefficients equal to copies of themselves with placeholder parameter values and finding a Gröebner basis. In particular, we set $\alpha = 2$, $\beta = 3$, $\mu_1 = 5$, $\tilde{\alpha} = 7$, $\tilde{\beta} = 11$, $\tilde{\mu}_1 = 13$, $\mu_0 X = 17$, and $\sigma X = 19$. The output of the Solve function in Mathematica is shown eqs. 6.21 and 6.22 for the two models respectively.

$$
\begin{aligned}
\alpha &= \frac{2}{17}\mu_0 X \\
\tilde{\alpha} &= \frac{7}{19}\sigma X \\
\beta &= \frac{1}{17}\left(2\mu_0 X - 17\mu_1 - 2\sqrt{17}\sqrt{323 - 2\mu_0 X \mu_1}\right) \\
\tilde{\beta} &= \frac{1}{38}\left(1360 + \frac{35409}{\sigma X} - \frac{119\mu_0 X \mu_1}{\sigma X} + 14\sigma X \right. \\
&\qquad \left. + \frac{680\sqrt{17}\sqrt{323 - 2\mu_0 X \mu_1}}{\sigma X} + 14\sqrt{17}\sqrt{323 - 2\mu_0 X \mu_1}\right) \\
\tilde{\mu}_1 &= \frac{1}{38\sigma X}\left(-35409 + 119\mu_0 X \mu_1 - 680\sqrt{17}\sqrt{323 - 2\mu_0 X \mu_1}\right)
\end{aligned}
\tag{6.21}
$$

$$
\begin{aligned}
\alpha &= \frac{2}{17}\mu_0 X \\
\sigma X &= \frac{19}{7}\tilde{\alpha} \\
\mu_1 &= \frac{86}{\mu_0 X} \\
\tilde{\mu}_1 &= \frac{91}{\tilde{\alpha}} \\
\beta &= 6 - \frac{85}{\mu_0 X} + \frac{2}{17}\mu_0 X \\
\tilde{\beta} &= 17 - \frac{91}{\tilde{\alpha}} + \tilde{\alpha}
\end{aligned}
\tag{6.22}
$$

CHAPTER VII

Conclusion

The human papillomavirus presents an inherently multiscale problem. Prevalence data is typically available at the population level, as is data for incidence of HPV-related cancers. However, transmission of the virus occurs on a local scale, and the transition from infectious disease to etiological agent of cancer—by HPV genome integration in host DNA—happens within an individual. Time, too, presents a challenge; infection and clearance are measured in months and years, but it may take more than a decade between the time of infection and the clinical detection of a tumor. This dissertation addresses, through a variety of mathematical models, the dynamics of HPV on different scales.

In Chapter III, I considered data in NHANES for oral and genital HPV prevalence as well as seroprevalence of HPV antibodies. I found that two-site concurrent infection and gentotype-concordant infection (or infection at the same time as the detection of antibodies in serum for that genotype) could differ significantly by age, by race, and by sex. The lack of correlation between tests suggests that there will be no easy test for being at risk for HPV-related cancer. There is current controversy among medical professionals as to whether cervicovaginal tests for HPV DNA should replace Pap smears in routine gynocological exams. That discussion, however, does not address risk of oropharyngeal or anal cancer. Our study suggests that the presence of serum antibodies is not a useful test for HPV presence, being poorly correlated with current oral and genital infection and varying (for oral) by sex; too,

vaccination typically causes seroconversion, making a test of serum antibodies unable to distinguish between a person who has been vaccinated and one who has seroconverted through infection.

Chapter III also analyzed, using age–cohort models, trends in the prevalence by age and relative prevalence by birth cohort of vaginal HPV infection and of seroprevalence among men and women. This is the first study to try to characterize large-scale trends in HPV infection in the United States. Further, this study highlights the racial differences in HPV prevalence. Unfortunately, testing for oral HPV infection is relatively recent, and testing for genital HPV in men is not being done at the population level. To better characterize HPV prevalence and link it to incidence of genital, anal, and oropharyngeal cancer, it is imperative that more comprehensive testing be undertaken. Additionally, as further NHANES survey data become available, we will be able to add confidence to our existing models.

In Chapter IV, I constructed a two-site infectious disease ODE model to better understand how the virus's ability to infect multiple sites affects its dynamics as an infectious disease. To this end, I considered the impact of of autoinoculation and how heterogeneity in the transmission pathways affected the basic reproduction number R_0, a widely used measure of a disease's potential to cause an epidemic. This is the first analysis of a model of a multisite infectious disease. I found that consideration of autoinoculation increases the complexity of the form of the basic reproductive number; we must be concerned, therefore, about the possible introduction of mispecification errors if only modeling HPV as a genital disease. Analysis of heterogeneity between the same-site parameters and between the cross-site parameters demonstrated that, for a fixed sum of transmission parameters, heterogeneity in the same-site terms increases R_0 while heterogeneity in the cross-site terms decreases it. This is an unusual finding, as heterogeneity is known to increase R_0 in classical models. Although these findings are suggestive and identify underlying dynamics, there are two obstacles to using this model currently to investigate HPV transmission in the United States. First, although some information is known

about clearance rates of HPV, little is known about transmission or autoinoculation rates. Second, assuming infectious contacts are well-mixed is a poor assumption for a sexually transmitted infection, even if taking heterosexuality into account, because of high demographic assortativity. The first problem will need to be addressed through observational studies. The second can be treated by further stratifying the model state space or reimagining the model with a network structure; each technique has its own challenges, however.

Chapter IV also addressed disease control. The basic reproduction number can provide information on the fraction of the population that would need to be vaccinated to force the disease to die out. The type and target reproduction numbers allow consideration of more finely tuned controls, such as vaccination of one sex or condom use. Once values of transmission and autoinoculation parameters are better known, it will be possible to identify reservoir host or site types that, if not targeted with controls, will make it difficult to control the disease in the overall population.

Chapter V leveraged age–period–cohort and multistage clonal expansion models to consider trends and racial disparities in oral (oropharyngeal and oral cavity) squamous cell carcinoma incidence in the United States. Using these models in combination allowed me to ground the model in the underlying biology of tumorigenesis, resolve the unidentifiability problem of the APC model, and consider temporal trends in tumor initiation rates. This is the first study to look at oral cancer using the multistage clonal expansion model paradigm. Although the primary aim of this project was to consider HPV-related subsites, consideration of HPV-unrelated subsites allowed deeper insight. Carcinomas of the oral tongue had different tumor promotion rates from cancers at the other two subsite groups, corroborating previous hypotheses about different etiologies. Further, for all three subsite groups considered, men had higher initiation rates than women and black men and women had higher promotion rates than white men and women. If one were considering HPV-related sites alone, it would have been reasonable to hypothesize that these differences and the relative incidence were related to the relative prevalence of oral

HPV in the United States. However, since all three subgroups had these similar patterns, they are more likely attributable to male–female biological differences and risk factor differences between racial groups.

Chapter VI extended the two-stage clonal expansion model considered in Chapter V to consider to models incorporating infection-related initiation pathways. I derive model equations under the assumption that the infection-related pathway leads to promotion and malignant conversion rates identical to infection-unrelated initiation and under the assumption that the rates differ. These models are a novel approach to connecting infectious disease prevalence to cancer incidence. I also addressed the identifiability of these models, which is necessary if one wishes to do parametric inference from cancer incidence data, using a differential algebra approach. Behavior of the models is considered for a range of prevalence functions, and the behavior of the different cancer phenotype model was compared to that of the same cancer phenotype model by varying the relative magnitudes of their analogous identifiable combinations. The different phenotype model was found to display a wider range of behavior and sensitivity to the prevalence functions, raising the possibility that information about prevalence could be inferred from incidence data, though issues of practical identifiability may make confident estimation of the identifiable combinations difficult.

These four chapters considered the prevalence of HPV, the dynamics of HPV as an infectious disease, and incidence of HPV-related oropharyngeal cancer. This dissertation lays the groundwork for a multiscale approach to the problem and describes one possible method to connect prevalence to incidence without an intermediate within-host model.

Bibliography

Adler, F. R. (1992). The Effects of Averaging on the Basic Reproductive Ratio. Mathematical Biosciences, 111(1):89–98.

Ali, H., Donovan, B., Wand, H., Read, T. R. H., Regan, D. G., Grulich, A. E., Fairley, C. K., and Guy, R. J. (2013). Genital warts in young Australians five years into national human papillomavirus vaccination programme: national surveillance data. BMJ (Clinical research ed.), 346:2032–2032.

Anderson, A. R. and Chaplain, M. A. (1998). Continuous and discrete mathematical models of tumor-induced angiogenesis. Bulletin of Mathematical Biology, 60(5):857–99.

Anderson, A. R., Chaplain, M. A. J., and McDougall, S. (2012). A Hybrid Discrete-Continuum Model of Tumour Induced Angiogenesis. In Jackson, T. L., editor, Modeling Tumor Vasculature, pages 105–133. Springer, New York, NY.

Anderson, R. M. and May, R. M. (1991). Infectious diseases of humans: dynamics and control. Oxford University Press, New York.

Anfinsen, K. P., Devesa, S. S., Bray, F., Troisi, R., Jonasdottir, T. J., Bruland, O. S., and Grotmol, T. (2011). Age-period-cohort analysis of primary bone cancer incidence rates in the United States (1976-2005). Cancer Epidemiology, Biomarkers & Prevention, 20(8):1770–7.

Armitage, P. and Doll, R. (1954). The age distribution of cancer and a multi-stage theory of carcinogenesis. British Journal of Cancer, VIII(I):1–12.

Armitage, P. and Doll, R. (1957). A two-stage theory of carcinogenesis in relation to the age distribution of human cancer. British Journal of Cancer, 11(2):161–169.

Audoly, S., Bellu, G., D'Angiò, L., Saccomani, M. P., and Cobelli, C. (2001). Global identifiability of nonlinear models of biological systems. IEEE Transactions on Biomedical Engineering, 48(1):55–65.

Barnabas, R. V., Laukkanen, P., Koskela, P., Kontula, O., Lehtinen, M., and Garnett, G. P. (2006). Epidemiology of HPV 16 and cervical cancer in Finland and the potential impact of vaccination: mathematical modelling analyses. PLoS Medicine, 3(5):e138.

Bartlett, M. (1953). Stochastic processes or the statistics of change. Journal of the Royal Statistical Society. Series C (Applied Statistics), 2(1):44–64.

Baussano, I., Lazzarato, F., Ronco, G., Dillner, J., and Franceschi, S. (2013). Benefits of catch-up in vaccination against human papillomavirus in medium- and low-income countries. International Journal of Cancer, 133(8):1876–81.

Bellman, R. and Åström, K. (1970). On structural identifiability. Mathematical Biosciences, 7:329–339.

Bergeron, C., Largeron, N., McAllister, R., Mathevet, P., and Remy, V. (2008). Cost-effectiveness analysis of the introduction of a quadrivalent human papillomavirus vaccine in France. International Journal of Technology Assessment in Health Care, 24(1):10–9.

Bogaards, J. a., Coupé, V. M. H., Xiridou, M., Meijer, C. J. L. M., Wallinga, J., and Berkhof, J. (2011). Long-term impact of human papillomavirus vaccination on infection rates, cervical abnormalities, and cancer incidence. Epidemiology, 22(4):505–15.

Botman, S., Moore, T., Moriarty, C., and Parsons, V. (2000). Design and Estimation for the National Health Interview, 1995-2004. Vital Health Stat 2, 130:1–31.

Brisson, M., Van de Velde, N., and Boily, M.-C. (2009). Economic evaluation of human papillomavirus vaccination in developed countries. Public health genomics, 12(5-6):343–51.

Brisson, M., Van de Velde, N., De Wals, P., and Boily, M.-C. (2007a). Estimating the number needed to vaccinate to prevent diseases and death related to human papillomavirus infection. Canadian Medical Association Journal, 177(5):2–6.

Brisson, M., Van de Velde, N., De Wals, P., and Boily, M.-C. (2007b). The potential cost-effectiveness of prophylactic human papillomavirus vaccines in Canada. Vaccine, 25(29):5399–408.

Brisson, M., van de Velde, N., Franco, E. L., Drolet, M., and Boily, M.-C. (2011). Incremental impact of adding boys to current human papillomavirus vaccination programs: role of herd immunity. Journal of Infectious Diseases, 204(3):372–6.

Brown, L. M., Check, D. P., and Devesa, S. S. (2011). Oropharyngeal cancer incidence trends: diminishing racial disparities. Cancer Causes & Control, 22(5):753–63.

Brown, L. M., Check, D. P., and Devesa, S. S. (2012). Oral cavity and pharynx cancer incidence trends by subsite in the United States: changing gender patterns. Journal of Oncology, 2012:649498.

Burchell, A. N., Coutlée, F., Tellier, P.-P., Hanley, J., and Franco, E. L. (2011). Genital transmission of human papillomavirus in recently formed heterosexual couples. Journal of Infectious Diseases, 204(11):1723–9.

Centers for Disease Control and Prevention (2012). National and State Vaccination Coverage Among Adolescents Aged 13–17 Years — United States, 2011. Morbidity and Mortality Weekly Report, 61(34):671–677.

Centers for Disease Control and Prevention (2013). National and State Vaccination Coverage Among Adolescents Aged 13–17 Years — United States, 2012. Morbidity and Mortality Weekly Report, 62(34):685–693.

Centers for Disease Control and Prevention (2014a). Human Papillomavirus Vaccination Coverage Among Adolescents, 2007–2013, and Postlicensure Vaccine Safety Monitoring, 2006–2014 — United States. Morbidity and Mortality Weekly Report, 63(29):620–4.

Centers for Disease Control and Prevention (2014b). National Health and Nutrition Examination Survey. http://www.cdc.gov/nchs/nhanes.htm. Accessed February 13, 2014.

Chappell, M. J., Godfrey, K. R., and Vajda, S. (1990). Global identifiability of the parameters of nonlinear systems with specified inputs: A comparison of methods. Mathematical Biosciences, 102:41–73.

Chaturvedi, A. K., Anderson, W. F., Lortet-Tieulent, J., Curado, M. P., Ferlay, J., Franceschi, S., Rosenberg, P. S., Bray, F., and Gillison, M. L. (2013). Worldwide trends in incidence rates for oral cavity and oropharyngeal cancers. Journal of Clinical Oncology, 31(36):4550–9.

Chaturvedi, A. K., Engels, E. A., Anderson, W. F., and Gillison, M. L. (2008). Incidence trends for human papillomavirus-related and -unrelated oral squamous cell carcinomas in the United States. Journal of Clinical Oncology, 26(4):612–9.

Chaturvedi, A. K., Engels, E. A., Pfeiffer, R. M., Hernandez, B. Y., Xiao, W., Kim, E., Jiang, B., Goodman, M. T., Sibug-Saber, M., Cozen, W., Liu, L., Lynch, C. F., Wentzensen, N., Jordan, R. C., Altekruse, S., Anderson, W. F., Rosenberg, P. S., and Gillison, M. L. (2011). Human papillomavirus and rising oropharyngeal cancer incidence in the United States. Journal of Clinical Oncology, 29(32):4294–301.

Clayton, D. and Schifflers, E. (1987a). Models for temporal variation in cancer rates. I: Age-period and age-cohort models. Statistics in Medicine, 6(4):449–67.

Clayton, D. and Schifflers, E. (1987b). Models for temporal variation in cancer rates. II: Age-period-cohort models. Statistics in Medicine, 6(4):469–81.

Cobelli, C. and DiStefano, J. J. (1980). Parameter and structural identifiability concepts and ambiguities: a critical review and analysis. American Journal of Physiology, 239:R7–R24.

Conway, J. M., Tuite, A. R., Fisman, D. N., Hupert, N., Meza, R., Davoudi, B., English, K., van den Driessche, P., Brauer, F., Ma, J., Meyers, L. A., Smieja, M., Greer, A., Skowronski, D. M., Buckeridge, D. L., Kwong, J. C., Wu, J., Moghadas, S. M., Coombs, D., Brunham, R. C., and Pourbohloul, B. (2011). Vaccination against 2009 pandemic H1N1 in a population dynamical model of Vancouver, Canada: timing is everything. BMC Public Health, 11(1):932.

Crump, K. S., Subramaniam, R. P., and Van Landingham, C. B. (2005). A numerical solution to the nonhomogeneous two-stage MVK model of cancer. Risk Analysis, 25(4):921–6.

Dasbach, E. J., Insinga, R. P., and Elbasha, E. H. (2008). The epidemiological and economic impact of a quadrivalent human papillomavirus vaccine (6/11/16/18) in the UK. BJOG : an international journal of obstetrics and gynaecology, 115(8):947–56.

De-Camino-Beck, T., Lewis, M. A., and van den Driessche, P. (2009). A graph-theoretic method for the basic reproduction number in continuous time epidemiological models. Journal of Mathematical Biology, 59(4):503–16.

Dewanji, A., Jeon, J., Meza, R., and Luebeck, E. G. (2011). Number and size distribution of colorectal adenomas under the multistage clonal expansion model of cancer. PLoS Computational Biology, 7(10):e1002213.

Diekmann, O. and Heesterbeek, J. (2000). Mathematical epidemiology of infectious diseases: model building, analysis, and interpretation. New York John Wiley, Chichester.

Diekmann, O., Heesterbeek, J., and Metz, J. (1990). On the definition and the computation of the basic reproduction ratio R 0 in models for infectious diseases in heterogeneous populations. Journal of Mathematical Biology, pages 365–382.

Diekmann, O., Heesterbeek, J. A. P., and Roberts, M. G. (2010). The construction of next-generation matrices for compartmental epidemic models. Journal of the Royal Society, Interface, 7(47):873–885.

Doob, J. (1942). Topics in the theory of Markoff chains. Transactions of the American Mathematical Society, 52(1):37–64.

Doob, J. (1945). Markoff Chains – Denumerable Case. Transactions of the American Mathematical Society, 58(3):455–473.

Dunne, E. F., Unger, E. R., Sternberg, M., McQuillan, G., Swan, D. C., Patel, S. S., and Markowitz, L. E. (2007). Prevalence of HPV infection among females in the United States. Journal of the American Medical Association, 297(8):813–9.

Dushoff, J. and Levin, S. (1995). The effects of population heterogeneity on disease invasion. Mathematical Biosciences, 128(1-2):25–40.

Edelstein, Z. R., Schwartz, S. M., Hawes, S., Hughes, J. P., Feng, Q., Stern, M. E., O'Reilly, S., Lee, S.-K., Fu Xi, L., and Koutsky, L. a. (2012). Rates and determinants of oral human papillomavirus infection in young men. Sexually Transmitted Diseases, 39(11):860–7.

Eisenberg, M. (2013). Generalizing the differential algebra approach to input-output equations in structural identifiability. arXiv:1302.5484v1.

Eisenberg, M. C., Kim, Y., Li, R., Ackerman, W. E., Kniss, D. A., and Friedman, A. (2011). Mechanistic modeling of the effects of myoferlin on tumor cell invasion. Proceedings of the National Academy of Sciences, 108(50):20078–83.

Eisenberg, M. C., Robertson, S. L., and Tien, J. H. (2013). Identifiability and estimation of multiple transmission pathways in cholera and waterborne disease. Journal of Theoretical Biology, 324:84–102.

Elbasha, E. H. and Dasbach, E. J. (2010). Impact of vaccinating boys and men against HPV in the United States. Vaccine, 28(42):6858–67.

Elbasha, E. H., Dasbach, E. J., and Insinga, R. P. (2007). Model for assessing human papillomavirus vaccination strategies. Emerging Infectious Diseases, 13(1):28–41.

Elbasha, E. H., Dasbach, E. J., Insinga, R. P., Haupt, R. M., and Barr, E. (2009). Age-based programs for vaccination against HPV. Value in Health, 12(5):697–707.

Eubank, S., Guclu, H., and Kumar, V. (2004). Modelling disease outbreaks in realistic urban social networks. Nature, 429(May):180–184.

Evans, N. D. and Chappell, M. J. (2000). Extensions to a procedure for generating locally identifiable reparameterisations of unidentifiable systems. Mathematical Biosciences, 168:137–159.

Fisher, J. (1958). Multiple-mutation theory of carcinogenesis. Nature, 181(4609):651–652.

Franco, E. L., Villa, L. L., Sobrinho, J. P., Prado, J. M., Rousseau, M. C., Désy, M., and Rohan, T. E. (1999). Epidemiology of acquisition and clearance of cervical human papillomavirus infection in women from a high-risk area for cervical cancer. Journal of Infectious Diseases, 180(5):1415–23.

Friedman, A. and Jain, H. (2013). A partial differential equation model of metastasized prostatic cancer. Mathematical Biosciences and Engineering, 10(3):591–608.

Gerberding, J. (2004). Prevention of Genital Human Papillomavirus Infection. Technical Report January.

Gillespie, D. (1977). Exact stochastic simulation of coupled chemical reactions. The journal of Physical Chemistry, 81(25):2340–2361.

Gillespie, D. T. (1976). A general method for numerically simulating the stochastic time evolution of coupled chemical reactions. Journal of Computational Physics, 22(4):403–434.

Gillison, M. L., Alemany, L., Snijders, P. J. F., Chaturvedi, A., Steinberg, B. M., Schwartz, S., and Castellsagué, X. (2012a). Human papillomavirus and diseases of the upper airway: head and neck cancer and respiratory papillomatosis. Vaccine, 30 Suppl 5:F34–54.

Gillison, M. L., Broutian, T., Pickard, R. K. L., Tong, Z.-y., Xiao, W., Kahle, L., Graubard, B. I., and Chaturvedi, A. K. (2012b). Prevalence of oral HPV infection in the United States, 2009-2010. Journal of the American Medical Association, 307(7):693–703.

Giuliano, A. R., Lee, J.-H., Fulp, W., Villa, L. L., Lazcano, E., Papenfuss, M. R., Abrahamsen, M., Salmeron, J., Anic, G. M., Rollison, D. E., and Smith, D. (2011). Incidence and clearance of genital human papillomavirus infection in men (HIM): a cohort study. Lancet, 377(9769):932–40.

Goldie, S. J., Kohli, M., Grima, D., Weinstein, M. C., Wright, T. C., Bosch, F. X., and Franco, E. (2004). Projected Clinical Benefits and Cost-effectiveness of a Human Papillomavirus 16/18 Vaccine. Journal of the National Cancer Institute, 96(8):604–615.

Goodman, M. T., Shvetsov, Y. B., McDuffie, K., Wilkens, L. R., Zhu, X., Thompson, P. J., Ning, L., Killeen, J., Kamemoto, L., and Hernandez, B. Y. (2010). Sequential acquisition of human papillomavirus (HPV) infection of the anus and cervix: the Hawaii HPV Cohort Study. The Journal of Infectious Diseases, 201(9):1331–9.

Gravitt, P. E., Rositch, A. F., Silver, M. I., Marks, M. A., Chang, K., Burke, A. E., and Viscidi, R. P. (2013). A cohort effect of the sexual revolution may be masking an increase in human papillomavirus detection at menopause in the United States. Journal of Infectious Diseases, 207(2):272–80.

Günther, O. P., Ogilvie, G., Naus, M., Young, E., Patrick, D. M., Dobson, S., Duval, B., Noël, P.-A., Marra, F., Miller, D., Brunham, R. C., and Pourbohloul, B. (2008). Protecting the next generation: what is the role of the duration of human papillomavirus vaccine-related immunity? Journal of Infectious Diseases, 197(12):1653–61.

Hariri, S., Unger, E. R., Sternberg, M., Dunne, E. F., Swan, D., Patel, S., and Markowitz, L. E. (2011). Prevalence of genital human papillomavirus among females in the United States, the National Health And Nutrition Examination Survey, 2003-2006. Journal of Infectious Diseases, 204(4):566–73.

Harris, T. E. (1963). Theory of Branching Processes. Springer-Verlag OHG, Berlin.

Harrison, C., Britt, H., Garland, S., Conway, L., Stein, A., Pirotta, M., and Fairley, C. (2014). Decreased Management of Genital Warts in Young Women in Australian General Practice Post Introduction of National HPV Vaccination Program: Results from a Nationally Representative Cross-Sectional General Practice Study. PloS One, 9(9):e105967.

Hazelton, W. D., Moolgavkar, S. H., Curtis, S. B., Zielinski, J. M., Ashmore, J. P., and Krewski, D. (2006). Biologically based analysis of lung cancer incidence in a large Canadian occupational cohort with low-dose ionizing radiation exposure, and comparison with Japanese atomic bomb survivors. Journal of Toxicology and Environmental Health. Part A, 69(11):1013–38.

Heesterbeek, J. and Dietz, K. (1996). The concept of R_0 in epidemic theory. Statistica Neerlandica, 50(1):89–110.

Heesterbeek, J. a. P. and Roberts, M. G. (2007). The type-reproduction number T in models for infectious disease control. Mathematical Biosciences, 206(1):3–10.

Heidenreich, W. F., Luebeck, E. G., and Moolgavkar, S. H. (1997). Some properties of the hazard function of the two-mutation clonal expansion model. Risk Analysis, 17(3):391–9.

Hernandez, B. Y., McDuffie, K., Zhu, X., Wilkens, L. R., Killeen, J., Kessel, B., Wakabayashi, M. T., Bertram, C. C., Easa, D., Ning, L., Boyd, J., Sunoo, C., Kamemoto, L., and Goodman, M. T. (2005). Anal human papillomavirus infection in women and its relationship with cervical infection. Cancer Epidemiology, Biomarkers & Prevention, 14(11 Pt 1):2550–6.

Hernandez, B. Y., Wilkens, L. R., Zhu, X., Thompson, P., McDuffie, K., Shvetsov, Y. B., Kamemoto, L. E., Killeen, J., Ning, L., and Goodman, M. T. (2008). Transmission of human papillomavirus in heterosexual couples. Emerging infectious diseases, 14(6):888–94.

Hethcote, H. (2000). The mathematics of infectious diseases. SIAM Review, 42(4):599–653.

Ho, G. and Bierman, R. (1998). Natural history of cervicovaginal papillomavirus infection in young women. New England Journal of Medicine, 338(7):423–428.

Holford, T. R. (1983). The Estimation of Age, Period and Cohort Effects for Vital Rates. Biometrics, 39(2):311–324.

Holford, T. R. (1991). Understanding the Effects of Age, Period, and Cohort on Incidence and Mortality Rates. Annual Review of Public Health, 12(1):425–457.

Holford, T. R., Cronin, K. A., Mariotto, A. B., and Feuer, E. J. (2006). Changing patterns in breast cancer incidence trends. Journal of the National Cancer Institute Monographs, 8034(36):19–25.

Holford, T. R., Levy, D. T., McKay, L. A., Clarke, L., Racine, B., Meza, R., Land, S., Jeon, J., and Feuer, E. J. (2014). Patterns of birth cohort-specific smoking histories, 1965-2009. American Journal of Preventive Medicine, 46(2):e31–7.

Hughes, J. P., Garnett, G. P., and Koutsky, L. (2002). The theoretical population-level impact of a prophylactic human papilloma virus vaccine. Epidemiology, 13(6):631–9.

IARC (2007). IARC monographs on the evaluation of carcinogenic risks to humans, volume 90, human papillomaviruses. IARC Monographs on the Evaluation of Carcinogenic Risks to Humans, 90:1–636.

Jackson, T. and Zheng, X. (2010). A cell-based model of endothelial cell migration, proliferation and maturation during corneal angiogenesis. Bulletin of Mathematical Biology, 72(4):830–68.

Jackson, T. L. and Zheng, X. (2012). A Cell-Based Model of Endothelial Cell Migration, Proliferation, and Maturation in Corneal Angiogenesis. In Jackson, T. L., editor, Modeling Tumor Vasculature, pages 151–165. Springer, New York, NY.

Jemal, A., Simard, E. P., Dorell, C., Noone, A.-M., Markowitz, L. E., Kohler, B., Eheman, C., Saraiya, M., Bandi, P., Saslow, D., Cronin, K. A., Watson, M., Schiffman, M., Henley, S. J., Schymura, M. J., Anderson, R. N., Yankey, D., and Edwards, B. K. (2013). Annual Report to the Nation on the Status of Cancer, 1975-2009, Featuring the Burden and Trends in Human Papillomavirus (HPV)-Associated Cancers and HPV Vaccination Coverage Levels. Journal of the National Cancer Institute, 105(3):175–201.

Jeon, J., Luebeck, E. G., and Moolgavkar, S. H. (2006). Age effects and temporal trends in adenocarcinoma of the esophagus and gastric cardia (United States). Cancer Causes & Control, 17(7):971–81.

Jeon, J., Meza, R., Moolgavkar, S. H., and Luebeck, E. G. (2008). Evaluation of screening strategies for pre-malignant lesions using a biomathematical approach. Mathematical Biosciences, 213(1):56–70.

Jit, M., Choi, Y. H., and Edmunds, W. J. (2008). Economic evaluation of human papillomavirus vaccination in the United Kingdom. BMJ, 337(jul17 2):a769–a769.

Joura, E. A., Giuliano, A. R., Iversen, O.-E., Bouchard, C., Mao, C., Mehlsen, J., Moreira, E. D., Ngan, Y., Petersen, L. K., Lazcano-Ponce, E., Pitisuttithum, P., Restrepo, J. A., Stuart, G., Woelber, L., Yang, Y. C., Cuzick, J., Garland, S. M., Huh, W., Kjaer, S. K., Bautista, O. M., Chan, I. S., Chen, J., Gesser, R., Moeller, E., Ritter, M., Vuocolo, S., and Luxembourg, A. (2015). A 9-Valent HPV Vaccine against Infection and Intraepithelial Neoplasia in Women. New England Journal of Medicine, 372:711–723.

Keeling, M. J. and Rohani, P. (2008). Modeling infectious dieases in humans and animals. Princeton University Press, Princeton.

Kendall, D. G. (1960). Birth-and-Death Processes, and the Theory of Carcinogenesis. Biometrika, 47:13–21.

Kermack, W. O. and McKendrick, A. G. (1927). A Contribution to the Mathematical Theory of Epidemics.

Kilfoy, B. A., Devesa, S. S., Ward, M. H., Zhang, Y., Rosenberg, P. S., Holford, T. R., and Anderson, W. F. (2009). Gender is an age-specific effect modifier for papillary cancers of the thyroid gland. Cancer Epidemiology, Biomarkers & Prevention, 18(4):1092–100.

Kim, J. and Goldie, S. (2008). Health and economic implications of HPV vaccination in the United States. New England Journal of Medicine, pages 821–832.

Kim, J. and Goldie, S. (2009). Cost effectiveness analysis of including boys in a human papillomavirus vaccination programme in the United States. BMJ, 339.

Kim, J. J. (2010). Targeted human papillomavirus vaccination of men who have sex with men in the USA: a cost-effectiveness modelling analysis. Lancet Infectious Diseases, 10(12):845–52.

Kopp-Schneider, A. (1997). Carcinogenesis models for risk assessment. Statistical Methods in Medical Research, (6):317–340.

Kreimer, A. R. (2014). Prospects for prevention of HPV-driven oropharynx cancer. Oral Oncology, 50(6):555–9.

Kreimer, A. R., Campbell, C. M. P., Lin, H.-Y., Fulp, W., Papenfuss, M. R., Abrahamsen, M., Hildesheim, A., Villa, L. L., Salmerón, J. J., Lazcano-Ponce, E., and Giuliano, A. R. (2013). Incidence and clearance of oral human papillomavirus infection in men: the HIM cohort study. Lancet, 6736(13):1–11.

Kulasingam, S. L., Connelly, L., Conway, E., Hocking, J. S., Myers, E. R., Regan, D. G., Roder, D., Ross, J., and Wain, G. (2007). A cost-effectiveness analysis of adding a human papillomavirus vaccine to the Australian National Cervical Cancer Screening Program. Sexual Health, 4(3):165–175.

Kulasingam, S. L. and Myers, E. R. (2003). Potential Health and Economic Impact of Adding a Human Papillomavirus Vaccine. Journal of the American Medical Association, 290(6):781–789.

Lansdorp-Vogelaar, I., Kuntz, K. M., Knudsen, A. B., van Ballegooijen, M., Zauber, A. G., and Jemal, A. (2012). Contribution of screening and survival differences to racial disparities in colorectal cancer rates. Cancer Epidemiology, Biomarkers & Prevention, 21(5):728–36.

Little, M. P. (1995). Are two mutations sufficient to cause cancer? Some generalizations of the two-mutation model of carcinogenesis of Moolgavkar, Venzon, and Knudson, and of the. Biometrics, 4:1278–1291.

Little, M. P., Haylock, R. G. E., and Muirhead, C. R. (2002). Modelling lung tumour risk in radon-exposed uranium miners using generalizations of the two-mutation model of Moolgavkar, Venzon and Knudson. International Journal of Radiation Biology, 78(1):49–68.

Little, M. P., Heidenreich, W. F., and Li, G. (2009). Parameter identifiability and redundancy in a general class of stochastic carcinogenesis models. PLoS One, 4(12):1–6.

Lu, B., Viscidi, R. P., Wu, Y., Nyitray, A. G., Villa, L. L., Lazcano-Ponce, E., Carvalho da Silva, R. J., Baggio, M. L., Quiterio, M., Salmerón, J., Smith, D. C., Abrahamsen, M., Papenfuss, M., and Giuliano, A. R. (2012). Seroprevalence of human papillomavirus (HPV) type 6 and 16 vary by anatomic site of HPV infection in men. Cancer Epidemiology, Biomarkers & Prevention, 21(9):1542–6.

Lu, B., Wu, Y., Nielson, C. M., Flores, R., Abrahamsen, M., Papenfuss, M., Harris, R. B., and Giuliano, A. R. (2009). Factors associated with acquisition and clearance of human papillomavirus infection in a cohort of US men: a prospective study. The Journal of Infectious Diseases, 199(3):362–71.

Luebeck, E., Curtius, K., Jeon, J., and Hazelton, W. (2013). Impact of tumor progression on cancer incidence curves. Cancer research, 73(3):1086–1096.

Luebeck, E. G. and Moolgavkar, S. H. (1991). Stochastic analysis of intermediate lesions in carcinogenesis experiments. Risk Analysis, 11(1):149–57.

Luebeck, E. G. and Moolgavkar, S. H. (2002). Multistage carcinogenesis and the incidence of colorectal cancer. Proceedings of the National Academy of Sciences, 99(23):15095–100.

Luebeck, E. G., Moolgavkar, S. H., Liu, A. Y., Boynton, A., and Ulrich, C. M. (2008). Does folic acid supplementation prevent or promote colorectal cancer? Results from model-based predictions. Cancer Epidemiology, Biomarkers & Prevention, 17(6):1360–7.

Luebeck, G. and Meza, R. (2013). Bhat: General likelihood exploration. R package version 0.9-10.

Markowitz, L. E., Hariri, S., Lin, C., Dunne, E. F., Steinau, M., McQuillan, G., and Unger, E. R. (2013). Reduction in Human Papillomavirus (HPV) Prevalence Among Young Women Following HPV Vaccine Introduction in the United States, National Health and Nutrition Examination Surveys, 2003-2010. Journal of Infectious Diseases, pages 1–9.

Markowitz, L. E., Sternberg, M., Dunne, E. F., McQuillan, G., and Unger, E. R. (2009). Seroprevalence of human papillomavirus types 6, 11, 16, and 18 in the United States: National Health and Nutrition Examination Survey 2003-2004. Journal of Infectious Diseases, 200(7):1059–67.

Marur, S., D'Souza, G., Westra, W. H., and Forastiere, A. a. (2010). HPV-associated head and neck cancer: a virus-related cancer epidemic. Lancet Oncology, 11(8):781–9.

May, R. and Anderson, R. (1987). Transmission dynamics of HIV infection. Nature, 326:137–142.

Mayhew, A., Mullins, T. L. K., Ding, L., Rosenthal, S. L., Zimet, G. D., Morrow, C., and Kahn, J. a. (2014). Risk Perceptions and Subsequent Sexual Behaviors After HPV Vaccination in Adolescents. Pediatrics, 133(3):404–11.

Mbulawa, Z. Z. a., Johnson, L. F., Marais, D. J., Coetzee, D., and Williamson, A.-L. (2013). The impact of human immunodeficiency virus on human papillomavirus transmission in heterosexually active couples. Journal of Infection, 67(1):51–58.

Meshkat, N., Eisenberg, M., and Distefano, J. J. (2009). An algorithm for finding globally identifiable parameter combinations of nonlinear ODE models using Gröbner Bases. Mathematical Biosciences, 222(2):61–72.

Meyers, L. A., Newman, M. E. J., and Pourbohloul, B. (2006). Predicting epidemics on directed contact networks. Journal of Theoretical Biology, 240:400–418.

Meza, R. (2006). Some Extensions and Applications of Multistage Carcinogenesis Models. PhD thesis.

Meza, R., Jeon, J., and Moolgavkar, S. (2010a). Quantitative Cancer Risk Assessment of Nongenotoxic Carcinogens. In Hsu, C.-H. and Stedeford, T., editors, Cancer Risk Assessment, chapter 25, pages 636–658. John Wiley & Sons, Inc.

Meza, R., Jeon, J., Moolgavkar, S. H., and Luebeck, E. G. (2008). Age-specific incidence of cancer: Phases, transitions, and biological implications. Proceedings of the National Academy of Sciences, 105(42):16284–9.

Meza, R., Jeon, J., Renehan, A. G., and Luebeck, E. G. (2010b). Colorectal cancer incidence trends in the United States and United kingdom: evidence of right- to left-sided biological gradients with implications for screening. Cancer Research, 70(13):5419–29.

Meza, R., Luebeck, E. G., and Moolgavkar, S. H. (2005). Gestational mutations and carcinogenesis. Mathematical Biosciences, 197(2):188–210.

Meza, R., Pourbohloul, B., and Brunham, R. C. (2010c). Birth cohort patterns suggest that infant survival predicts adult mortality rates. Journal of Developmental Origins of Health and Disease, 1(03):174–183.

Molano, M., van den Brule, A., Plummer, M., Weiderpass, E., Posso, H., Arslan, A., Meijer, C. J. L. M., Munoz, N., and Franceschi, S. (2003). Determinants of Clearance of Human Papillomavirus Infections in Colombian Women with Normal Cytology: A Population-based, 5-Year Follow-up Study. American Journal of Epidemiology, 158(5):486–494.

Moolgavkar, S. and Luebeck, G. (1990). Two-event model for carcinogenesis: Biological, mathematical, and statistical considerations. Risk Analysis.

Moolgavkar, S. H. and Knudson, A. G. (1981). Mutation and cancer: a model for human carcinogenesis. Journal of the National Cancer Institute, 66(6):1037–52.

Moolgavkar, S. H., Meza, R., and Turim, J. (2009). Pleural and peritoneal mesotheliomas in SEER: age effects and temporal trends, 1973-2005. Cancer Causes & Control, 20(6):935–44.

Moolgavkar, S. H. and Venzon, D. J. (1979). Two-event models for carcinogenesis: incidence curves for childhood and adult tumors. Mathematical Biosciences, 47(1-2):55–77.

Morris, M., Kurth, A. E., Hamilton, D. T., Moody, J., and Wakefield, S. (2009). Concurrent partnerships and HIV prevalence disparities by race: linking science and public health practice. American Journal of Public Health, 99(6):1023–31.

Moscicki, A.-B., Schiffman, M., Burchell, A., Albero, G., Giuliano, A. R., Goodman, M. T., Kjaer, S. K., and Palefsky, J. (2012). Updating the natural history of human papillomavirus and anogenital cancers. Vaccine, 30 Suppl 5:F24–33.

Moscicki, A.-B., Shiboski, S., Broering, J., Powell, K., Clayton, L., Jay, N., Darragh, T. M., Brescia, R., Kanowitz, S., Miller, S. B., Stone, J., Hanson, E., and Palefsky, J. (1998). The natural history of human papillomavirus infection as measured by repeated DNA testing in adolescent and young women. Journal of Pediatrics, 132(2):277–84.

Muñoz, N., Bosch, F. X., de Sanjosé, S., Herrero, R., Castellsagué, X., Shah, K. V., Snijders, P. J. F., and Meijer, C. J. L. M. (2003). Epidemiologic classification of human papillomavirus types associated with cervical cancer. New England Journal of Medicine, 348(6):518–27.

Myers, E. R., McCrory, D. C., Nanda, K., Bastian, L., and Matchar, D. B. (2000). Mathematical model for the natural history of human papillomavirus infection and cervical carcinogenesis. American Journal of Epidemiology, 151(12):1158–71.

Neri, F. M., Bates, A., Füchtbauer, W. S., Pérez-Reche, F. J., Taraskin, S. N., Otten, W., Bailey, D. J., and Gilligan, C. a. (2011). The effect of heterogeneity on invasion in spatial epidemics: from theory to experimental evidence in a model system. PLoS Computational Biology, 7(9):e1002174.

Newman, M. (2002). Spread of epidemic disease on networks. Physical Review E, 66(1):016128.

Neyman, J. and Scott, E. (1967). Statistical aspect of the problem of carcinogenesis. Proceedings of the Fifth Berkeley Symposium on Mathematical Statistics and Probability., (3):745–776.

Nordling, C. (1954). Evidence regarding the multiple mutation theory of the cancer-inducing mechanism. Human Heredity, 5:93–104.

Nordling, C. O. (1953). A new theory on cancer-inducing mechanism. British Journal of Cancer, 7(1):68–72.

Patel, S. C., Carpenter, W. R., Tyree, S., Couch, M. E., Weissler, M., Hackman, T., Hayes, D. N., Shores, C., and Chera, B. S. (2011). Increasing incidence of oral tongue squamous cell carcinoma in young white women, age 18 to 44 years. Journal of Clinical Oncology, 29(11):1488–94.

Perez, L. and Dragicevic, S. (2009). An agent-based approach for modeling dynamics of contagious disease spread. International Journal of Health Geographics, 8:50.

Pickard, R. K. L., Xiao, W., Broutian, T. R., He, X., and Gillison, M. L. (2012). The prevalence and incidence of oral human papillomavirus infection among young men and women, aged 18-30 years. Sexually Transmitted Diseases, 39(7):559–66.

Raue, A., Karlsson, J., Saccomani, M. P., Jirstrand, M., and Timmer, J. (2014). Comparison of approaches for parameter identifiability analysis of biological systems. Bioinformatics, 30:1440–1448.

Raue, A., Kreutz, C., Maiwald, T., Bachmann, J., Schilling, M., Klingmüller, U., and Timmer, J. (2009). Structural and practical identifiability analysis of partially observed dynamical models by exploiting the profile likelihood. Bioinformatics, 25(15):1923–1929.

Rimer, B. K., Harper, H., and Witte, O. N. (2014). Accelerating HPV Vaccine Uptake: Urgency for Action to Prevent Cancer. A Report to the President of the United States from the PresidentâĂŹs Cancer Panel. Technical report, National Cancer Institute, Bethesda, MD.

Ritt, J. F. (1950). Differential Algenra. American Mathematical Society, New York.

Roberts, M. G. and Heesterbeek, J. A. P. (2003). A new method for estimating the effort required to control an infectious disease. Proceedings of the Royal Society B. Biological Sciences, 270(1522):1359–64.

Robertson, S. L., Eisenberg, M. C., and Tien, J. H. (2013). Heterogeneity in multiple transmission pathways: modelling the spread of cholera and other waterborne disease in networks with a common water source. Journal of Biological Dynamics, 7(1):254–75.

Rotherberg, T. J. (1971). Identification in Parametric Models. Econometrica, 39(3):577–591.

Saba, N. F., Goodman, M., Ward, K., Flowers, C., Ramalingam, S., Owonikoko, T., Chen, A., Grist, W., Wadsworth, T., Beitler, J. J., Khuri, F. R., and Shin, D. M. (2011). Gender and ethnic disparities in incidence and survival of squamous cell carcinoma of the oral tongue, base of tongue, and tonsils: a surveillance, epidemiology and end results program-based analysis. Oncology, 81(1):12–20.

Saccomani, M. P., Audoly, S., Bellu, G., and D'Angio, L. (2001). A new differential algebra algorithm to test identifiability of nonlinear systems with given initial conditions. Proceedings of the 40th IEEE Conference on Decision and Control, 4:3108–3113.

Sanders, G. D. and Taira, A. V. (2003). Cost-effectiveness of a potential vaccine for human papillomavirus. Emerging Infectious Diseases, 9(1):37–48.

Schöllnberger, H., Beerenwinkel, N., Hoogenveen, R., and Vineis, P. (2010). Cell selection as driving force in lung and colon carcinogenesis. Cancer Research, 70(17):6797–803.

Shuai, Z., Heesterbeek, J. A. P., and van den Driessche, P. (2013). Extending the type reproduction number to infectious disease control targeting contacts between types. Journal of Mathematical Biology, 67(5):1067–82.

Siebert, U., Alagoz, O., Bayoumi, A. M., Jahn, B., Owens, D. K., Cohen, D. J., and Kuntz, K. M. (2012). State-transition modeling: a report of the ISPOR-SMDM Modeling Good Research Practices Task Force–3. Value in Health, 15(6):812–20.

Skiest, D. J. and Margolis, D. M. (2008). Reply to Cooper et al. Journal of Infectious Diseases, 197(5):775–776.

Steinau, M., Hariri, S., Gillison, M. L., Broutian, T. R., Dunne, E. F., Tong, Z.-y., Markowitz, L. E., and Unger, E. R. (2014). Prevalence of cervical and oral human papillomavirus infections among US women. Journal of Infectious Diseases, 209(11):1739–43.

Sturgis, E. M., Wei, Q., and Spitz, M. R. (2004). Descriptive epidemiology and risk factors for head and neck cancer. Seminars in Oncology, 31(6):726–733.

Tabrizi, S. N., Brotherton, J. M. L., Kaldor, J. M., Skinner, S. R., Cummins, E., Liu, B., Bateson, D., McNamee, K., Garefalakis, M., and Garland, S. M. (2012). Fall in human papillomavirus prevalence following a national vaccination program. Journal of Infectious Diseases, 206(11):1645–51.

Taira, A. V., Neukermans, C. P., and Sanders, G. D. (2004). Evaluating human papillomavirus vaccination programs. Emerging Infectious Diseases, 10(11):1915–23.

Vajda, S., Godfrey, K. R., and Rabitz, H. (1989). Similarity transformation approach to identifiability analysis of nonlinear compartmental models. Mathematical Biosciences, 93:217–248.

Valente, T. W. (2012). Network interventions. Science, 337(6090):49–53.

Van de Velde, N., Boily, M.-C., Drolet, M., Franco, E. L., Mayrand, M.-H., Kliewer, E. V., Coutlée, F., Laprise, J.-F., Malagón, T., and Brisson, M. (2012). Population-level impact of the bivalent, quadrivalent, and nonavalent human papillomavirus vaccines: a model-based analysis. Journal of the National Cancer Institute, 104(22):1712–23.

Van de Velde, N., Brisson, M., and Boily, M.-C. (2007). Modeling human papillomavirus vaccine effectiveness: quantifying the impact of parameter uncertainty. American Journal of Epidemiology, 165(7):762–75.

Van de Velde, N., Brisson, M., and Boily, M.-C. (2010). Understanding differences in predictions of HPV vaccine effectiveness: A comparative model-based analysis. Vaccine, 28(33):5473–84.

van den Driessche, P. and Watmough, J. (2002). Reproduction numbers and sub-threshold endemic equilibria for compartmental models of disease transmission. Mathematical Biosciences, 180:29–48.

Walline, H. M., Komarck, C., McHugh, J. B., Byrd, S. a., Spector, M. E., Hauff, S. J., Graham, M. P., Bellile, E., Moyer, J. S., Prince, M. E., Wolf, G. T., Chepeha, D. B., Worden, F. P., Stenmark, M. H., Eisbruch, A., Bradford, C. R., and Carey, T. E. (2013). High-risk human papillomavirus detection in oropharyngeal, nasopharyngeal, and oral cavity cancers: comparison of multiple methods. JAMA Otolaryngology– Head & Neck Surgery, 139(12):1320–7.

Whittemore, A. and Keller, J. (1978). Quantitative theories of carcinogenesis. Siam Review, 20(1):1–30.

Widdice, L., Ma, Y., Jonte, J., Farhat, S., Breland, D., Shiboski, S., and Moscicki, A.-B. (2013). Concordance and transmission of human papillomavirus within heterosexual couples observed over short intervals. Journal of Infectious Diseases, 207(8):1286–94.